論文 / 著書情報
Article / Book Information

題目(和文)	120GHz帯無線における10Gbpsデータ伝送のための偏波多重方式の研究
Title(English)	Study of Polarization Multiplexing for 10-Gbps Data Transmission over 120-GHz-band Wireless Links
著者(和文)	竹内淳
Author(English)	jun takeuchi
出典(和文)	学位:博士（工学）, 学位授与機関:東京工業大学, 報告番号:甲第9782号, 授与年月日:2015年3月26日, 学位の種別:課程博士, 審査員:廣川　二郎,安藤　真,水本　哲弥,淺田　雅洋,西方　敦博
Citation(English)	Degree:, Conferring organization: Tokyo Institute of Technology, Report number:甲第9782号, Conferred date:2015/3/26, Degree Type:Course doctor, Examiner:,,,,
学位種別(和文)	博士論文
Type(English)	Doctoral Thesis

Doctoral Dissertation

Study of Polarization Multiplexing for 10-Gbps Data Transmission over 120-GHz-band Wireless Links

January, 2015

Under the Supervision of

Associate Professor Jiro Hirokawa

Presented by

Jun Takeuchi

Department of Electrical and Electronic Engineering

Tokyo Institute of Technology

Contents

Chapter 1
Introduction

1-1 Background of this study

Demand for higher data rates in wireless systems is increasing dramatically, because of the spread of broadband network, smart phone, and HDTV. The 10-Gigabit Ethernet (10-GbE) comes to be adopted at datacenter as a mainstream of Ethernet equipments, and 10-GbE market continues growing up. The 40-GbE or 100-GbE will soon become the next growing segment in the Ethernet market. Wireless technologies that can handle those standardized wired network are useful for the cable less connection between datacenter, fixed wireless access, and temporal connections during the recovery from disaster.

In the mobile network regime, smart phones and tablets are rapidly spreading in our modern life and it causes dramatic increase of mobile data traffic. Next generation mobile network of LTE-Advanced will require maximum data rate of 1-Gbps for down link and it means that mobile base stations or mobile backhauls require more than 1-Gbps of access network. Recently mobile base stations and mobile backhauls come to be connected by wireless access network for easy and rapid installation.

In the broadcasting regime, HDTV (1.5 Gbps) become common technology for TV program production. 4K Ultra-HDTV (12-Gbps) is the next growing segment in the Television market. 4K broadcasting trial service had already started in Japan. Moreover, 8K Ultra-HDTV (more than 24-Gbps) are researched and developed as the future television system [1]. Transmitting uncompressed HDTV signals or Ultra-HDTV signals with wireless technology is important issue for the practical use in the live-relay broadcasting. To meet those demands, multi-gigabit wireless data transmission system is required.

Recently, millimeter-wave (MMW) wireless technology is attracting a lot of interest because of its sufficient bandwidth for higher bit rate. Figure 1 shows bit rates and distances between wireless terminals for recently reported MMW wireless transmissions. This figure covers only experimental results for wireless transmission using antennas. Table 1 shows a

comparison of frequency, modulation scheme, key technology and antenna in the reports.

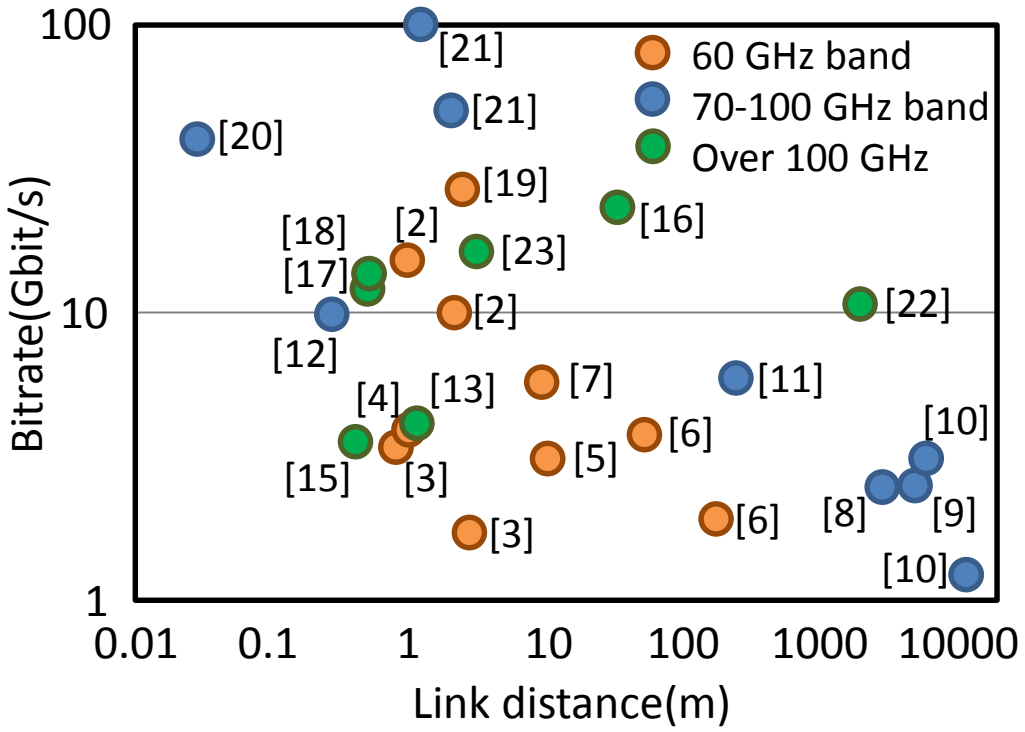

Figure 1-1. Recently reported bit rates and transmission distances in experimental demonstrations of MMW wireless transmission. (Modified from H. Takahashi, T. Kosugi, A. Hirata, and K. Murata, "Supporting Fast and Clear Video," IEEE Microwave Magazine vol. 13, Issue 6, pp. 54-64, 2012.)

Ref.	Frequency	Modulation	Technology	Antenna
[2]	60-GHz band	16-QAM	65 nm CMOS	Packaged array antennas
[3]	60-GHz band	QPSK/16-QAM	65 nm CMOS	Packaged antenna (6 dBi)
[4]	60-GHz band		65 nm CMOS	Horn (25 dBi)
[5]	60-GHz band	16-QAM OFDM	65 nm CMOS	Packaged array antennas
[6]	60-GHz band	16-QAM OFDM	65 nm CMOS	Packaged array antennas
[7]	60-GHz band	16-QAM OFDM	SiGe BiCMOS	Packaged patch-array antennas
[8]	71–76 GHz/ 81–86 GHz	QPSK	-	Cassegrain
[9]	71–76 GHz/ 81–86 GHz	BPSK	-	Cassegrain (51 dBi)
[10]	71–76 GHz/ 81–86 GHz	QPSK	-	Cassegrain (44 dBi, 51 dBi)
[11]	81–86 GHz	8 PSK	GaAs pHEMT	Conical lens horn (45 dBi)
[12]	73–93 GHz	Impluse radio	InP HEMT	Horn (23 dBi)
[13]	140-GHz band	ASK	130-nm SiGe BICMOS	Horn
[14] [15]	120/140-GHz band	ASK	65 nm CMOS	Horn (25 dBi)
[16]	240-GHz band	8 PSK	35 nm mHEMT	Lens and horn
[17]	300-GHz band	ASK	Photonics-based transmitter	Dielectric lens and horn (~25 dBi)
[18]	300-GHz band	ASK	Photonics-based transmitter	Dielectric lens and horn (~25 dBi)
[19]	57.4–64.4 GHz	16-QAM OFDM	Photonics-based transmitter	Horn (23 dBi)
[20]	W band (75–110 GHz)	16-QAM	Photonics-based transmitter	Horn
[21]	W band (75–110 GHz)	16-QAM	Photonics-based transmitter	Horn (24 dBi)
[22]	120-GHz band	ASK	100-nm InP HEMT	Cassegrain (49 dBi)
[23]	120-GHz band	QPSK	100-nm InP HEMT	Horn (23 dBi)

Table 1-1. Comparison of frequency bands, modulations, device technologies and antennas in experimental demonstrations of MMW wireless transmission. (Modified from H. Takahashi, T. Kosugi, A. Hirata, and K. Murata, “Supporting Fast and Clear Video,” IEEE Microwave Magazine vol. 13, Issue 6, pp. 54-64, 2012.)

60-GHz-band wireless technology [2-7] is permitted to use as license-free band. Current Si CMOS technology enables the 60-GHz ICs for mass production. Those ICs offer higher order modulation such as QPSK or 16QAM for multi-gigabit data rate. Some wireless standard for transmission of HDTV signals have already been established and wireless HDTV systems are already commercially available [5]. However, atmospheric attenuation by Oxygen is large at 60-GHz-band thus 60-GHz-band cannot be used for outdoor long range data transmission usage model as shown in Figure 1.
Higher frequency range of 71-76 GHz / 81-86 GHz [8-12] can be applied for the long range data transmission because atmospheric attenuation of those bands are less than that of 60-GHz band. However in general, using higher frequency range of more than 100-GHz band increases loss of components of the circuit, such as inductors or capacitors. The loss of components increases the phase noise which deteriorates the modulation accuracy. Thus, it is difficult to use higher order modulation in the higher frequency range of more than 100-GHz band [13-15].
Recent progress in designing and fabricating the MMIC enables higher order modulation in the frequency range of more than 100-GHz band [16].
Photonic based technology [17-21] enables higher order modulation because of the accuracy of controlling phase and amplitude. However in general, size of photonic based equipment is larger than size of ICs.
NTT laboratories have been working on development of 120-GHz-band wireless link systems [22, 23]. 120-GHz-band can be applied for the long range data transmission same as 71-76 GHz or 81-86 GHz band, and NTT have already succeeded in error-free 10-Gbps data transmission for more than 3-km. 120-GHz-band wireless system was first developed with photonic based technology and current system is developed with InP HEMT MMICs. 120-GHz-band wireless system has compatibility to fiber optic system so that it can be used for last-mile access of 10-Gbps Ethernet.
NTT has also developed QPSK technology in 120-GHz-band and has succeeded in making the wireless link systems for outdoor use [23].

As explained above, demand for higher data rates in wireless systems is increasing so that improvement to increase the spectral efficiency is required. One of the promising methods is to use the polarization multiplexing. Polarization multiplexing is a simple method which uses horizontal and

vertical polarization for simply double the spectral efficiency. Moreover we can use both polarization multiplexing and higher order modulation at the same time to increase spectral efficiency much more. It means that using polarization multiplexing doubles the data rate of MMW wireless transmission systems which are referred in Table 1.

Tsunemitsu et al. demonstrated bidirectional data transmissions in the 26-GHz band using orthogonally arranged slot array antennas [24]. Kwang Seon Kim et al. demonstrated bidirectional data transmissions in the 90-GHz band using orthogonally arranged Cassegrain antennas [25]. Frequency range of over 100 GHz, polarization multiplexing is rarely used for data transmission. Thus, evaluating the polarization multiplexing data transmission characteristics of more than 100 GHz region is important for both scholarly pursuits and practical application.

There are two important characteristics for polarization multiplexing: isolation between orthogonal ports (Iop) and cross-polarization isolation (XPI). Iop is required for bidirectional data transmission and XPI is required for unidirectional 2-ch data transmissions. These two characteristics are mostly deteriorated by polarization rotation and multi-reflection of radio waves which causes polarization rotation. In the millimeter wave region, radio waves have high straightness. Thus, using high gain antenna for long range data transmission of millimeter wave results in line-of-sight propagation and multi-reflection problem hardly occurs. Therefore, using polarization multiplexing in millimeter wave region is one of the promising methods.

1-2 Polarization multiplexing for 120-GHz-band wireless links

The objective of this study is to evaluate the practical use of polarization multiplexing for millimeter wave data transmission. We decided to use 120-GHz-band wireless link for its evaluation. Figure 1-2, 1-3, and 1-4

shows the outward appearance and schematic view of 120-GHz-band wireless link. 120-GHz-band wireless link was developed by NTT laboratories [22, 23] and can transmit 10 Gbps data stream. 120-GHz-band wireless link includes all of RF components and has the maximum link distance of more than 3 km. The 120-GHz-band wireless link employs amplitude shift keying (ASK) for the modulation scheme and uses the occupied band width of 17 GHz (from 116.5 to 133.5 GHz) because ASK is the simplest architecture for both modulation and demodulation. 120-GHz-band wireless link is allowed to use outdoor because it has experimental radio station license from the Ministry of Internal Affairs and Communications of Japan. Therefore we decided to use 120-GHz-band wireless link for polarization multiplexing of 10 Gbps data stream because we can evaluate its characteristic both indoors and outdoors.

Figure 1-2. Outward appearance of 120-GHz band wireless transmitter

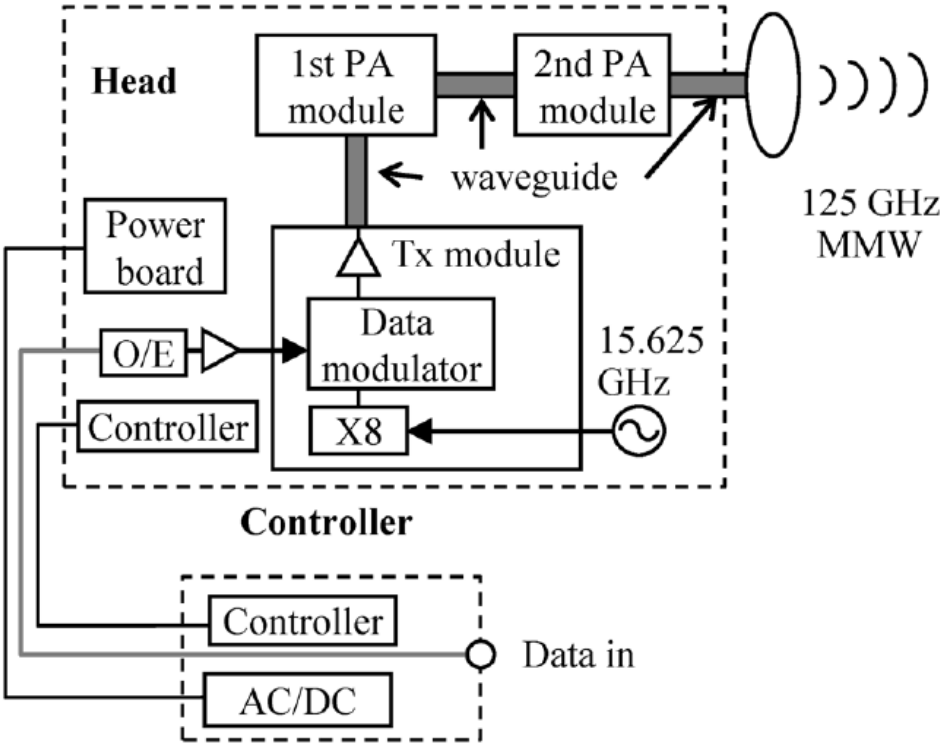

Figure 1-3. Schematic of 120-GHz band wireless transmitter

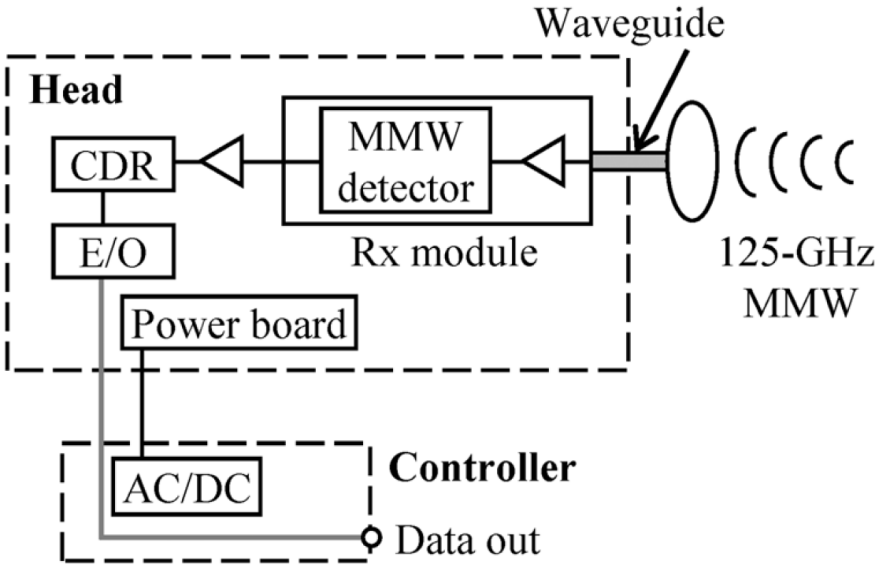

Figure 1-4. Schematic of 120-GHz band wireless receiver

1-3 Outline of remaining chapters

In this dissertation, we demonstrate feasibility of using polarization multiplexing for 120-GHz-band wireless link systems.

Fig. 1-5 shows flow chart of this dissertation. Chapter 2 presents system requirement for polarization multiplexing of 120-GHz-band wireless link. In Chapter 2, required value of Iop and XPI are shown.

Chapter 3, 4 and 5 present the experimental results of polarization multiplexing by each method.

There are two types of polarization multiplexing, shown in Fig. 1-6. One is using two pairs of antennas for V and H wave. Using two pairs of antennas doubles size of wireless equipment, but physically isolated two pairs of antennas enables high Iop.

The other is using one antenna and orthomode transducer (OMT). An OMT multiplexes and de-multiplexes V and H wave with one antenna. Using OMT enables space-saving assembly of wireless equipment, but physically connected V and H wave by OMT increases difficulty of achieving high Iop.

Chapter 3 and 4 describes two pairs of antennas arrangements for polarization multiplexing. In Chapter 3, experimental results of polarization multiplexing by Cassegrain antennas are shown. In Chapter 4, experimental results of polarization multiplexing by planar slot array antennas are shown.

Chapter 5 describes one antenna with OMT arrangement for polarization multiplexing. In Chapter 5, design and fabrication of OMT and experimental results of polarization multiplexing by OMT are shown.

Finally, Chapter 6 summarizes this study and discusses the future study.

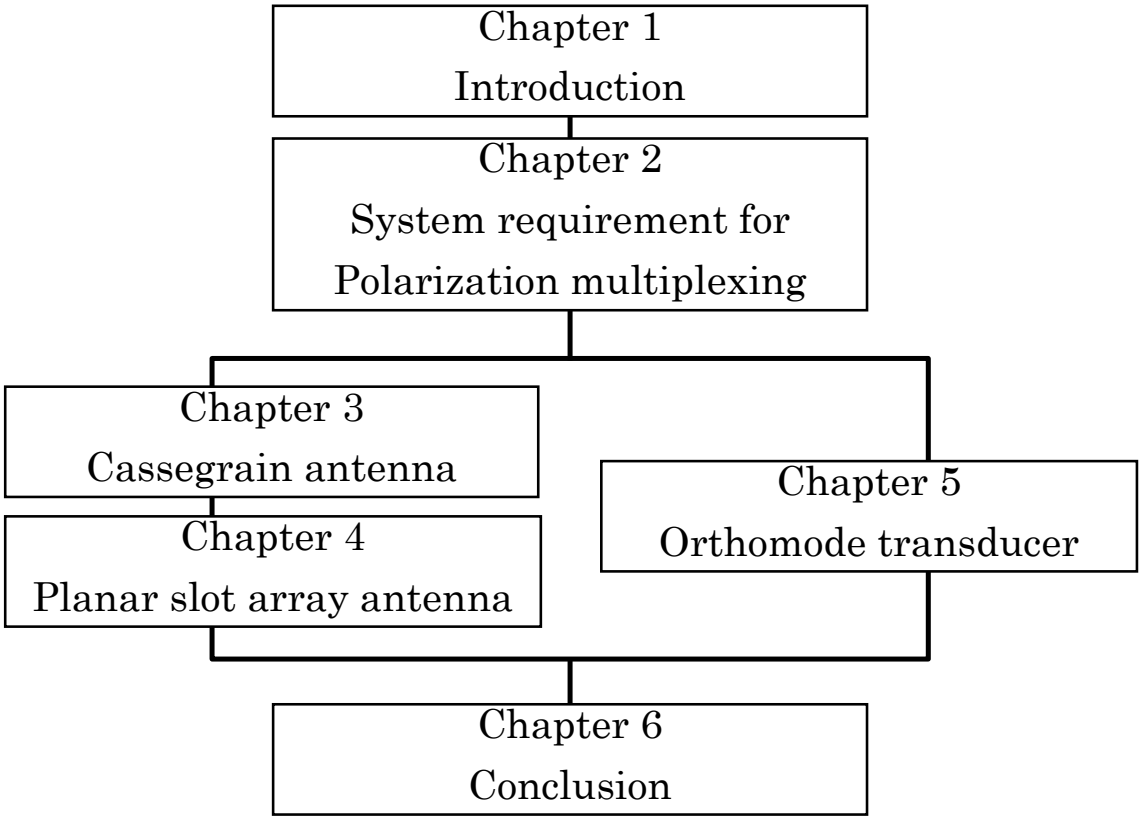

Fig. 1-5. Flow chart of this dissertation

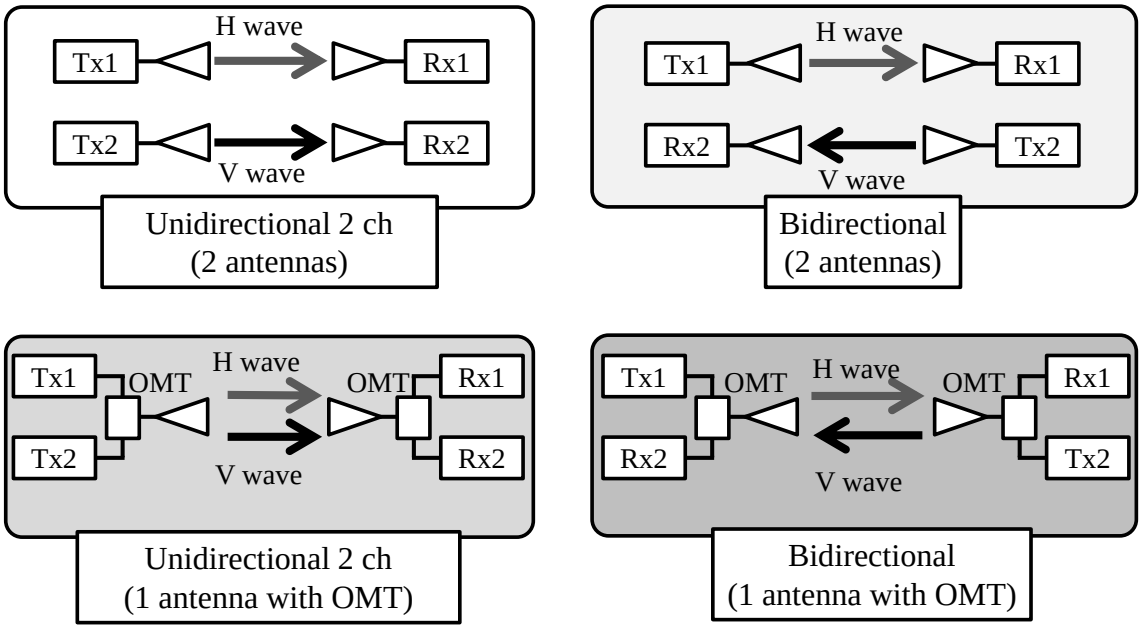

Fig. 1-6. Schematic view of different types of polarization multiplexing methods. (V: Vertical, H: Horizontal)

References in Chapter 1

[1] M. Maeda, Y. Shishikui, F. Suginoshita, Y. Takiguchi, T. Nakatogawa, M. Kanazawa, K. Mitani, K. Hamasaki, M. Iwaki, and Y. Nojiri, "Steps toward the practical use of Super Hi-Vision," NAB Broadcast Engineering Conference, pp. 450-455, 2006.

[2] D. Dawn, S. Pinel, S. Sarkar, P. Sen, B. Perumana, D. Yeh and J. Laskar, "Development of CMOS Based Circuits for 60GHz WPAN applications," ICUWB 2007, Digt., pp. 129 – 133.

[3] K. Okada, K. Kondou, M. Miyahara, M. Shinagawa, H. Asada, R. Minami, T. Yamaguchi, A. Musa, Y. Tsukui, Y. Asakura, S. Tamonoki, H. Yamagishi,Y. Hino, T. Sato, H. Sakaguchi, N. Shimasaki, T. Ito, Y. Takeuchi, Ning Li, Qinghong Bu, R. Murakami, K. Bunsen, K. Matsushita, M. Noda, and A. Matsuzawa, " Full Four-Channel 6.3-Gb/s 60-GHz CMOS Transceiver With Low-Power Analog and Digital Baseband Circuitry," IEEE Journal of Solid-State Circuits, Vol. 48 , Issue 1, pp. 46 – 65, 2013.

[4] C. Marcu, D. Chowdhury, C. Thakkar, Jung-Dong Park, Ling-Kai Kong, M. Tabesh, Wang Yanjie Wang, B. Afshar, A. Gupta, A. Arbabian, S. Gambini, R. Zamani, E. Alon, and A.M. Niknejad, "A 90 nm CMOS Low-Power 60 GHz Transceiver With Integrated Baseband Circuitry," IEEE Journal of Solid-State Circuits, Vol. 44 , Issue 12, pp. 3434 – 3447, 2009.

[5] Wireless HD. homepage [Online]. Available:

http://www.wirelesshd.org/

[6] S. Emami, R.F. Wiser, E. Ali, M.G. Forbes, M.Q. Gordon, Guan Xiang, S. Lo, P.T. McElwee, J. Parker, J.R. Tani, J.M. Gilbert, and C.H. Doan, "A 60GHz CMOS phased-array transceiver pair for multi-Gb/s wireless communications," ISSCC 2011 Digt., pp. 164-166.

[7] A. Valdes-Garcia, S. Reynolds, A. Natarajan, Dong Kam, Duixian Liu, Jie-Wei Lai, Y.-L.O. Huang, Ping-Yu Chen, Ming-Da Tsai, J.-H.C. Zhan, S. Nicolson, and B. Floyd, " Single-element and phased-array transceiver chipsets for 60-ghz Gb/s communications," IEEE Communications Magazine, vol. 49, Issue 4, pp. 120-131, 2011.

[8] NEC Corp. homepage [Online]. Available: http://www.nec.com/en/global/prod/nw/pasolink/products/epaso.html/

[9] Loea Corp. homepage [Online]. Available: http://www.loeacom.com/pages/products_l2250.htm

[10] BridgeWave Communications, Inc. homepage [Online]. Available: http://www.bridgewave.com/downloads/BridgeWave_products_at_a_glance_brochure.pdf

[11] V. Dyadyuk, J. D. Bunton, J. Pathikulangara, R. Kendall, O. Sevimli, L.Stokes, and D. A. Abbott, "A multigigabit millimeter-wave communication system with improved spectral efficiency," IEEE Trans. on Microwave Theory and Techniques, vol. 55, no. 12, pp. 2813-2821, 2007.

[12] Y. Nakasha, M. Sato, T. Tajima, Y. Kawano, T. Suzuki, T. Takahashi, K. Makiyama, T. Ohki, and N. Hara, "W -band Transmitter and Receiver for 10-Gb/s Impulse Radio

With an Optical-Fiber Interface," IEEE Transactions on Microwave Theory and Techniques, Vol. 57, Issue 12 , Part 2, pp. 3171 – 3180, 2009.

[13] E. Laskin, P. Chevalier, B. Sautreuil, and S. P. Voinigescu, "A 140-GHz double-sideband transceiver with amplitude and frequency modulation operating over a few meters," IEEE BCTM 2009., pp. 178-181.

[14] R. Fujimoto, R. M. Motoyoshi, U. Yodprasit, K. Takano, and M. Fujishima, "A 120-GHz transmitter and receiver chipset with 9-Gbps data rate using 65-nm CMOS technology," A-SSCC 2010 Digt., pp.1-4.

[15] R. Fujimoto, R. M. Motoyoshi, K. Takano, and M. Fujishima, "A 120 GHz / 140 GHz dual-channel ASK receiver using standard 65 nm CMOS technology," EuMC 2011 41st European Digt., pp. 1189 - 1192

[16] J. Antes, S. Koenig, D. Lopez-Diaz, F. Boes, A. Tessmann, R. Henneberger, O. Ambacher, T. Zwick, I. Kallfass, " Transmission of an 8-PSK Modulated 30 Gbit/s Signal Using an MMIC-Based 240 GHz Wireless Link," 2013 IEEE MTT-S International Microwave Symposium (IMS) Digt. pp. 1 - 3

[17] Ho-Jin Song, K. Ajito, A. Wakatsuki, Y. Muramoto, N. Kukutsu, Y. Kado, and T. Nagatsuma, "Terahertz wireless communication link at 300 GHz," MWP 2010, Digt., pp. 42 - 45

[18] T. Nagatsuma, T. Takada, Ho-Jin Song, K. Ajito, N. Kukutsu, and Y. Kado, "Millimeter- and THz-wave photonics towards 100-Gbit/s wireless transmission," IEEE Photonics Society, 2010 Digt. pp. 385 – 386.

[19] M. Weiss, A. Stohr, F. Lecoche, and B. Charbonnier, “27 Gbit/s photonic wireless 60 GHz transmission system using 16-QAM OFDM,” MWP '09. Digt. pp. 1 – 3.

[20] A. Kanno, K. Inagaki, I. Morohashi, T. Sakamoto, T. Kuri, I. Hosako, T. Kawanishi, Y. Yoshida, and K. Kitayama, “40 Gb/s W-band (75–110 GHz) 16-QAM radio-over-fiber signal generation and its wireless transmission,” ECOC 2011, Digt., pp. 1 – 3.

[21] X. Pang, C. Antonio, D. Anton, A. Valeria, B. Robert, J. S. Pedersen, Lei Deng, F. Karinou, F. Roubeau, D. Zibar, Xianbin Yu, and I.T. Monroy, “100 Gbit/s hybrid optical fiber-wireless link in the W-band (75–110 GHz),” Optics Express, Vol. 19, Issue 25, pp. 24944-24949, 2011.

[22] A. Hirata, T. Kosugi, H. Takahashi, J. Takeuchi, H. Togo, M. Yaita, N. Kukutsu, K. Aihara, K. Murata, Y. Sato, T. Nagatsuma, Y. Kado, “ 120-GHz-Band Wireless Link Technologies for Outdoor 10-Gbit/s Data Transmission,” IEEE Transactions on Microwave Theory and Techniques, vol. 60, no.3, pp. 881-895, March 2012.

[23] H. Takahashi, T. Kosugi, A. Hirata, J. Takeuchi, K. Murata, and N. Kukutsu, “120-GHz-Band 10-Gbit/s Fully Integrated Wireless Link using Quadrature-Phase-Shift Keying,” 2013 IEEE MTT-S International Microwave Symposium (IMS) Digt. pp. 1 – 4.

[24] Y. Tsunemitsu, K. Kojima, G. Yoshida, M. Nagayasu, N. Goto, J.Hirokawa, M. Ando, ”Orthogonally-Arranged Center-Feed Single-Layer Slotted Waveguide Array Antennas for Polarization Division Duplex,” EuCAP 2007, pp. 1-5, 2007.

[25] Kwang Seon Kim, Bong-Su Kim, Min-Soo Kang, Woo-Jin Byun, Hyung Chul Park, ”16-QAM OFDM-Based W-Band Polarization-Division Duplex Communication

System with Multi-gigabit Performance," ETRI Journal, Volume 36, Number 2, April 2014

Chapter 2
System Requirement for Polarization Multiplexing

Chapter 2 describes system requirement of isolation between orthogonal ports (Iop) and cross-polarization isolation (XPI) for polarization multiplexing. Iop is required for bidirectional data transmission and XPI is required for unidirectional 2-ch data transmissions.

2-1 System requirement for 10-Gbps data transmission of 120-GHz-band wireless link system

We first calculated the required C/N ratio for 120-GHz-band wireless link. The 120-GHz-band wireless link system employs amplitude shift keying (ASK) for modulation and envelope detection for demodulation. The center frequency of the wireless link is 125 GHz, the occupied bandwidth is from 116.5 to 133.5 GHz. In this system, the probability of error in a spacing signal $P_{e,M\to S}$ and the probability of error in a spacing signal $P_{e,S\to M}$ are given by [1]

$$P_{e,M\to S} = \sqrt{\rho_0}\Phi(y) \quad (1)$$

$$P_{e,S\to M} = e^{-R\rho_0^2} \quad (2)$$

$$\Phi(y) = \frac{1}{\sqrt{2\pi}}\int_{-\infty}^{-y} e^{-\frac{x^2}{2}}\,dx \quad (3)$$

$$y = \sqrt{2R}(1-\rho_0) \quad (4)$$

where Φ(y) is the error function, ρ_0 is a threshold level ($\rho_0 = 0.5$), and R is the C/N ratio. Total error rate P_e is expressed as

$$P_e = \frac{1}{2}P_{e,M\to S} + \frac{1}{2}P_{e,S\to M} \quad (5)$$

Figure 2-1 show the dependence of error rate on the C/N ration given by Eq.(5).

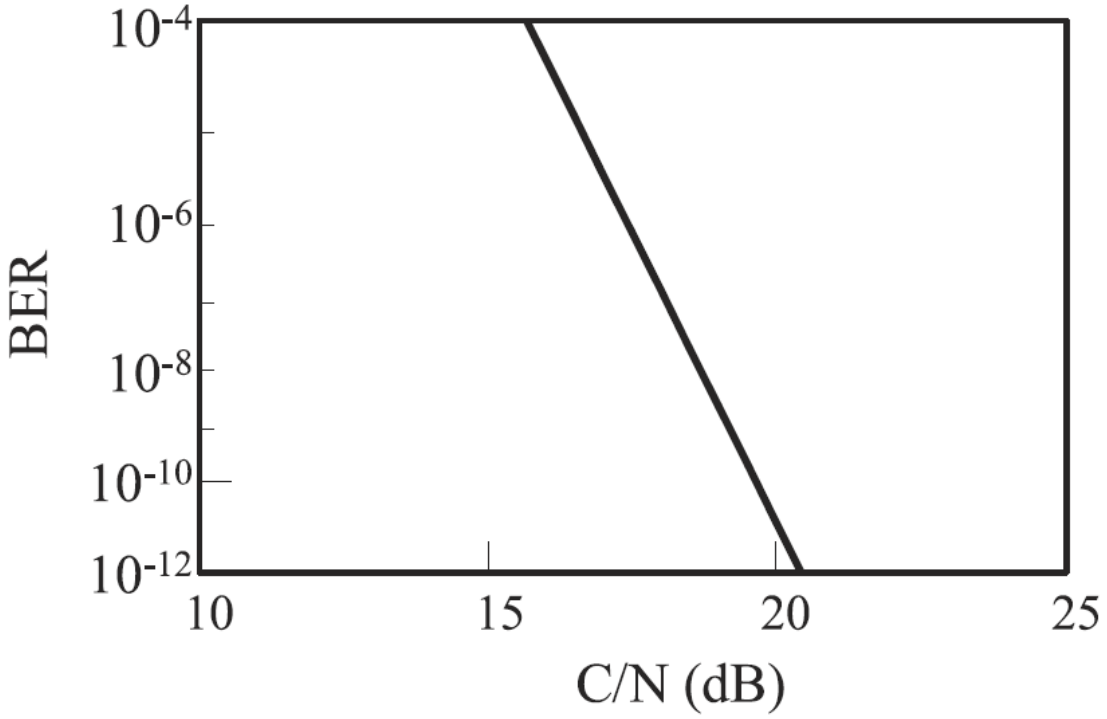

Figure 2-1. Dependence of BER on C/N ratio in the wireless link using ASK modulation.

Figure 2-1 indicates that a C/N ratio of over 20.2 dB is required for a Bit Error Rate (BER) of below 10^{-12}. BER of below 10^{-12} is required in order to meet the standards for general optical-fiber communications, such as OC-192 and 10-GbE. Moreover, using Forward Error Correction (FEC) decreases the required C/N ratio by coding gain. We use Reed Solomon (RS)(255,239) coding FEC, which is defined in ITU-T Recommendation G.709 Interfaces, for 120 GHz band wireless link in order to increase the reliability of the wireless link. The coding gain of RS(255, 239) coding FEC is about 6 dB; therefore, the required C/N ratio for a BER of below 10^{-12} becomes 14.2 dB when we use FEC in our system.

The C/N ratio of the wireless system is expressed as

$$C/N = P_r/(N_{thr}) \qquad (6)$$

where P_r is a received power from Transmitter (Tx) and N_{thr} is the noise power at the receiver.
The noise power at the receiver N_{thr} mainly comes from the thermal noise of the LNA, which is given by

$$N_{thr} = k_b T \cdot NF_r \cdot \Delta f \qquad (7)$$

Where k_b is Boltzmann's constant, NF_r is the Noise Figure (NF) of the receiver, T is temperature, and Δf is the bandwidth of the receiver.

In our system, the NF is about 5.6 dB and Δf is 20 GHz. N_{thr} therefore becomes -65.2 dBm. As described in Ref. [2, 3, 4], the received power necessary for a BER below 10^{-12} is about -37 dBm without FEC. This value varies and is higher than the theoretical value discussed above. We suppose that the difference between the experimental results and the theoretical value is due to the group delay of the MMW amplifier, thermal noise of the baseband amplifier, and process variation in device and module.

2-2 System requirement of XPI for polarization multiplexing unidirectional 2 ch data transmission

We next calculated the required XPI and Iop for polarization multiplexing data transmission of 120-GHz-band wireless link.

A schematic view of the unidirectional 2-ch data transmission system by polarization multiplexing is shown in Fig. 2-2, where V means vertical and H means horizontal. A small number of cross-polarization (Ex: H waves) are converted into co-polarization (Ex: V waves), which become noise for the

Receiver (Rx) module. For unidirectional 2-ch data transmission, the received powers of both the V and H waves are the same because they are equally weakened by the propagation loss. The thermal noise of the receiver module is sufficiently smaller than the noise from cross-polarization. Therefore, the C/N ratio of unidirectional 2-ch data transmission is determined by the ratio between the co-polarization and noise from the cross-polarization. As explained above, a C/N ratio of over 20.2 dB is necessary to obtain a BER below 10^{-12}. Thus, an XPI value of more than 20.2 dB across the entire occupied bandwidth of the 120-GHz-band wireless link is necessary. We decided on a target value of the XPI of more than 23 dB which is about 3 dB higher than the required value.

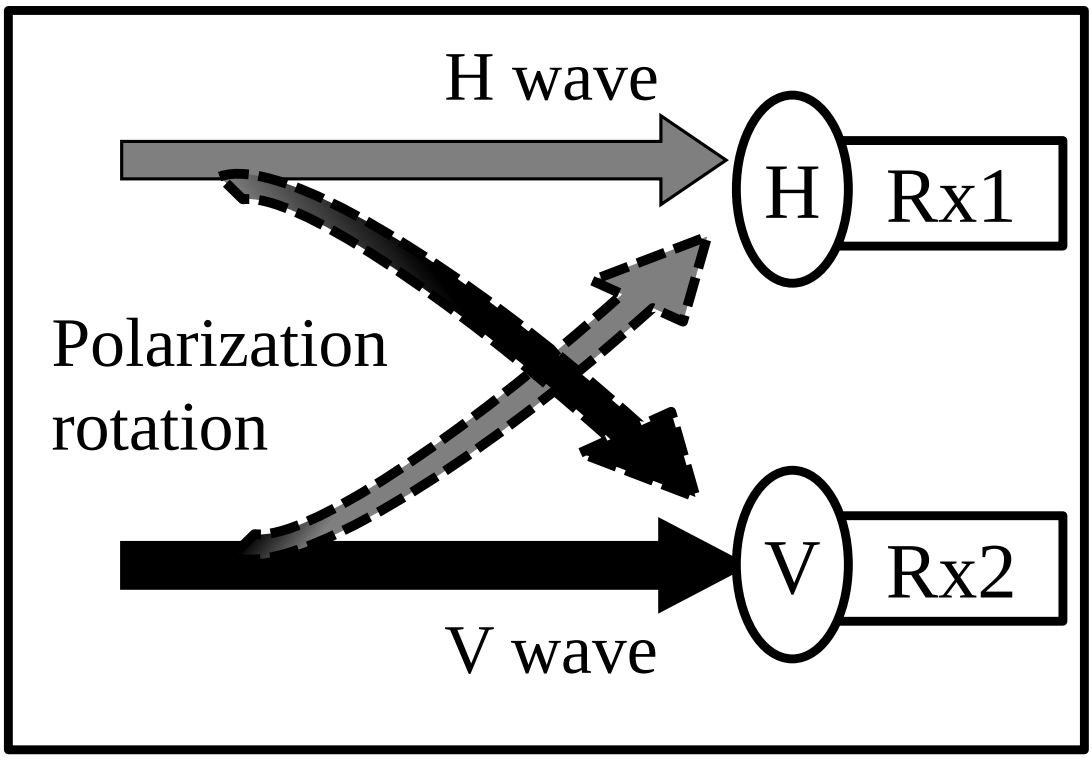

Fig. 2-2. Schematic view of a unidirectioinal 2-ch data transmission system by polarization multiplexing. (V: Vertical, H: Horizontal)

Figure 2-3 shows measured spectrum characteristics of ASK modulated signal of 120-GHz band wireless link. The occupied bandwidth of the 120-GHz-band wireless link is 116.5 ~ 133.5 GHz. In Fig. 2-3, there is a peak at the carrier frequency of 125 GHz. From system requirements, the peak with an amplitude of 50 percent of the total power appears at the carrier frequency when ASK modulation is used. Furthermore, there is leakage of carrier signals in actual devices. The data component of a 120-GHz-band wireless signal is broad and has a low spectral density. Thus the data component does not require as much isolation as the carrier component when ASK modulation is used.

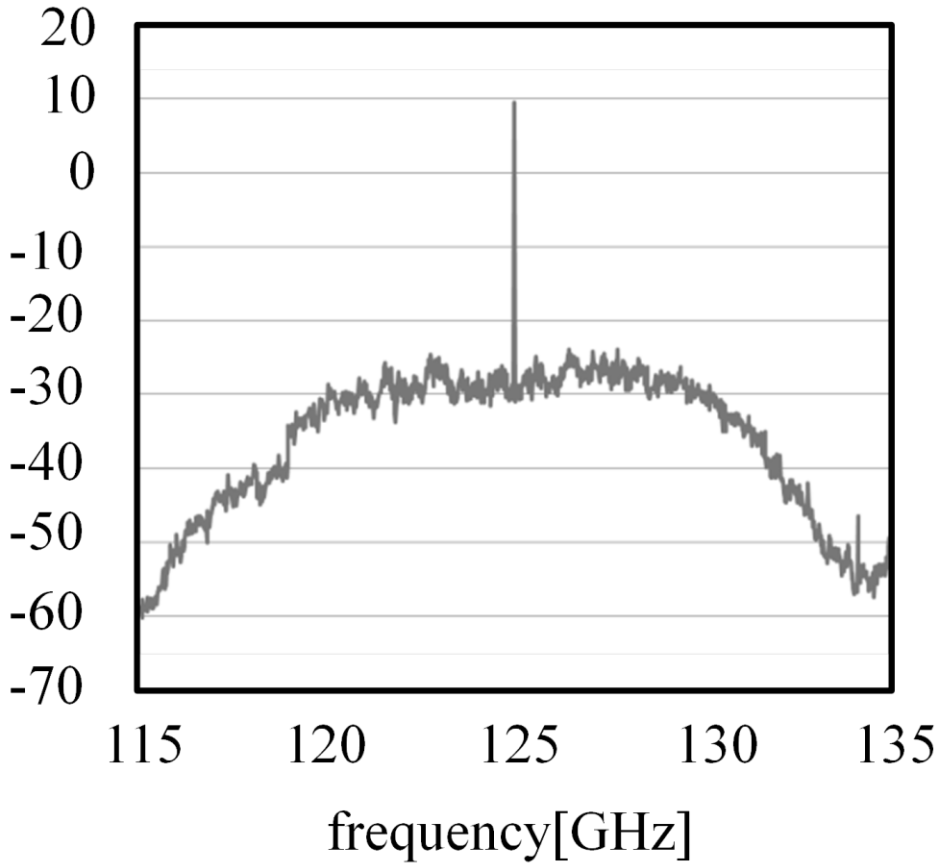

Fig. 2-3. Measured spectrum characteristics of ASK modulated signal of 120-GHz band wireless link.

2-3 System requirement of Iop for polarization multiplexing bidirectional data transmission

A schematic view of the bidirectional wireless data transmission by polarization multiplexing is shown in Fig. 2-4, where V means vertical and H means horizontal. Iop can be expressed as the transmission characteristics between co-pol and cross-pol in Fig. 2-4. A small amount of the Tx module output power is converted from co-pol into cross-pol and input into cross-pol. This polarization-rotated signal becomes noise for the Rx module. Our goal is to achieve Iop of over 60 dB. In this case, the received power of co-pol becomes more than -37 dBm.

As explained above, a C/N ratio of over 20.2 dB is necessary to obtain a BER below 10^{-12}.

Therefore, the required noise level is lower than -57.2 dBm across the entire occupied bandwidth of the 120-GHz-band wireless link. Compared with the noise from cross-polarization, the thermal noise of the receiver module is negligible; that is, we only have to consider the noise from polarization-rotated signal. We decided on a target value of Iop of more than 60 dB, which is about 3 dB higher than the required value. Noise power from the cross-polarization becomes lower than -57 dBm in this condition.

As explained in Section 2-2, when ASK modulation is used, high isolation is required for the carrier frequency and the data component does not require as much isolation as the carrier component.

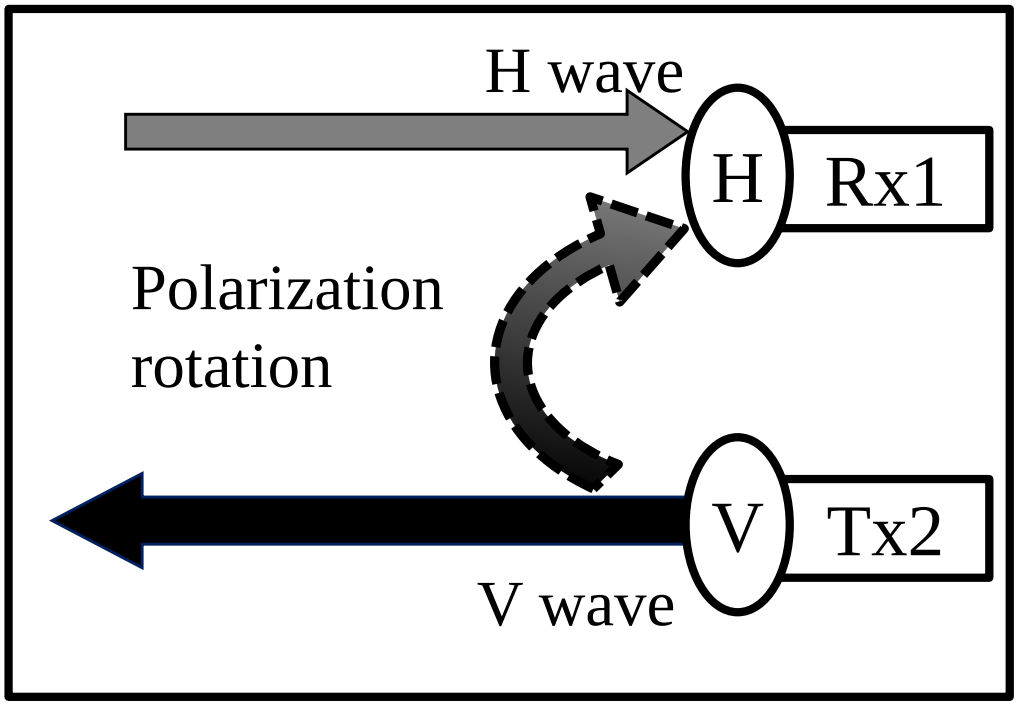

Fig. 2-4. Schematic view of a bidirectional data transmission system by polarization multiplexing. (V: Vertical, H: Horizontal)

2-4 Conclusion of Chapter 2

Chapter 2 describes system requirement of isolation between orthogonal ports (Iop) and cross-polarization isolation (XPI) for polarization multiplexing. Iop is required for bidirectional data transmission and XPI is required for unidirectional 2-ch data transmissions. The required value of Iop is more than 60 dB, and the required value of XPI of more than 23 dB.

References in Chapter 2

[1] S. Seki, “Basis of digital modulation and demodulation circuit,” Ohm Publ., pp. 30-35, (in Japanese).

[2] A. Hirata, T. Kosugi, H. Takahashi, R. Yamaguchi, F. Nakajima, T. Furuta, H. Ito, H. Sugahara, Y. Sato, and T. Nagatsuma, “120-GHz-Band Millimeter-Wave Photonic Wireless Link for 10-Gbit/s Data Transmission,” IEEE Transactions on Microwave Theory and Techniques, vol. 54, no.5, pp. 1937-1944, May, 2006.

[3] T. Kosugi, M. Tokumitsu, K. Murata, T. Enoki, H. Takahashi, A.Hirata, T. Nagatsuma,” 120-GHz Tx/Rx Waveguide Modules for 10-Gbit/s Wireless Link System,” IEEE CSIC Symp. Digest, pp.25-28, 2006.

[4] A. Hirata, R. Yamaguchi, T. Kosugi, H. Takahashi, K. Murata, T.Nagatsuma, N. Kukutsu, Y. Kado, N. Iai, S. Okabe, S. Kimura, H.Ikegawa, H. Nishikawa, T. Nakayama, T. Inada, ” 10-Gbit/s Wireless Link Using InP HEMT MMICs for Generating 120-GHz-Band Millimeter-Wave Signal,” IEEE Trans. MTT, vol. 57, pp. 1102-1109, 2009.

Chapter 3
Polarization Multiplexing by Two Pairs of Cassegrain Antennas

Chapter 3 describes polarization multiplexing by two Cassegrain antennas. The Cassegrain antenna is commercially available one with a diameter of 450 mm [1]. The Cassegrain antennas, which we own, are allowed to use in outdoor environment by ministry of internal affairs and communications as test license.
We first measured radiation pattern of Cassegrain antenna. The radiation pattern is important factor for two pairs of antennas arrangement because radiation patterns affect for XPI and isolation between parallel links. Next, we measured interference power level at unidirectional 2 ch data transmission and at bidirectional data transmission for evaluation of XPI and isolation between parallel links. Then, we measured transmission characteristics of V and H polarizations at outdoor circumstance. The purpose of the measurement is to evaluation how weather affects for transmission characteristics of V and H polarizations. Finally, we measured data transmission characteristics of polarization multiplexing by two Cassegrain antennas.

3-1 Radiation pattern of the Cassegrain antenna

Figure 3-1 shows the vertical- and horizontal-radiation pattern of the antenna with a diameter of 450 mm [1]. The measurement frequency was 125 GHz. Typical antenna gain is about 49 dBi, and the half-power beamwidth is about 0.4 degree. Side lobes appear every 0.4~0.5 degrees.

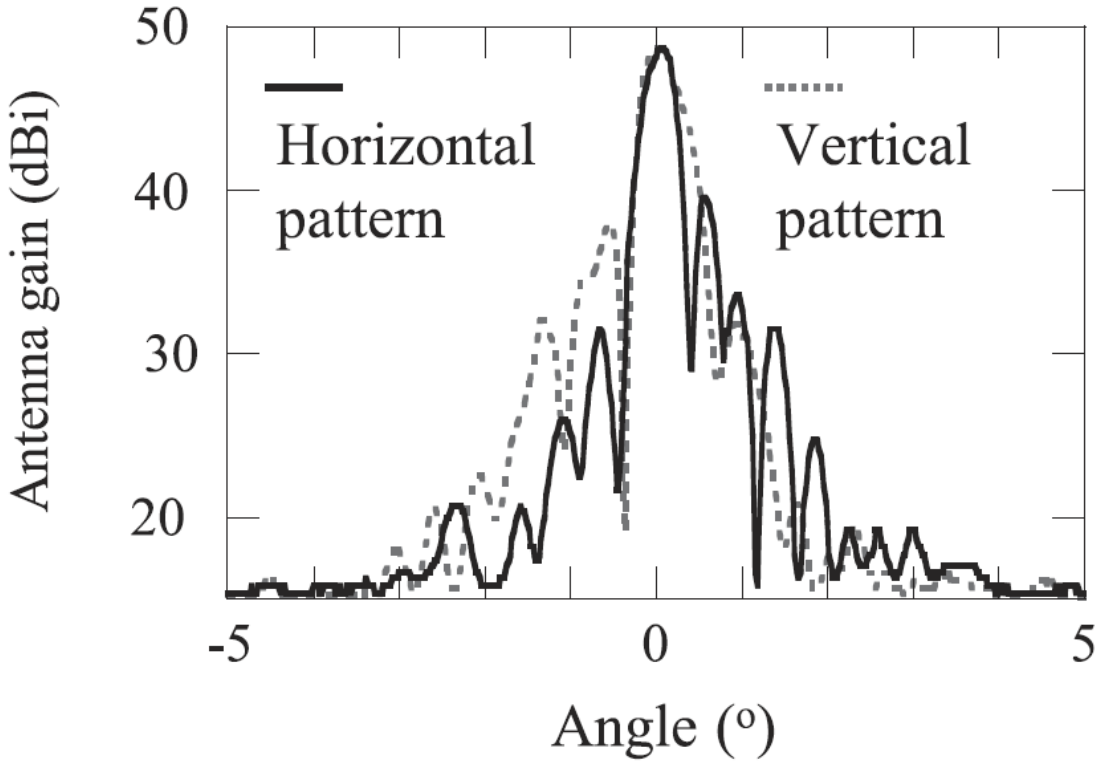

Figure 3-1. Measured radiation pattern of the Cassegrain antenna with a diameter of 450 mm. The measurement frequency is 125 GHz.

3-2 Interference power level at unidirectional 2 ch data transmission

We measured the interference power between the parallel 120-GHz-band wireless links in outdoor environment. The output power of the 120-GHz-band wireless links is 10 dBm, and Cassegrain antennas with a diameter of 450 mm are used. Figure 3-2 shows a schematic of the transmission experiment. Transmission distance was 800 m. One link consisted of Tx1 and Rx1, both of which were stationary. The other consisted

of Tx2 and Rx2. These were movable so that we could vary the distance between the two Txs, D_T, and that between two Rxs, D_R. The Tx's and Rx's can change the polarization of the MMW signal using polarization convertor. The Cassegrain antenna is attached to the transmitter with a bayonet mechanism. At the normal setting, the equipment outputs waves with V polarization. We can change that to H with a polarization convertor consisting of a waveguide twist, in which case we also have to rotate the antennas by 90 degrees. In this experiment, we evaluated the interference power that Tx1-Rx1 gives to the Tx2-Rx2 link. Figure 3-3 shows the D_T and D_R dependence of the interference power level. The power received by Rx1 from Tx1 was about -29 dBm. Here we define the received power that Rx2 received from Tx1 as the interference power. When both links use V polarization waves, the interference power level changes from -36 to -90 dBm as D_R increases. The interference power level decreases as D_T increases from 2 to 10 m. When D_T is constant, the interference power decreases as D_R increases from 2 to 6 m, and the interference power increases when D_R becomes 8 m, and it decreases again as D_R increases to over 10 m.

Next we evaluated the interference between the wireless links with different polarizations. Figure 3-4 shows the dependence of the interference power level on D_T and D_R. The link with Tx1 and Rx1 used vertical polarization waves (V polarization waves); the one with Tx2 and Rx2 used H polarization waves. The interference power levels are much smaller than that between the links with the same polarization. When both D_T and D_R are 2 m, the interference power level is -58 dBm. The power received by Rx1 from Tx1 was about -29 dBm, so that XPI becomes 29 dB. These results indicate that the use of V and H polarizations decreases interference power and that the configuration should provide a BER of better than 10^{-12}, even when two links are close to each other.

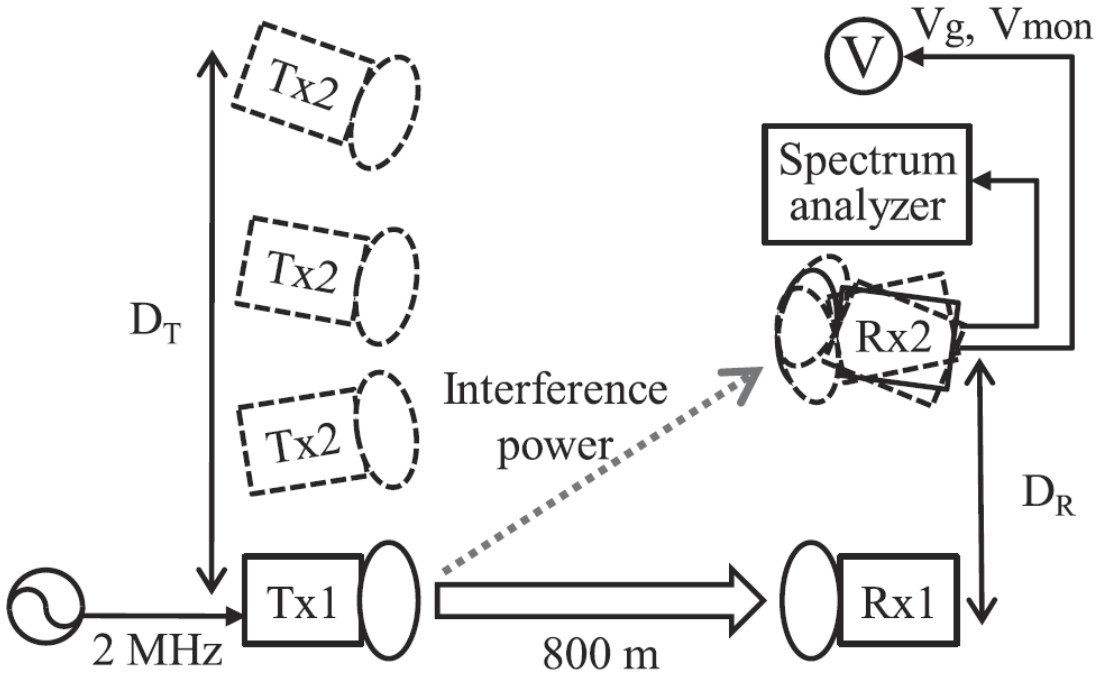

Figure 3-2. Schematic of transmission experiment to evaluate the interference power between the parallel wireless links.

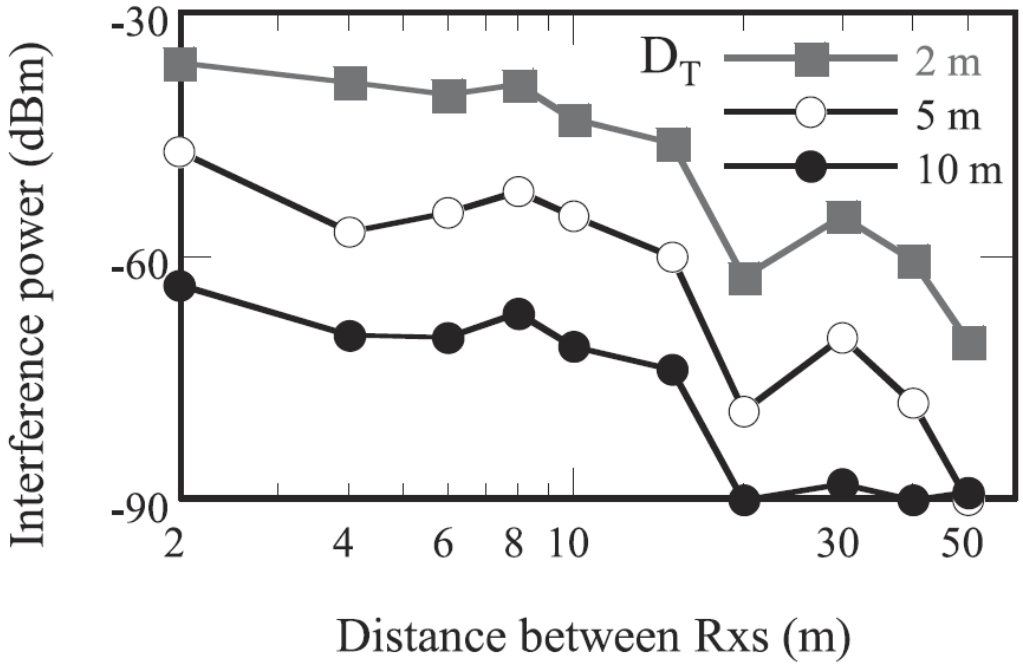

Figure 3-3. D_T and D_R dependence of the interference power level when both links use V polarization waves.

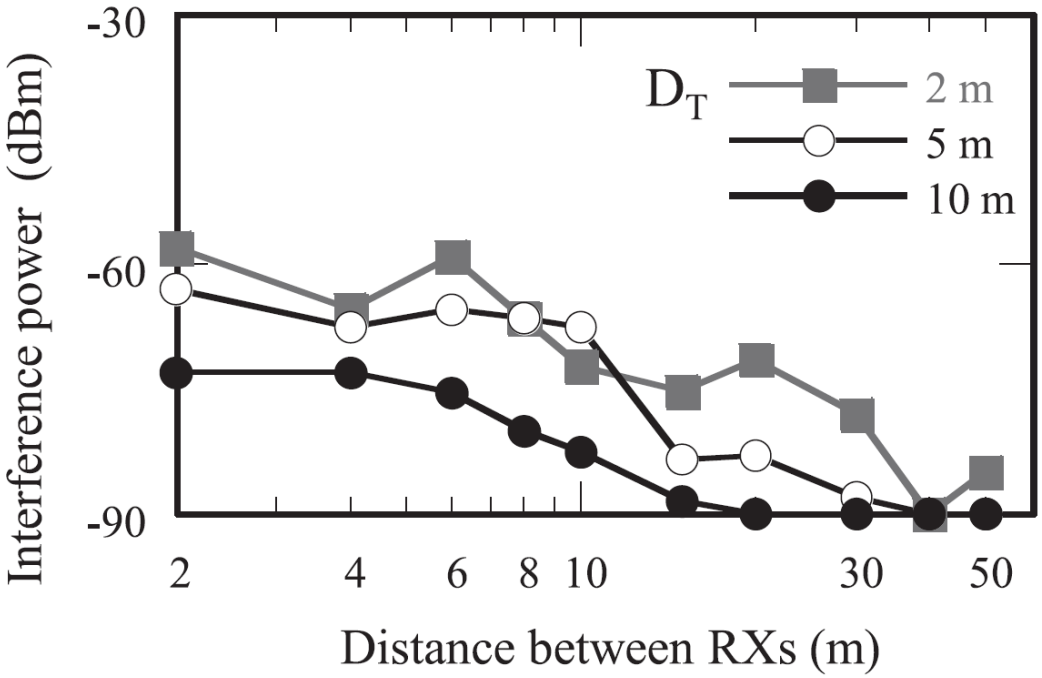

Figure 3-4. D_T and D_R dependence of the interference power level when one link uses V polarization wave and the other link uses H polarization.

3-3 Interference power level at bidirectional data transmission

We measured the interference power between the bidirectional 120-GHz-band wireless links in outdoor environment. The output power of the 120-GHz-band wireless links is 10 dBm, and Cassegrain antennas with a diameter of 450 mm are used. Figure 3-5 shows a schematic of the transmission experiment. The distance between Tx1 and Rx2 was 1 m. We measured the interference power level with the variation of antenna position of Rx2. Figure 3-6 shows the dependence of the interference power level on the antenna position of Rx2. Tx1 and Rx2 used same polarization (V polarization waves). From figure 3-6, interference power level was less than -75 dBm with the variation of ±2 m of antenna position. Thus, isolation between parallel links is 85 dB because output power is 10 dBm. As explained in Chapter 2, required isolation is more than 60 dB. Therefore, the interference power levels are much smaller than required value.

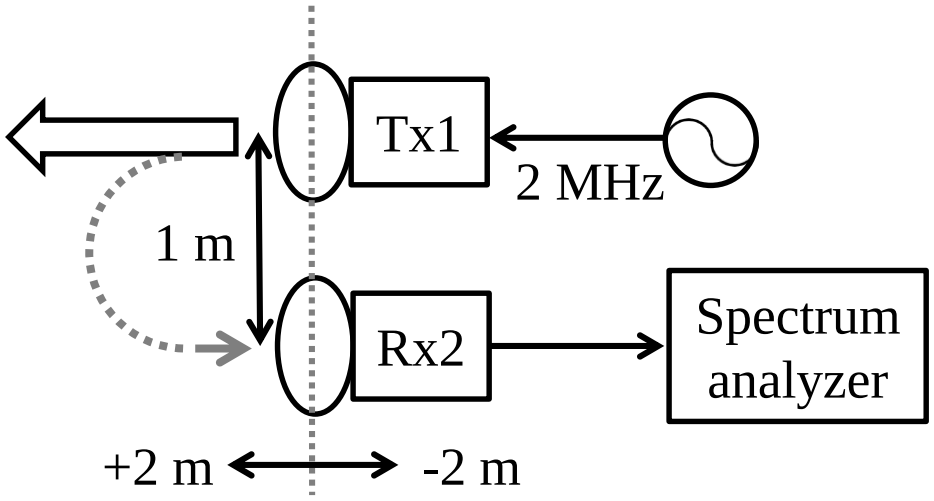

Figure 3-5. Schematic of transmission experiment to evaluate the interference power between the bidirectional wireless links with variation of position of antenna.

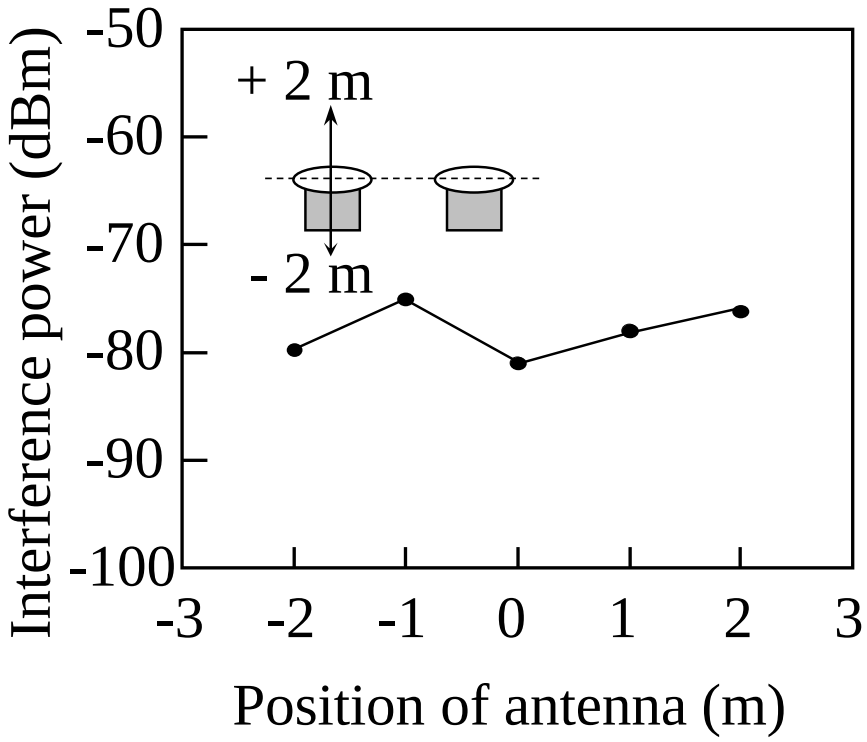

Figure 3-6. Interference power level with the variation of antenna position of Rx when both links use V polarization waves.

Next, we measured the interference power level with the variation of antenna direction of Tx1 as shown in Figure 3-7. Figure 3-8 shows the dependence of the interference power level on the direction of antenna of Tx1. Tx1 and Rx2 used same polarization (V polarization waves). From figure 3-8, interference power level was less than -65 dBm with antenna direction of 90 degree, which is smaller than the required value.

These results indicate that the configuration for bidirectional data transmission should provide a BER of better than 10^{-12}, even when two links use same polarization and are close to each other.

These high isolation characteristics are due to the use of high-gain antenna with narrow radio wave beam width, whose high directivity decreases the interference outside of the main beam.

Thus polarization multiplexing is not required in this configuration.

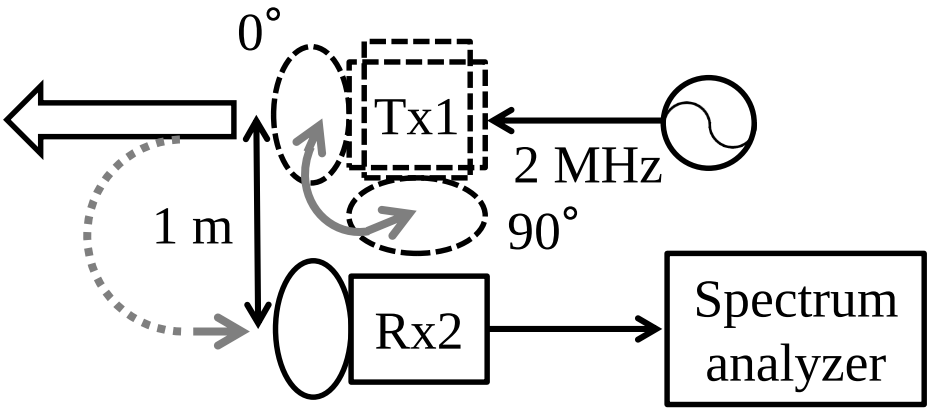

Figure 3-7. Schematic of transmission experiment to evaluate the interference power between the bidirectional wireless links with variation of direction of antenna.

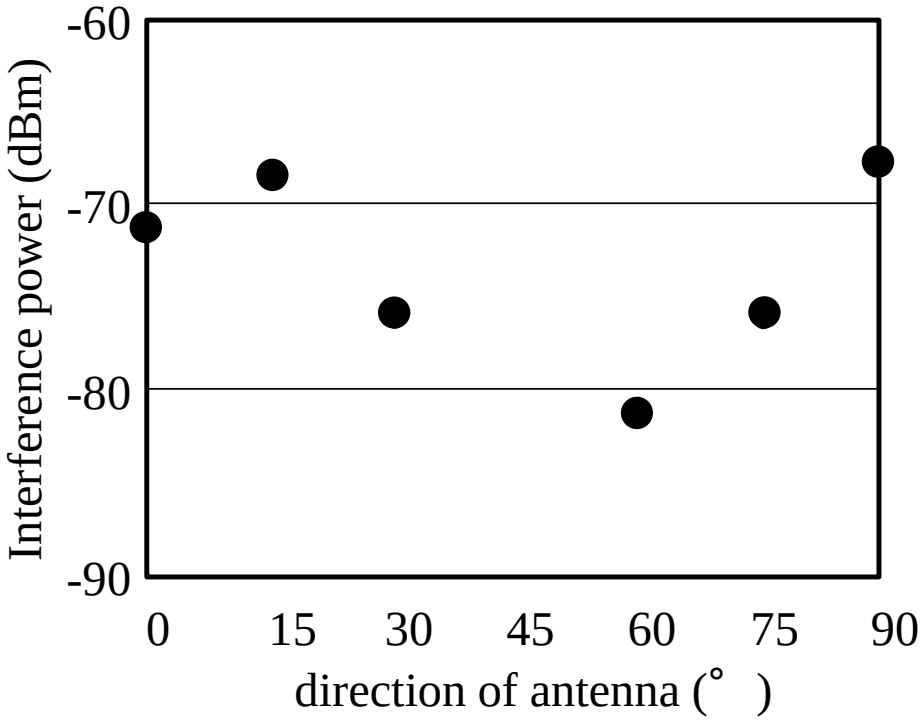

Figure 3-8. Interference power level with the variation of antenna position of Rx when both links use V polarization waves.

3-4 Transmission Characteristics of V and H polarization

As shown in Fig. 3-4, the use of cross-polarized waves is effective for reducing the distance between parallel wireless links. However, the rain attenuation of V polarization waves and H polarization waves is different. It is well known that the nonspherical shape of raindrops causes radio-wave propagation effects in rain to be polarization-dependent at microwave and MMW frequencies [2]. These differences in transmission characteristics affect the data transmission characteristics of H and V polarization 120-GHz-band wireless link. Several studies on the rain attenuation and availability of millimeter-wave wireless links have been reported [3-5]. At a frequency region of over 100 GHz, Utsunomiya et al. had conducted propagation experiments at 103 GHz [5]. However, the dependence of the rain attenuation characteristics of 120-GHz-band MMW signals on the polarization has not been evaluated. Therefore, we compared the transmission characteristics of V and H polarization waves.

ITU-R recommendation P.838-3 [6] defines the specific rain attenuation factor γ as

$$\gamma = k R^{\alpha} \ \text{(dB/km)} \qquad (1)$$

where R is the rain rate, and k and α are functions of frequency, drop-size distribution, rain temperature, and polarization of MMW signal. Table 3-1 shows the parameters (k, α) at 120 GHz described in the ITU-R recommendation P.838-3, the specific rain attenuation factors for V and H polarization waves calculated using the Eq.(1)and Table 3-1 are almost the same, 49.5 and 50.1 dB/km at a rain rate of 200 mm/hr, respectively.

We measured the rain attenuation characteristics of V and H polarization waves for 120-GHz-band MMW signals. The transmission distance was 1 km and the distance between Txs and Rxs was ($D_T = D_R$) 0.8 m.

Figure 3-9 shows the time dependence of the one-minute rain rate and 120-GHz-band signal attenuation due to the rain. During the experiment, the highest rain intensity was 11 mm/hr and the highest rain attenuation was about 10 dB. The rain attenuation of V and H polarization waves increases as the rain intensity increases, and no obvious difference between

the V and H polarization waves is observed.

Figure 3-9 shows the time dependence of the one-minute rain rate and 120-GHz-band signal attenuation due to the rain. During the experiment, the highest rain intensity was 11 mm/hr and the highest rain attenuation was about 10 dB. The rain attenuation of V and H polarization waves increases as the rain intensity increases, and no obvious difference between the V and H polarization waves is observed.

Figure 3-10 shows the relationship between the rain intensity and rain attenuation of V and H polarization waves. The experimental rain attenuation values are obtained by averaging the rain attenuation values in the same rain intensity condition. The theoretical values calculated by the Eq. (1) are also shown. The rain attenuation of V and H polarization waves is almost the same at the same rain intensity. Moreover, the experimental results coincide with the theoretical values in substance. Figure 3-11 shows the correlation of rain attenuation between V and H polarization waves. The rain attenuation of V and H polarization waves is almost the same in the same rain condition.

These results indicate that the rain attenuation characteristics between V and H polarization waves are almost the same when rain intensity is below 10 mm/hr.

Table 3-1 Parameters (k, α) at 120 GHz described in ITU-R recommendation P.838-3.

Frequency	k_H	α_H	k_V	α_V
120 GHz	1.4866	0.6640	1.4911	0.6609

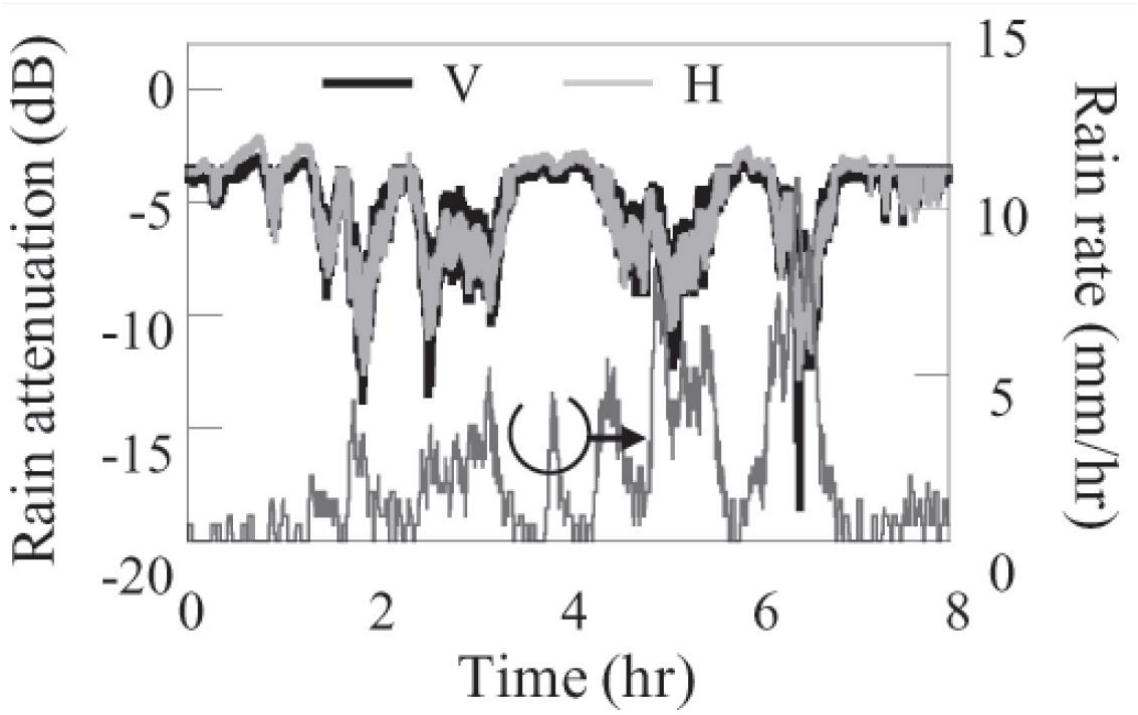

Figure 3-9. Rain attenuation of V and H polarization waves. The transmission distance is 1.0 km.

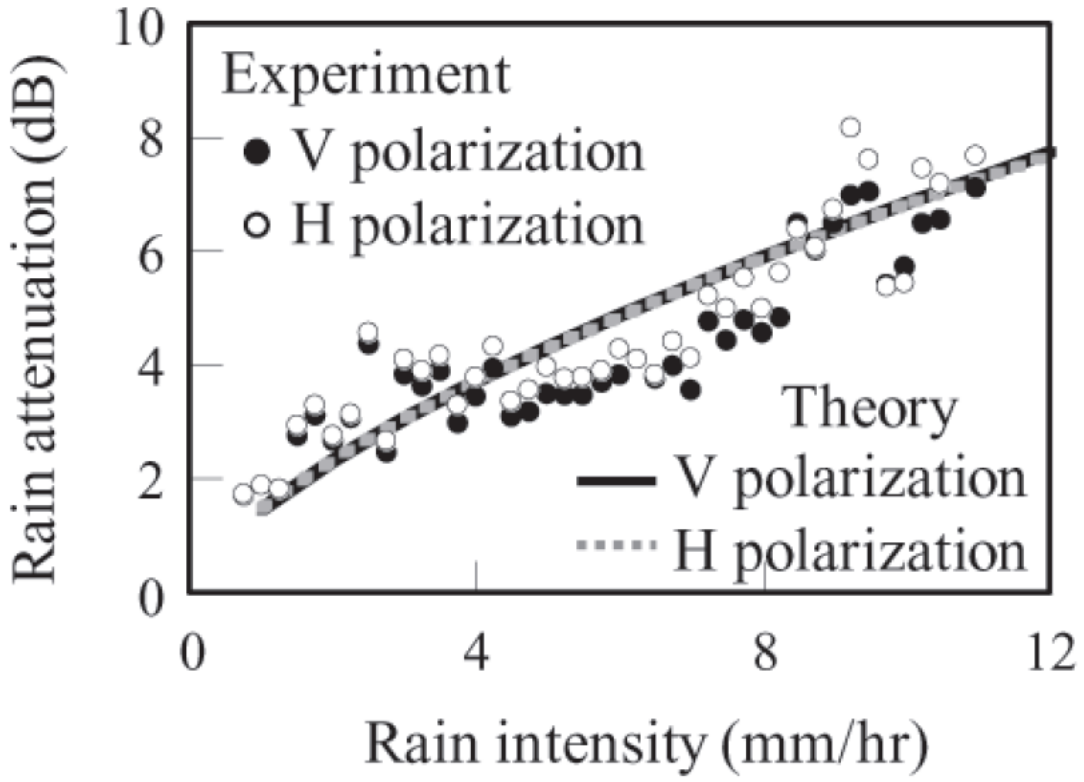

Figure 3-10. Relationship between rain attenuation and rain intensity. The theoretical values calculated using ITU-R recommendation P.838-3 are also shown.

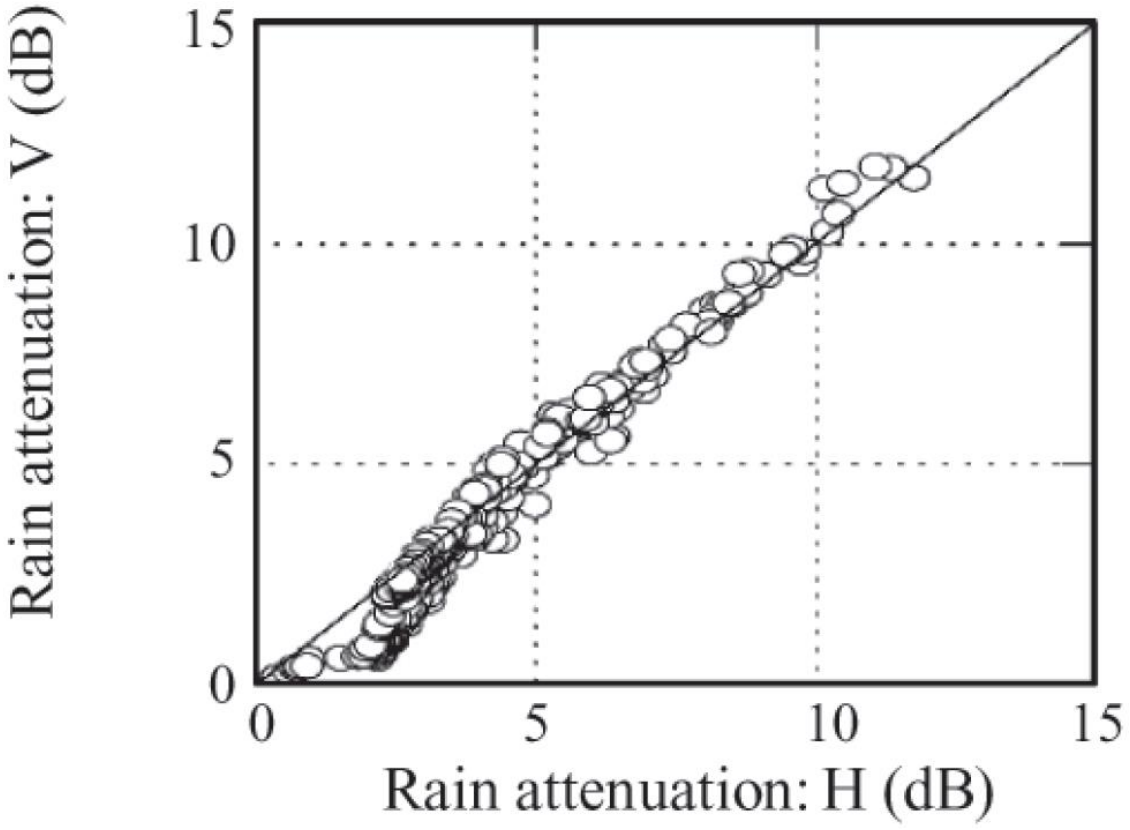

Figure 3-11. Correlation between the rain attenuation of V and H polarization waves.

3-5 Data Transmission Characteristics

First, we measured the unidirectional 2ch data transmission characteristics of the wireless links using polarization multiplexing. The configuration of the transmission experiment is shown in Fig. 3-12. Table 3-2 shows the received power and BER of the parallel links for unidirectional 2ch data transmission. The transmission data was PRBS data with a rate of 10.3 Gbps. The received power was about -34 dBm for both links. When FEC was not used, the BER of the wireless link using V polarization was below 10^{-12}, and that using H polarization was 3×10^{-7}. We suppose that the difference in the BER characteristics between the two wireless links arises from the

side-lobe pattern of the antennas the two wireless links used. These results indicate that we can obtain a BER below 10^{-12} even when two wireless links are set within 1 m of each other, when FEC and polarization multiplexing are used for each wireless link.

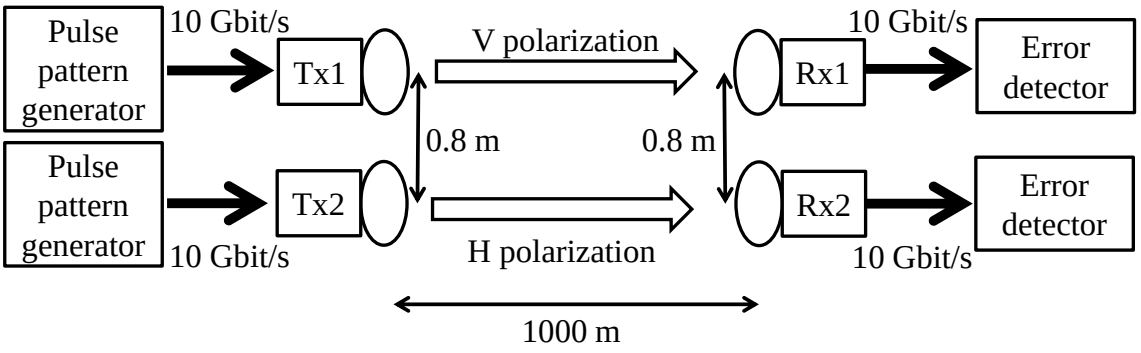

Figure 3-12. Configuration for outdoor unidirectional 2 ch data transmission experiment.

Table 3-2 Received power and BER of 120-GHz-band wireless links using polarization multiplexing for unidirectional 2ch data transmission. The transmission distance is 1 km and the distance between the two parallel wireless links is 0.8 m.

Polarization	Received power (dBm)	w/o FEC	With FEC
V	-34	$< 10^{-12}$	$< 10^{-12}$
H	-34	3×10^{-7}	$< 10^{-12}$

Next, we measured the bidirectional data transmission characteristics of the wireless links using same polarization. The configuration of the transmission experiment is shown in Fig. 3-13. In Fig. 3-13, there is a windowpane between Txs and Rxs because Rx1 and Tx2 were set inside the building and windowpane was not able to be opened. The attenuation by the windowpane is about 10 dB.

Table 3-3 shows the received power and BER of the parallel links for bidirectional data transmission. The transmission data was PRBS data with a rate of 10.3 Gbps. The received power was about -29 dBm for both links. When FEC was not used, the BER of both wireless links were 10^{-12}. These results indicate that we can obtain a BER below 10^{-12} even when two wireless links are set within 1 m of each other, when polarization multiplexing are not used for each wireless link.

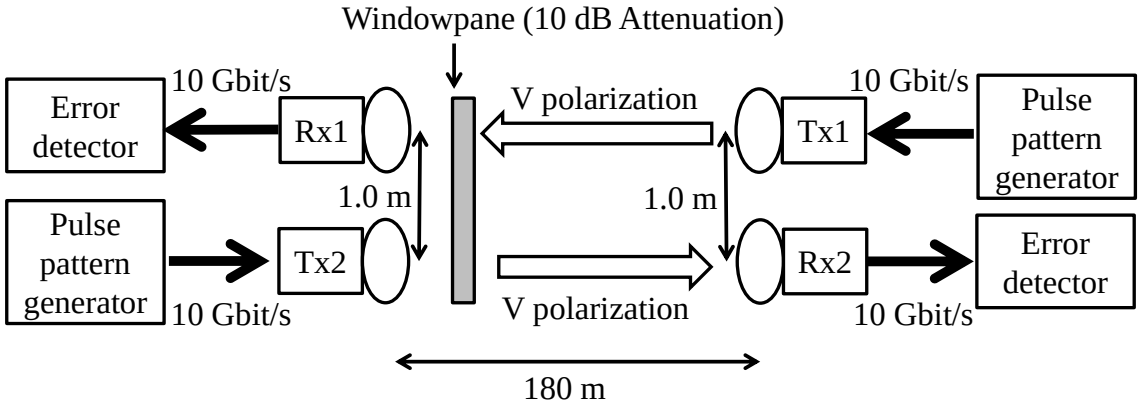

Figure 3-13. Configuration for outdoor bidirectional data transmission experiment.

Table 3-3 Received power and BER of 120-GHz-band wireless links using same polarization for bidirectional data transmission. The transmission distance is 180 m and the distance between the two parallel wireless links is 0.8 m.

Polarization	Received power (dBm)	w/o FEC	With FEC
V	-29	$< 10^{-12}$	$< 10^{-12}$
H	-29	$< 10^{-12}$	$< 10^{-12}$

3-6 Conclusion of Chapter 3

We first measured radiation pattern of Cassegrain antenna at 125 GHz. Typical antenna gain was about 49 dBi, and the half-power beamwidth was about 0.4 degree. Next, we measured interference power level for evaluation of XPI and isolation between parallel links. Measured XPI was 29 dB when distance between parallel links is set 2 m. Measured isolation between parallel links was 85 dB when distance between parallel links is set 1 m. Measured XPI and isolation between parallel links were high enough for our requirement explained in Chapter 2. Then, we measured transmission characteristics of V and H polarizations at outdoor circumstance. The measurement results show that the rain attenuation of V- and H-polarization is almost the same. Finally, we measured data transmission characteristics of polarization multiplexing by two Cassegrain antennas. We succeeded bidirectional 10 Gbps and unidirectional 2 ch 20 Gbps full duplex data transmission with BER below 10^{-12}. These results indicate that use of two pairs of Cassegrain antennas for space and polarization multiplexing is effective for frequency reuse in the 120-GHz-band wireless link system.

References in Chapter 3

[1] ELVA-1 Corp. homepage [Online]. Available:

http://www.elva-1.com/

[2] M. Thurai, V.N. Bringi, and A. Rocha, "Specific attenuation and depolarisation in rain from 2-dimensional video disdrometer data," IET Microwaves, Antennas & Propagation, vol.1, pp.373-380, 2007.

[3] R.L. Olsen, D.V. Rogers, and D.B. Hodge, "The aR^b relation in the calculation of rain attenuation," IEEE Trans. Antennas Propag., vol.AP-26, no.2,pp.318-329, 1978.

[4] G. Liu, J.T. Ong, E. Choo, and C.G. Teo, "Techniques to separate wet radome loss from measured rain attenuation data during rain events," Electron. Lett., vol.36, no.10, pp.904-905, 2000.

[5] T. Utsunomiya and M. Sekine, "Rain attenuation at 103 GHz in millimeter wave ranges," Int. J. Infrared and Millimeter Waves, vol.26, no.11, pp.1651-1660, 2005.

[6] Rec. ITU-R P.837-3 "Specific attenuation model for rain for use in prediction methods," ITU, 2005, Geneva, Switzerland.

Chapter 4
Polarization Multiplexing by Two Pairs of Plate-laminated Corporate-feed Waveguide Slot Array Antennas

Chapter 4 describes polarization multiplexing by two plate-laminated corporate-feed waveguide slot array antennas. The slot array antenna has been developed by author's research group [1-2]. Figure 4-1 shows the configuration of a 120-GHz-band planar slot array antenna. The antenna is made by diffusion bonding of copper laminated planes patterned by etching. Etching patterns in the laminated plates can provide high precision, and the diffusion bonding can provide perfect electrical contacts among the plates even at such higher frequencies. There are 16x16 radiating slots on the top layer fed by a corporate feeding network on the bottom layer. The total size of the 16x16-element array is 33.6 mm x 33.6 mm and the total thickness is only 1.6 mm. The thin structure of slot array antennas is suitable for two pairs of antennas configuration because the size of configuration becomes much smaller than size of using two Cassegrain antennas. We have succeeded in 10-Gbps data transmission over the 120-GH-band wireless link using them. Moreover, it has been shown that the planar slot array antenna is suitable for polarization multiplexing at 26-GHz-band wireless link [3].

We first measured radiation pattern of slot array antenna. The radiation pattern is important factor for two pairs of antennas arrangement because radiation patterns affect for XPI and isolation between parallel links. Next, we measured XPI and Iop. Finally, we measured data transmission characteristics of polarization multiplexing by two slot array antennas.

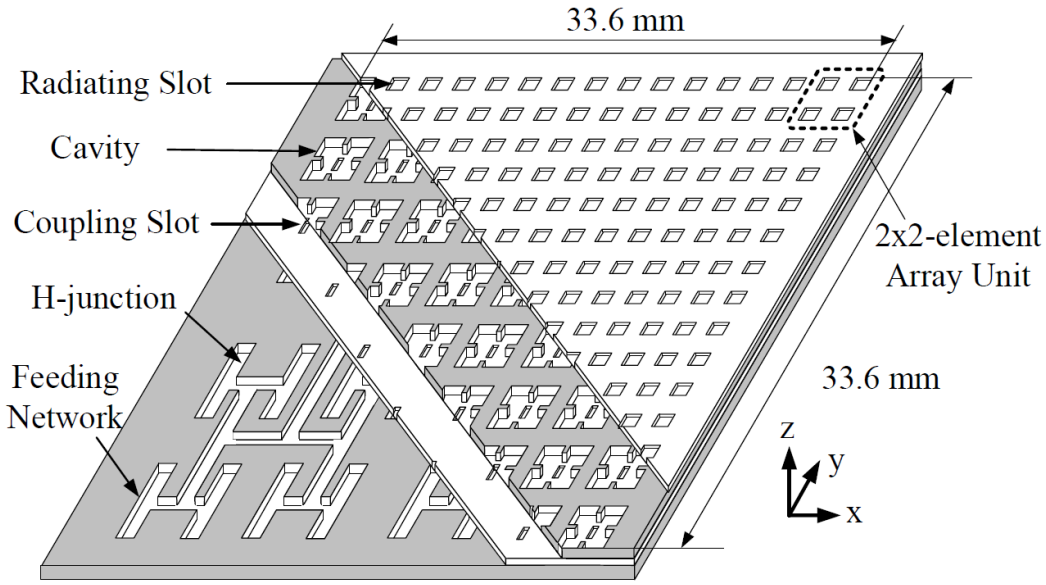

Figure 4-1 120-GHz-band plate-laminated corporate-feed waveguide slot array antennas. The measurement frequency is 125 GHz.

4-1 Radiation pattern of the plate-laminated corporate-feed waveguide slot array antennas

We first measured the vertical (E-plane)- and horizontal (H-plane)-radiation pattern of the antenna shown in Figure 4-2. The measurement frequency was 125 GHz. Typical antenna gain is about 32 dBi, and the half-power beamwidth is 3.5 degree.

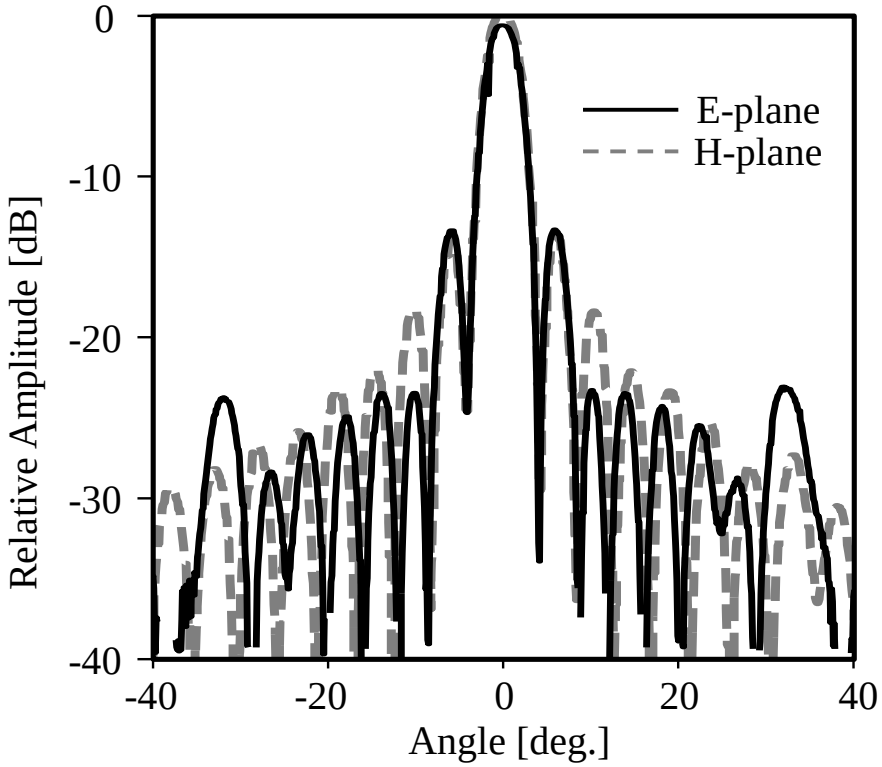

Figure 4-2. Measured radiation pattern of the 120-GHz-band plate-laminated corporate-feed waveguide slot array antennas. The measurement frequency is 125 GHz.

4-2 Evaluation of XPI for unidirectional 2 ch data transmission

We evaluated the XPI (cross-polarization isolation) of the antenna by using an F-band vector network analyzer. Figure 4-3 shows a schematic of the measurement setup. The XPI was calculated by the S21 difference of co-polarization and cross-polarization.

The measured XPI is shown in Fig. 4-4. The XPI is about 40 dB at 100-130 GHz, and it is over 32 dB above 130 GHz. With ASK modulation and an envelope detection scheme, the required carrier-to-noise (C/N) ratio is over 20 dB for a BER of below 10^{-12}. Therefore, the XPI value necessary for BER of below 10^{-12} for unidirectional 2-ch data transmission is over 20 dB. These results indicate that the planar slot array antenna can be employed for

unidirectional 2-ch data transmission using polarization multiplexing.

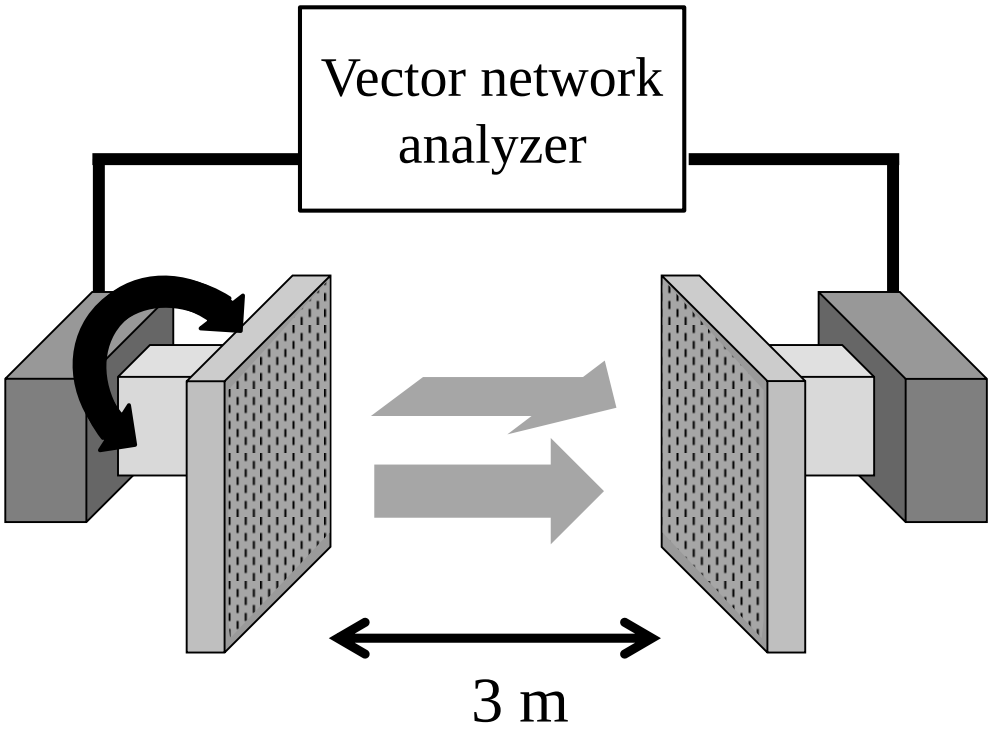

Figure 4-3. Schematic of the XPI measurement between two planar slot array antennas.

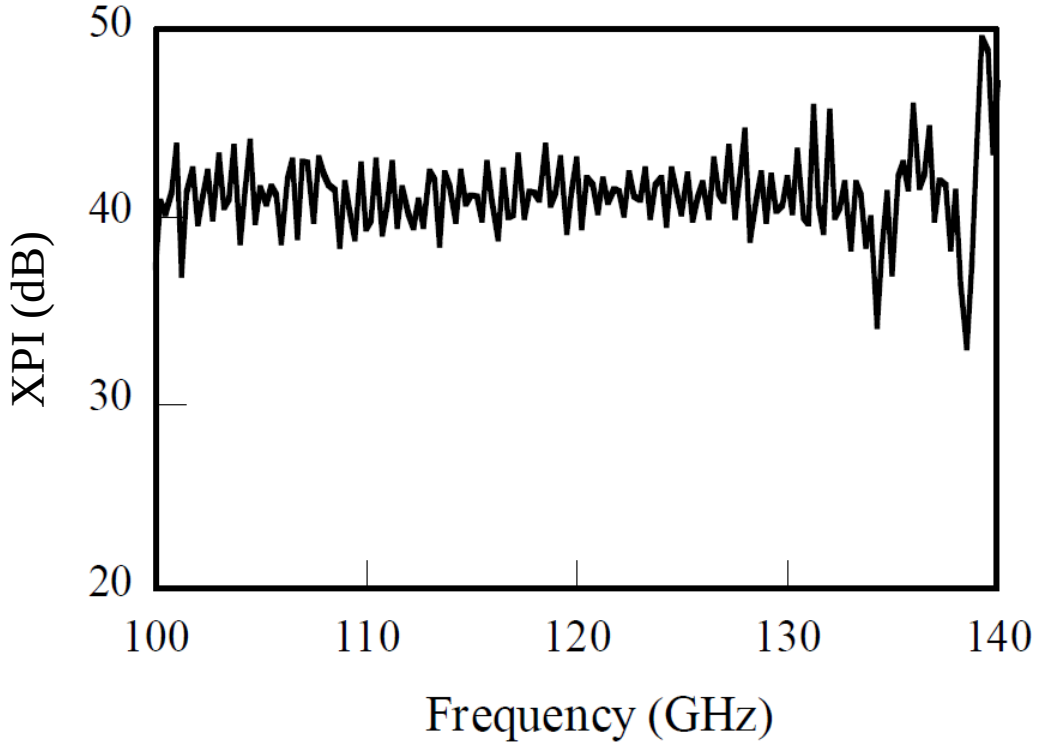

Figure 4-4. XPI of the planar slot array antenna.

4-3 Evaluation of isolation for bidirectional data transmission

We evaluated the isolation of two planar slot array antennas adjoined to each other. Figure 4-5 shows a schematic of the experiment. We arranged two planar slot array antennas, each of which is connected to the F-band vector network analyzer. In this experiment, the slot directions of the two antennas were the same polarization, and in the second one, the slots were orthogonally arranged (cross pol.). For the same polarization, there are two types of slot direction (same pol. 1 and same pol. 2). The schematics of the slot directions in cross pol., same pol. 1, and same pol. 2 are shown in Fig.

4-6.

Figure 4-7 shows the experimental results for the isolation, when 16 x 16 element planar slot array antennas were used. In this case, S21 corresponds to the isolation between two channels used for bidirectional communications. For same pol.2, isolation varies from -50 to -70 dB at 115-135 GHz, which is the occupied frequency band of our 120-GHz-band wireless link. When antennas are orthogonally arranged, S21 is below -70 dB at 115-135 GHz. The isolation in cross polarization (cross pol.) is higher than that in same polarization. When we compare the isolation between the same polarization arrangements, we find that that of same pol. 1 is much worse than that of same pol. 2. Figure 4-8 shows simulated E-field patterns of slot array antennas. The coupling between the slots placed with facing each side of the long sides of the rectangular waveguide (left side picture (a) of Figure 4-8) is stronger than that between those placed with facing each side of the short sides of the rectangular waveguide (right side picture (b) of Figure 4-8), because magnitude of E-field is strong at the center of the long sides of the rectangular waveguide and magnitude of E-field is weak at the end of the long sides of the rectangular waveguide. Transmission characteristic (S21) between each slot array antennas of picture (a) in Figure 4-8 is -16.5 dB, and that of picture (b) in Figure 4-8 is -31 dB.

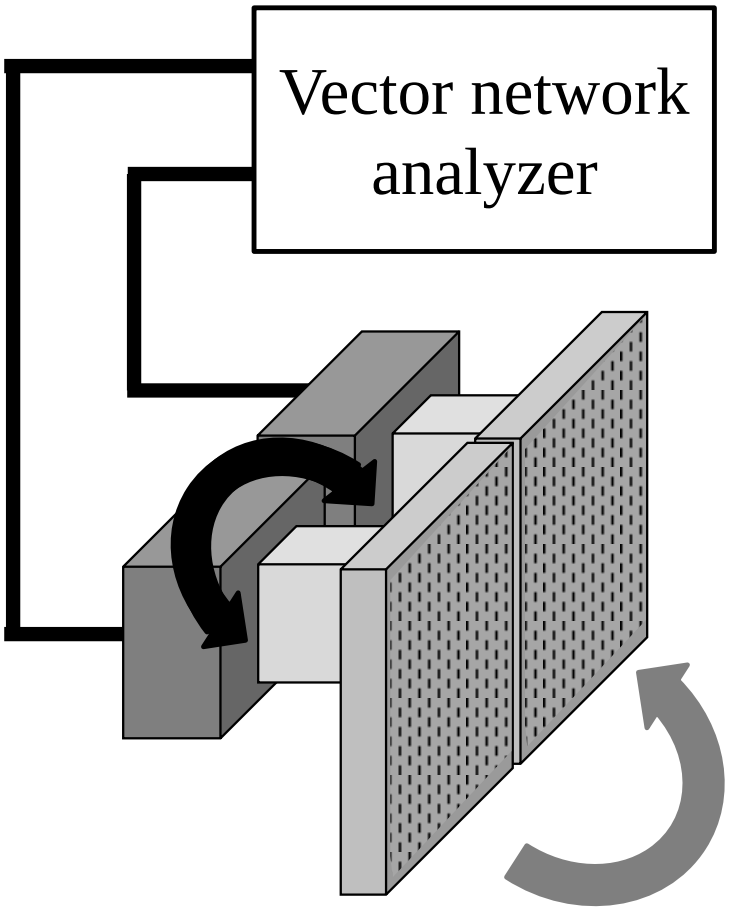

Figure 4-5. Schematic of the isolation measurement between two planar slot array antennas.

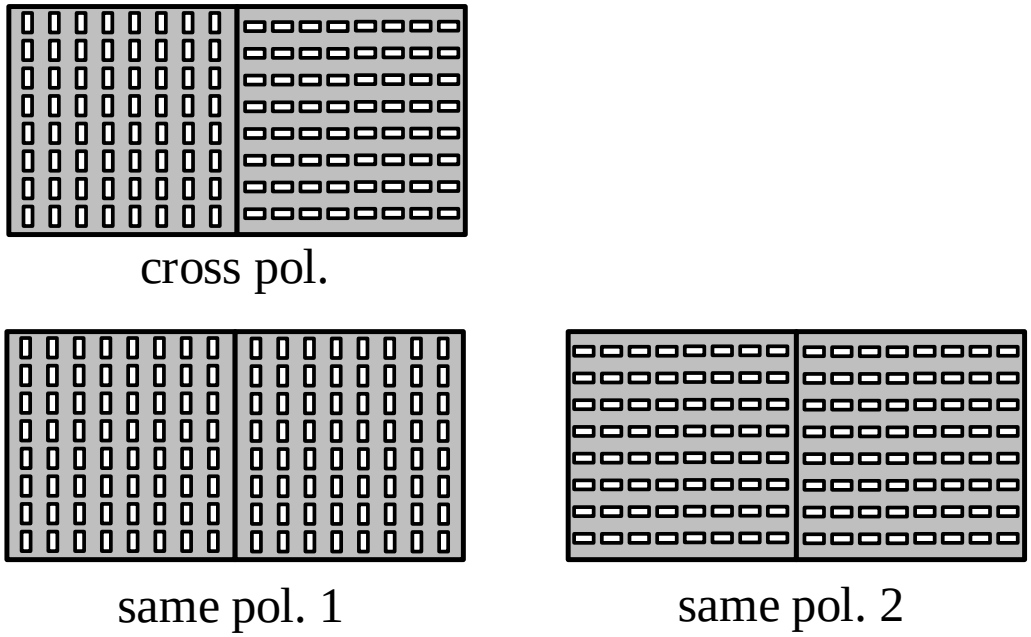

Figure 4-6. Schematics of the slot directions in cross pol., same pol. 1, and same pol. 2.

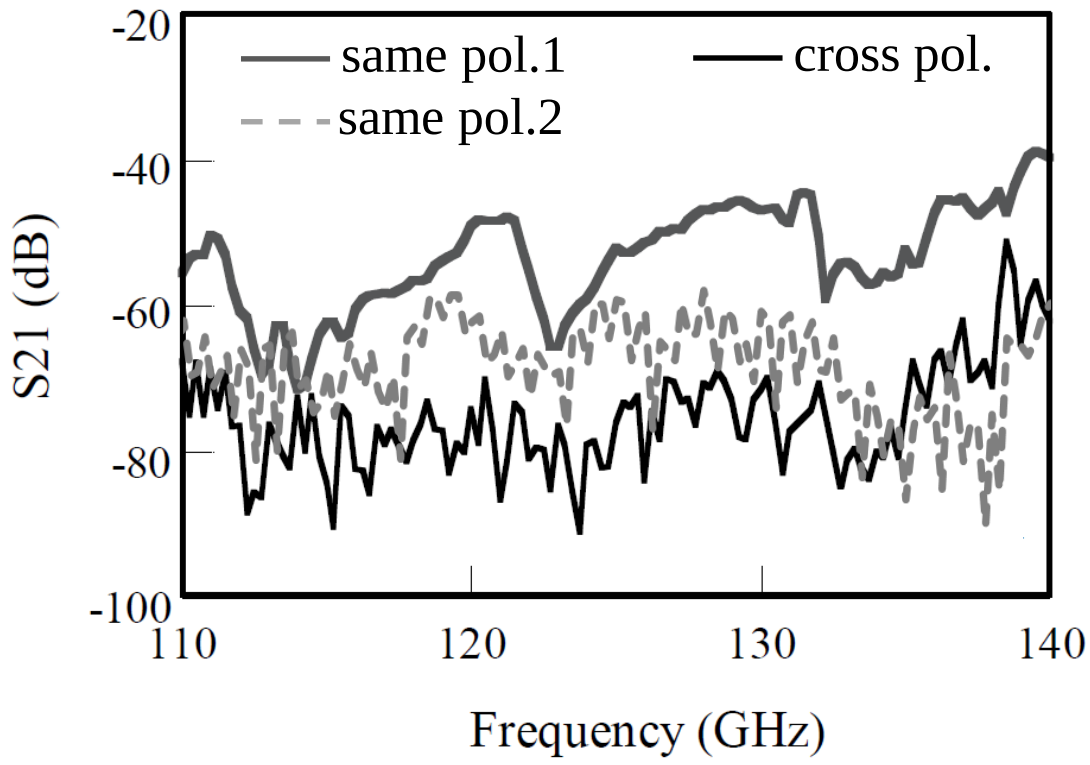

Figure 4-7. Isolation of two planar slot array antennas adjoined to each other.

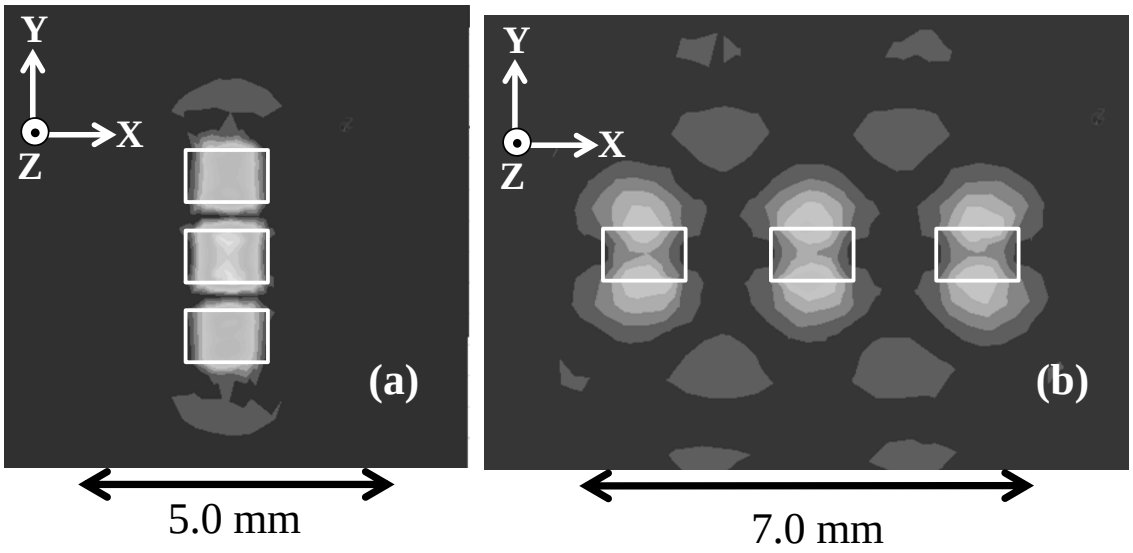

Figure 4-8. Simulated E-field patterns of slot array antennas.

4-4 Data Transmission Characteristics

First, we evaluated the BER characteristics of the dual channel unidirectional 120-GHz-band wireless links. Figure 4-9 shows the experimental setup. Two planar antennas were arranged orthogonally, and one link used V-polarization waves and the other one uses H-polarization waves. The two planar antennas were connected to receivers (Rxs), and two horn antennas are used at the transmitter (Tx) side. Details of the Tx and Rx are shown in Ref. 4. Waveguide variable attenuators (ATTs.) were used between the planar antennas and Rxs in order to adjust the power input into the Rxs. For the data signal, we used a 2^{23}-1 pseudo-random pattern bit stream (PRBS) data at 10.3125 Gbps. We evaluated the BER characteristics of the V-polarization link (Tx2-Rx2) when the H-polarization link (Tx1-Rx1) was ON or OFF. In this case, the received power of Rx2 from Tx1 becomes the interference power for V-polarization link.
The measurement results are shown in Fig. 4-10. The BER characteristics of the V link are almost the same and no deterioration has been observed when the H-polarization link is ON. These results indicate that the dual channel unidirectional wireless links using the planar slot array antennas can achieve sufficient isolation when two planar slot array antennas are orthogonally arranged.

Next, the BER characteristics of dual-channel bidirectional 120-GHz-band wireless links were evaluated. The experimental setup is shown in Fig. 4-11. The transmitted data signal was 2^{23}-1 pseudo-random pattern bit stream (PRBS) data at 10.3125 Gbps. In this experiment, one planar slot array antenna was connected to Tx1, and the other slot array antenna was connected to Rx2. Tx2 using horn antenna was installed facing the planar slot array antenna to which Rx2 was connected. In this case, the received power of Rx2 from Tx1 becomes the interference power for V-polarization link. Figure 4-12 shows the BER characteristics of the first wireless link that consists of Tx2 with the horn antenna and Rx2 connected to the planar slot array antenna. When the two links are set to same pol. 2 shown in Fig. 4-6, the BER characteristics deteriorate when the Tx1 connected with the planar

slot array antenna is ON. The received power necessary for BER of below 10^{-12} increases by 2.5 dB. When the second wireless link (Tx2-Rx2) is set to H polarization, no deterioration of BER characteristics is observed. These results coincide with the investigations shown in Sec. 4-3 based on the results shown in Fig. 4-7.

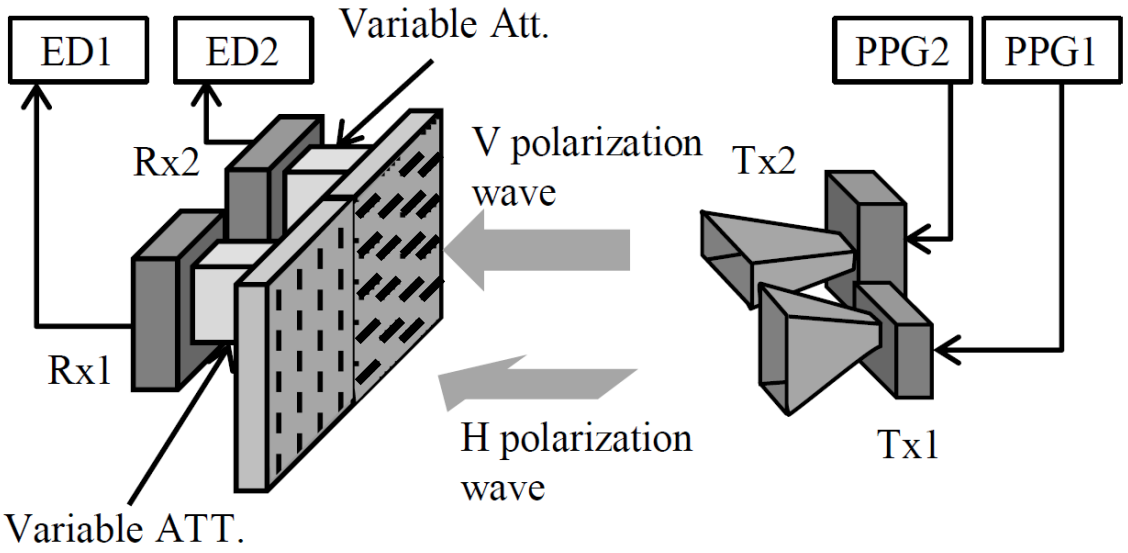

Figure 4-9. Experimental setup for dual-channel unidirectional data transmission.

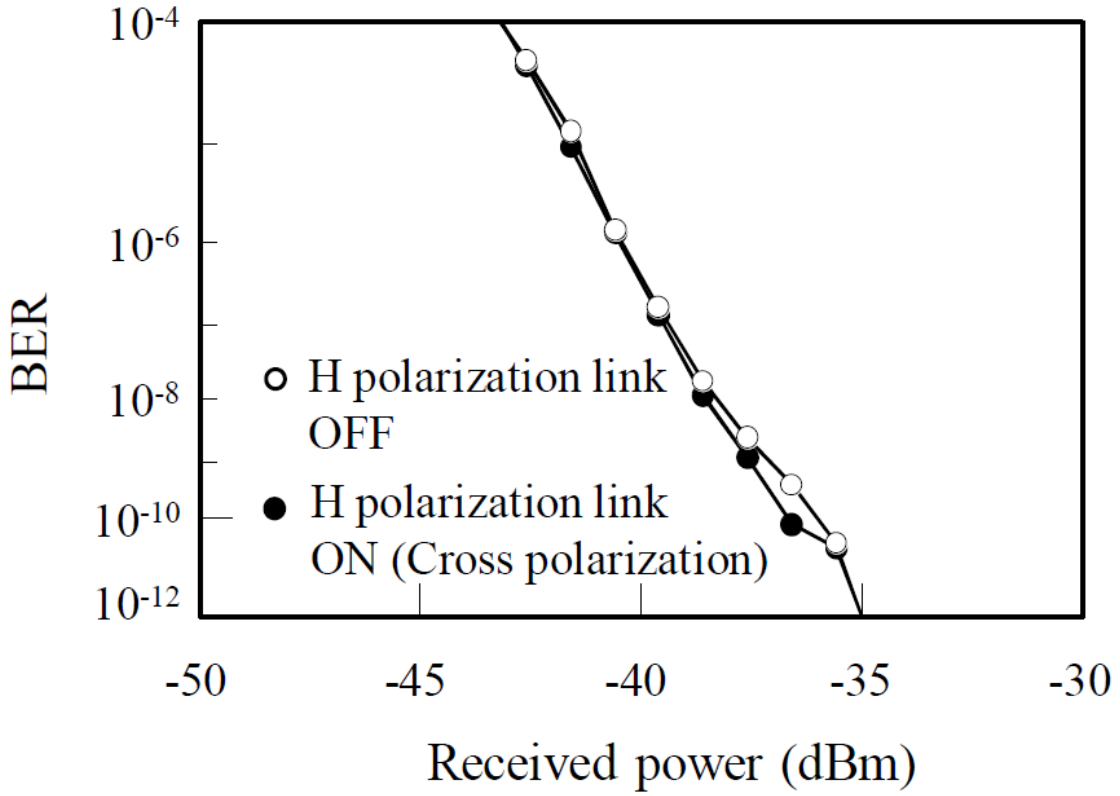

Figure 4-10. BER characteristics of V polarization link when H polarization link is ON or OFF. Data rate is 10.3125 Gbps.

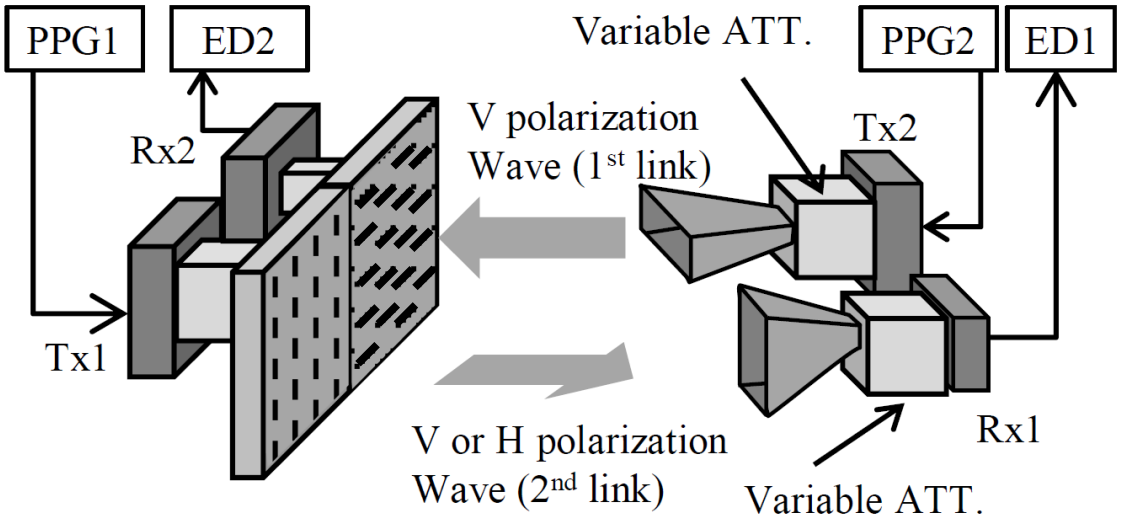

Figure 4-11. Experimental setup for dual-channel bidirectional data transmission.

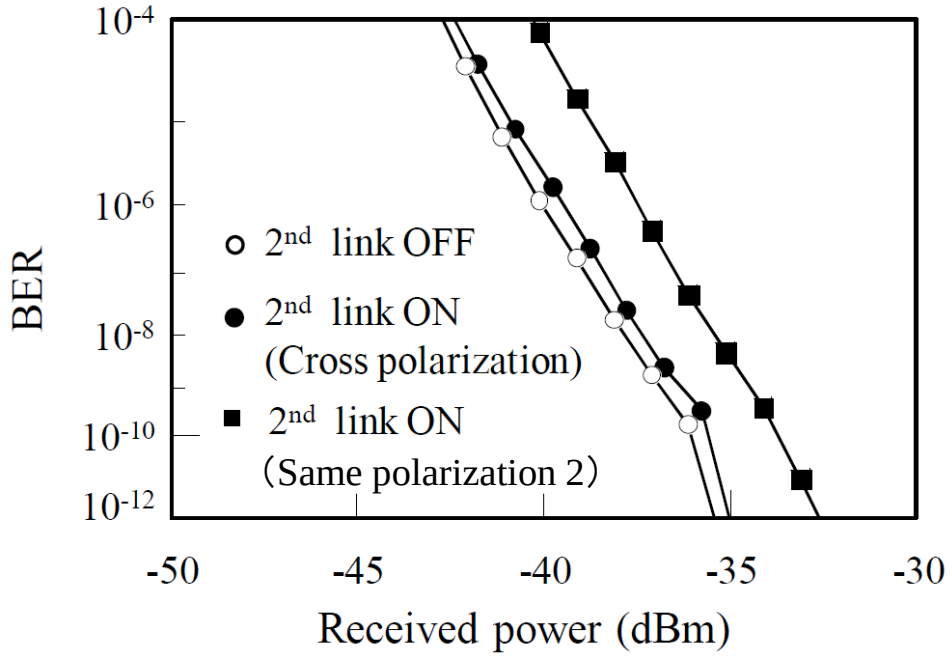

Figure 4-12. BER characteristics of the first wireless link (Tx2-Rx2) when second wireless link (Tx1-Rx1) is ON or OFF. Data rate is 10.3125 Gbps.

4-5 Conclusion of Chapter 4

We first measured radiation pattern of slot array antenna at 125 GHz. Typical antenna gain was about 32 dBi, and the half-power beamwidth was about 3.5 degree. Next, we measured XPI and Iop. Measured XPI was about 40 dB. Measured Iop was about 70 dB. Measured XPI and Iop were high enough for our requirement explained in Chapter 2. Finally, we measured data transmission characteristics of polarization multiplexing by two slot array antennas. We succeeded bidirectional 10 Gbps and unidirectional 2 ch 20 Gbps full duplex data transmission with BER below 10^{-12}. These results indicate that use of two slot array antennas for space and polarization multiplexing is also effective for frequency reuse in the 120-GHz-band wireless link system. Moreover, the thin structure of slot array antennas is suitable for two pairs of antennas configuration because the size of configuration becomes much smaller than size of using two Cassegrain antennas.

References in Chapter 4

[1] D. Kim, J. Hirokawa, M. Ando, J. Takeuchi, and A. Hirata、 “64x64-element and 32x32-element slot　array antennas using double-layer hollow-waveguide corporate-feed in the 120 GHz band,”　IEEE Trans. Antennas Propagation., vol.62, no.3, pp.1507-1512, March, 2014.

[2]D. Kim, J. Hirokawa, M. Ando, and T. Nagatsuma, “Design and fabrication of a corporate-feed plate-laminated waveguide slot array antenna for 120GHz-band,” IEEE APSURSI, 2011, pp. 3044 – 3047.

[3]Y. Tsunemitsu, K. Kojima, G. Yoshida, M. Nagayasu, G. Naohisa, J. Hirokawa, and M. Ando, “Orthogonally-Arranged Center-Feed Single-Layer Slotted Waveguide Array Antennas for Polarization Division Duplex,” European Conf. on Antennas and Propagation, pp. 1-5, 2007.

[4] A. Hirata, T. Kosugi, H. Takahashi, J. Takeuchi, H. Togo, M. Yaita, N. Kukutsu, K. Aihara, K. Murata, Y. Sato, T. Nagatsuma, and Y. Kado, “120-GHz-Band Wireless Link Technologies for Outdoor 10-Gbit/s Data Transmission, ” IEEE Transactions on Microwave Theory and Techniques, vol. 60, no. 3, pp. 881 - 895, March, 2012.

Chapter 5
Polarization multiplexing by Finline Orthomode Transducer

Chapter 5 describes polarization multiplexing by orthomode transducer. First, we designed and fabricated new OMT because there is no OMT which has sufficient Iop characteristics for our requirement explained in Chapter 2. Next, we made portable wireless equipment for polarization multiplexing data transmission experiments with OMT because the portable wireless equipment enables easy installation at any places. Finally, we measured data transmission characteristics of polarization multiplexing by the portable wireless equipment with OMT.

5-1 Introduction

As explained in Chapter 3 and 4, we have demonstrated unidirectional 2-ch data transmissions and bidirectional data transmission in the 120-GHz band using two orthogonally set antennas. Using two pairs of antennas easily doubles the spectral efficiency, but it makes the system large. The use of an orthomode transducer (OMT), which can divide and multiplex cross-polarized waves, enables polarization multiplexing with one antenna. OMTs are already used for satellite communications system [1] and radio astronomy [2]. An OMT is a waveguide-based component, and it is smaller than other quasi-optical components used for polarization multiplexing, such as Gaussian lens antennas with a wire grid. Using an OMT would therefore be one of the best ways to increase the spectral efficiency of the 120-GHz-band wireless link. However, OMTs for satellite communication system can double the spectral efficiency only for unidirectional 2-ch data transmission. For example, the required value of XPI for Ku-band satellite communications is around 30 dB [3] and is possible. However, in bidirectional data transmission, strong output power from the uplink

transmitter must be suppressed to a level below the weak received power of the adjacent downlink receiver to meet the required C/N ratio. Thus, the required value of Iop for Ku-band satellite communications becomes around 85 dB [3], which is impossibly high for an OMT. As a result, an OMT cannot double the spectral efficiency for bidirectional data transmission of Ku-band satellite communications.

However, the required Iop for bidirectional data transmission of the 120-GHz-band wireless link is 60 dB, which is also high but possible (Details are described in section 5-2). There are many kinds of OMTs based on different polarization multiplexing methods. The turnstile OMT [4] and the Boifot OMT [5] are designed with a three-dimensional (3D) symmetrical structure to achieve high Iop in broad-band operations; however, fabrication of these devices is difficult because it requires 3D machining. For over 100 GHz, 3D machining with high precision is quite difficult. The septum OMT is designed with a simple asymmetrical structure for easy fabrication, but its Iop is low [6]. The finline OMT is designed for achieving both high Iop and easy fabrication [7-10]. The finline OMT has a pair of thin tapered metal fins that separate orthogonal polarizations, and its simple structure allows easier fabrication without 3D machining. But in some frequency regions, unwanted resonance excites the finline structure and decrease the Iop. To decrease the resonance, a resistive card must be attached to the edge of finline. The finline OMTs in Refs. 8 and 9 achieved an Iop of over 50 dB at frequencies of 11 and 7 GHz, respectively. However, to achieve high Iop for frequencies over 100 GHz, the device has to be precisely scaled down and fine processing of a small resistive card on the finline is needed, which increase the difficulty of fabrication. For easier fabrication, we have developed a 120-GHzband compact and high Iop finline OMT without using a resistive card [11-13]. In this Chapter, we present the detailed design of our finline OMT for our 120-GHz-band wireless link and a method for improving Iop.

5-2 The First Design and Fabrication of the New Finline OMT1

5-2-1 Design of the New Finline OMT1

Fig. 5-1 shows a schematic view of the conventional finline OMT reported by S. D. Robertson [7]. Such OMTs consist of a thin metallic fin set inside a square waveguide. The polarization mode, in which there is an electric field parallel to the fin, is converted from a waveguide mode into a finline mode whose energy is confined to the space between the fins. This energy can then be brought out by curving the fin and bringing the fin out from the wall of the waveguide, after which the energy is converted back into the waveguide mode by a gradual outward taper. The orthogonal polarization has an electric field perpendicular to the fin and passes unperturbed if the fin is sufficiently thin. In a certain frequency range, unwanted resonant modes are excited on the finline and this deteriorates Iop, XPI, and the group delay of transmitted signals. As shown in Ref. 7, the resonance is due to the excitation of a dominant mode on the finline. The dominant mode is reflected at both edges of the finline on the X-axis in Fig. 1, and resonance excites the finline structure when the length between the two edges becomes an integral number of half wavelengths. To suppress the unwanted resonant modes, conventional finline OMTs use a resistive card on the edge of the finline as shown in Fig. 1. The OMT shown in Ref. 8 achieved an Iop of over 50 dB at a frequency of 11 GHz. However, very high resistance is required for the resistive card to eliminate the unwanted resonant modes and achieve high Iop of more than 50 dB. Furthermore, for a 120-GHz-band OMT, the integration of a small resistive card on the finline complicates the fabrication process. Thus, we improved the design of the finline OMT to obtain high Iop and XPI without using a resistive card.

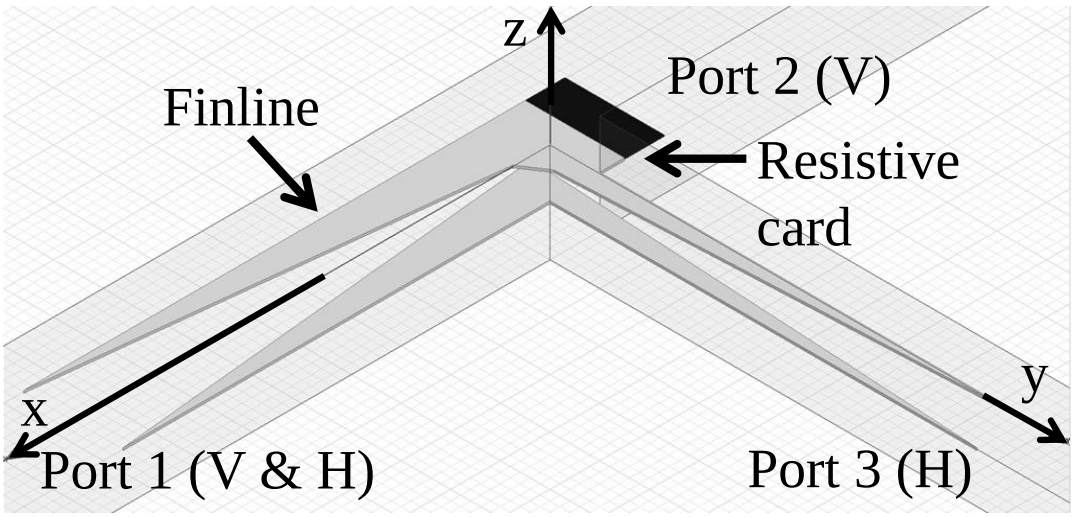

Figure 5-1. Schematic view of a conventional finline OMT.

Fig. 5-2 shows a schematic view of our newly designed finline OMT. Instead of using a resistive card, we suppress the resonance by reducing the length of the finline (La in Fig. 5-2). As explained above, the resonant frequency is related to the length between the two edges of the finline. In other words, the resonant frequency can be controlled by the length of the finline. Our length-reduced finline OMT is designed to expel unwanted resonance from the operation bandwidth of the 120-GHz-band wireless link. Reducing the finline length causes transmission loss of the horizontal waves because the horizontal waves propagate between the fins. Reducing the finline length also narrows the operation bandwidth of the OMT1-A conventional finline is designed for more than 30% or 70% of fractional bandwidth for use in radio astronomy.

Since our purpose is to make an OMT for our 120-GHzband wireless link, whose fractional bandwidth is less than 14%, our approach is sufficient for achieving high Iop within 116.5 to 133.5 GHz, which is the operation bandwidth of the link.

Fig. 5-3 shows the simulated S23 (Iop) of finline OMTs without a resistive card. In the conventional finline OMT, the finline length (La) is more than

five wavelengths of the operation frequency. Thus, we simulated the Iop with La of 12 mm (five wavelengths at 125 GHz). There are three peaks in the operation bandwidth of the 120-GHzband wireless link, and the Iop is deteriorated. These peaks are generated by the resonance on the finline.
When La is reduced to 1.42 mm, resonance appears at 114 and 137 GHz. As a result, there is no peak in the operation bandwidth of the 120-GHz-band wireless link. The simulated Iop (> 61 dB) is high enough for our purposes (> 50 dB). Fig. 6 shows the simulated S21, S31 (transmission loss) and S22, S33 (return loss) when La is 1.42 mm. The other lengths of finline OMT1 are as follows: Lb=1.67 mm, Lc=1.20 mm. Transmission losses are below 1 dB and return losses are over 13 dB from 116.5 to 133.5 GHz.

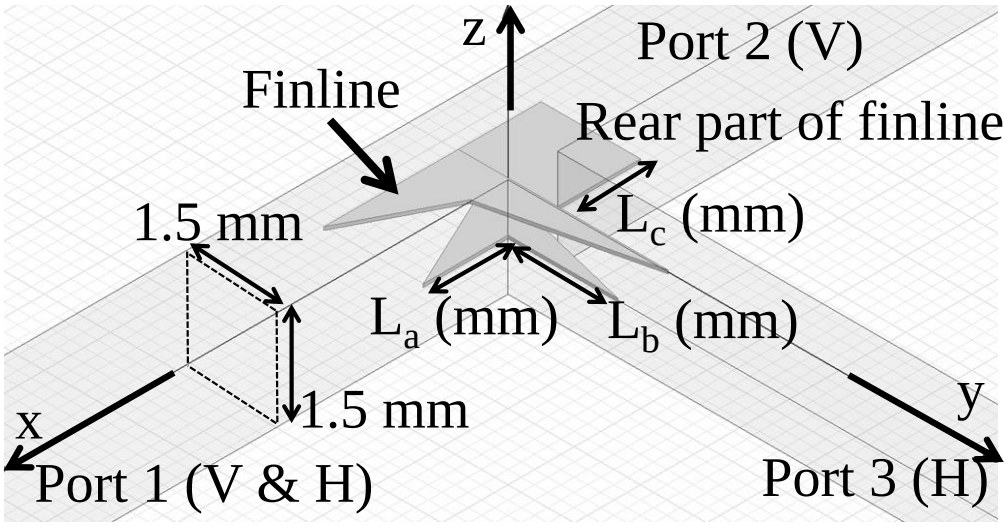

Figure 5-2　Schematic view of a new finline OMT.

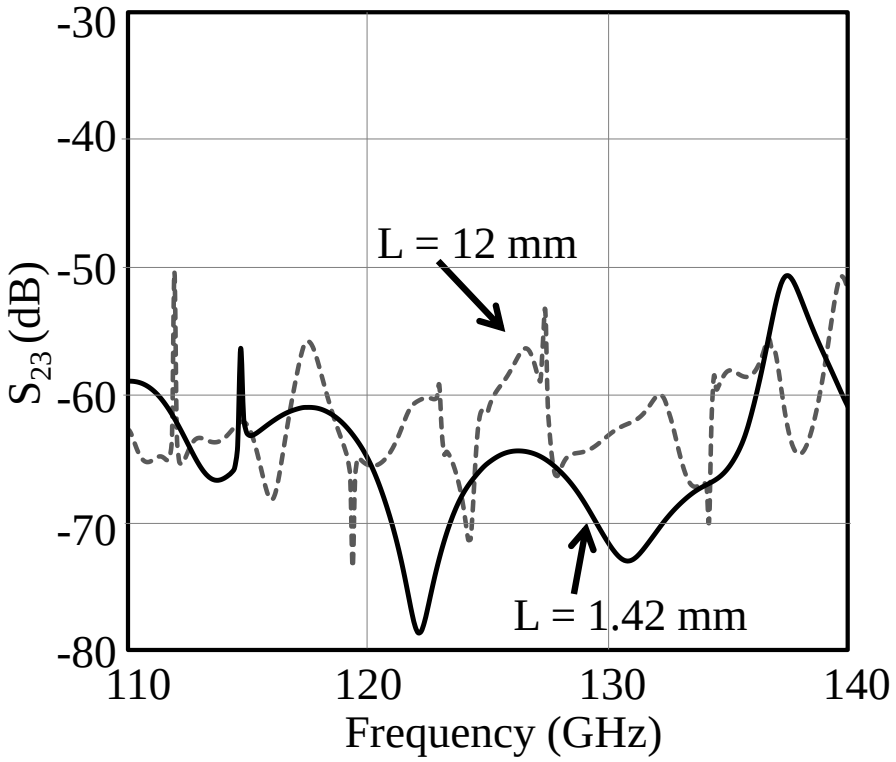

Figure 5-3 Simulated S_{23} (*Iop*) of a conventional (L=12 mm) and the new finline OMTs (L=1.42 mm) without a resistive card. The size of the port 1 waveguide is 1.5 mm × 1.5 mm.

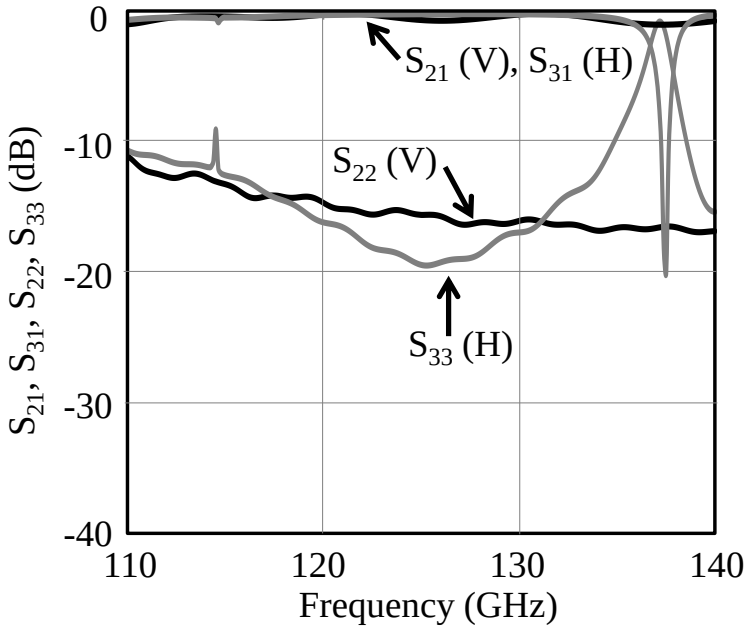

Figure 5-4 Simulated S_{21}, S_{31} (transmission loss) and S_{22}, S_{33} (return loss) of the new finline OMT1 (La = 1.42 mm). The size of the port 1 waveguide is 1.5 mm × 1.5 mm.

Next, we optimized the size of the square waveguide at port 1. Port 1 uses a square waveguide to handle both TE_{10} and TE_{01} basic modes for polarization multiplexing. However, higher-order modes TE_{11} and TM_{11}can also be excited at port 1 from 106 GHz if the size of the port 1 waveguide is 2 mm × 2 mm, which is the same value as the long sides of a standard F-band rectangular waveguide, and covers from 90 to 140 GHz. Fig. 5-5 shows basic modes and higher-order modes of the square waveguide, where the arrows denote electric field polarization.

As shown in Fig. 5-5, TE_{11} and TM_{11} have both vertical and horizontal electric waves and they deteriorate both the I_{op} and XPI. Fig. 5-6 shows the simulated propagation of horizontal waves inside a finline OMT1-at 125 GHz when the size of the waveguide is 2 mm × 2 mm square. In Fig. 5-6, there is leakage of millimeter-wave signal from port 3 to port 2. This leakage is caused by converted higher-order modes of the horizontal waves.

A square waveguide for data transmission should be designed so that port 1 allows only the basic modes of the operation bandwidth of the 120-GHz-band wireless link, and the basic modes should be used in a frequency band higher than the cutoff frequency of the basic modes to reduce group delay of signals. We therefore designed a smaller waveguide for port 1. Cutoff frequency f_c of a rectangular waveguide is expressed as

$$f_c = \frac{1}{2\sqrt{\varepsilon\mu}}\sqrt{\left(\frac{m}{a}\right)^2 + \left(\frac{n}{b}\right)^2} \quad (5\text{-}1)$$

where ε and μ denote the permittivity and permeability, a and b denote size of waveguide, and m and n denote the number of modes: (TE_{mn}, TM_{mn}). We finally decided to use a 1.5 mm × 1.5 mm square waveguide. The cutoff frequency f_c of TE_{10} and TE_{01} basic modes is 100 GHz, and that of TE_{11} and TM_{11} higher-order modes is 141 GHz. These characteristics are sufficient for meeting our requirements. Fig. 5-7 shows the simulated propagation of horizontal waves and vertical waves inside the finline OMT1-at 125 GHz for the waveguide. In Fig. 5-7 (a) and (b), there is no leakage between port 3 and port 2. These results indicate that the 1.5 mm × 1.5 mm square waveguide prevents the excitation of higher-order modes and suppresses leakage. In the simulations of the I_{op} and transmission and return losses (Figs. 5-3 and 5-4), we used 1.5 mm × 1.5 mm square waveguides for the same reason.

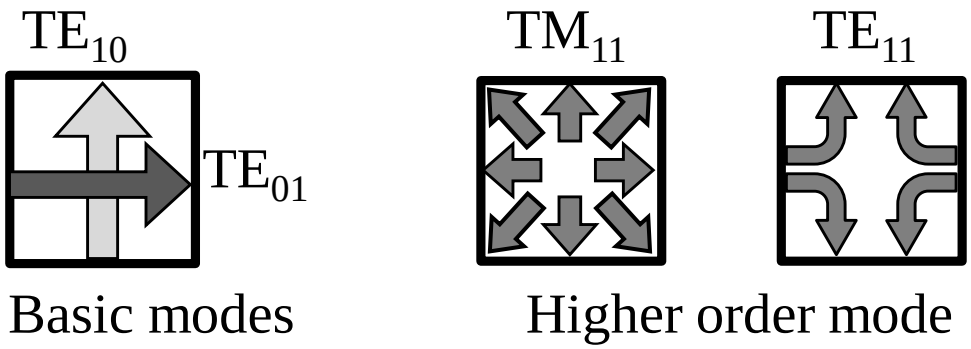

Figure. 5-5 Basic modes and higher-order modes of square waveguide, where the arrows denote electric field polarization.

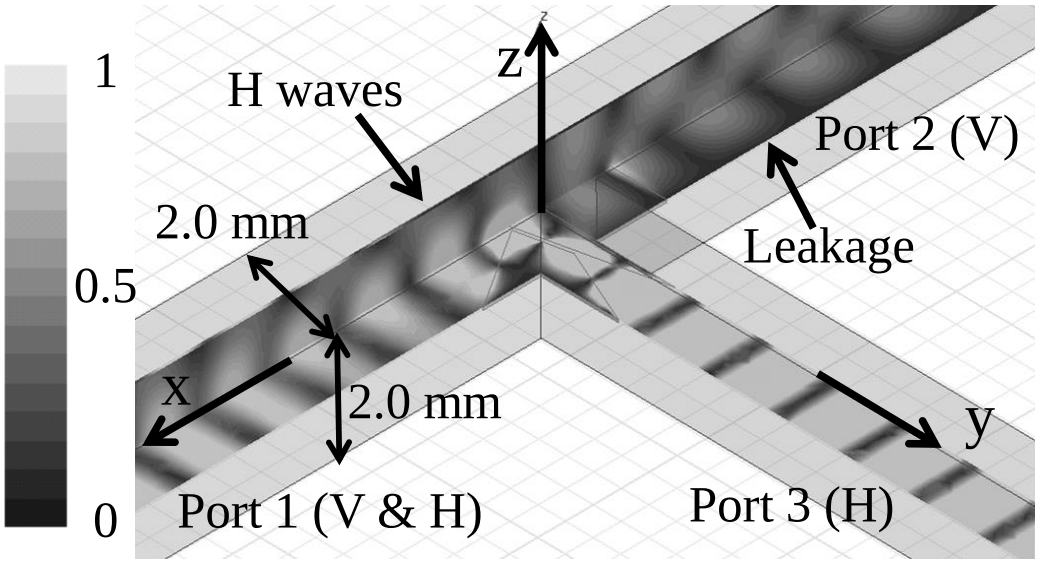

Figure. 5-6 Simulated propagation of horizontal waves inside a finline OMT1 whose waveguide is 2 mm × 2 mm square. E field scale is normalized with respect to the extreme values in each plot.

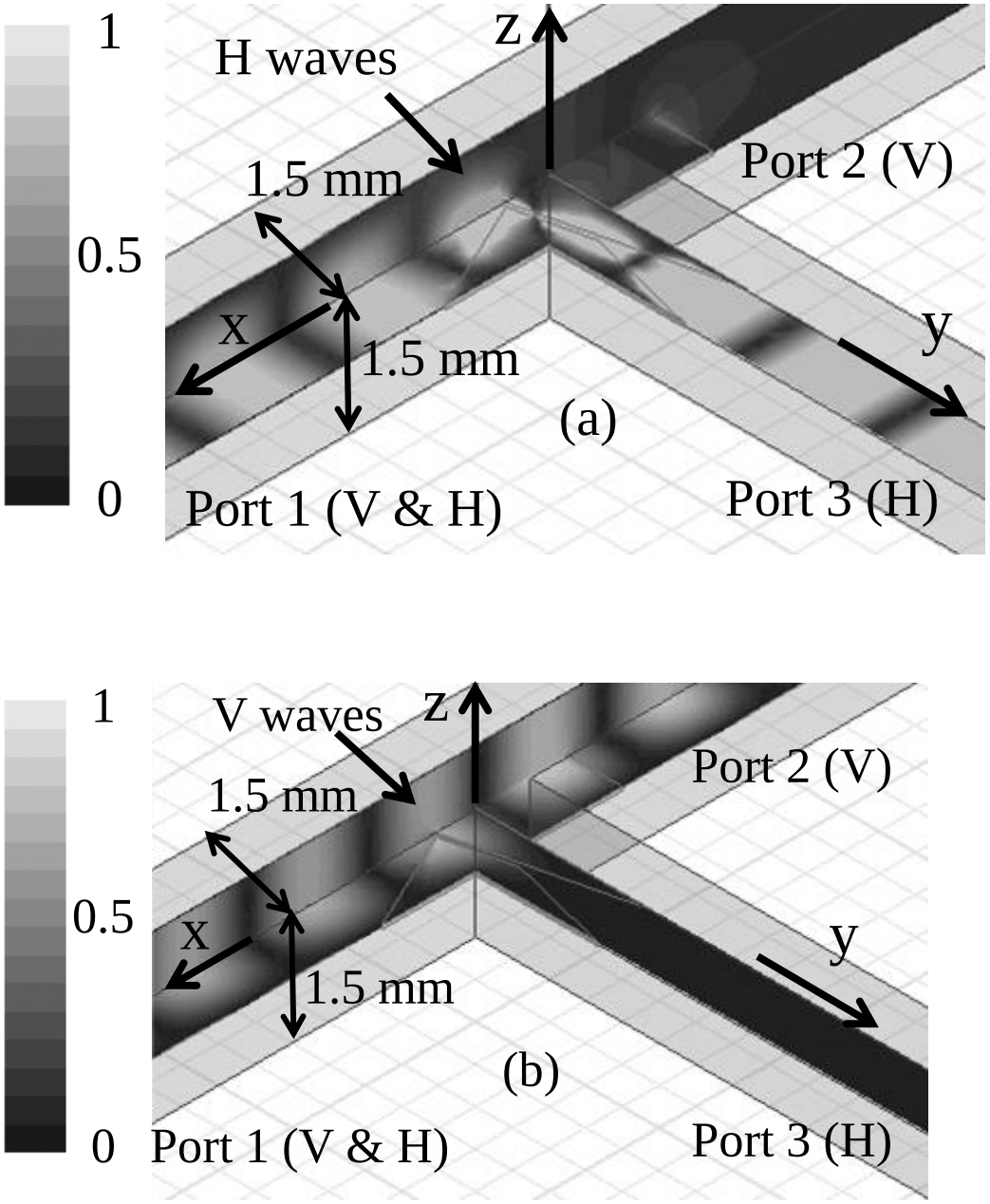

Figure. 5-7 (a) Simulated propagation of horizontal waves inside the new finline OMT1. The size of the port 1 waveguide is 1.5 mm × 1.5 mm. (b) Simulated propagation of vertical waves inside the new finline OMT1. The size of the port 1 waveguide is 1.5 mm × 1.5 mm. E field scale is normalized with respect to the extreme values in each plot.

5-2-2 Fabrication of finline OMT1 and its Characteristics

The waveguide structure of a finline OMT consists of a pair of metal parts. Normally, these metal parts are fabricated by end milling techniques. The fabrication error of end milling in the depth direction is ± 30 μm, and the two metal parts are combined to construct the waveguide. The waveguide structure could therefore have fabrication error in the depth direction of as much as ± 60 μm. Such fabrication errors deteriorate the I_{op} of the finline OMT. To achieve high I_{op}, the finline must be set at the center position of the waveguide in the depth direction, because the resulting symmetry prevents polarization rotation. Fig. 5-8 shows the relationship between S_{23} (I_{op}) and waveguide fabrication precision. In order to achieve more than 50 dB of I_{op}, fabrication precision of better than ± 10 μm is required. Thus, we decided to use milling techniques and laser measuring techniques by turns several times. By checking the depth after milling each time by the laser measuring technique, we achieved a waveguide structure with a precision of better than ± 10 μm.

We fabricated the new finline OMT1 and evaluated its performance. Fig. 5-9(a) shows the outward appearance of the new finline OMT1. Its total volume is 20 mm × 20 mm × 25 mm, and it weighs 74 g. This small volume and low weight make it easy to build the new finline OMT1 into portable wireless link systems. Fig. 5-9 (b) shows the inside of the new finline OMT1. We used 50-μm-thick metal plate fins, and the fin gap at the center is 70 μm. Fig. 5-9 (c) shows the cross section of the new finline OMT1. The lengths of the sides of the fabricated square waveguide of the OMT1 are 1505 and 1493 μm, which are within ± 10 μm of the designed length of 1500 μm. Thus, we succeeded in fine fabrication of the waveguide structure by combining milling and laser measurement techniques.

Fig. 5-10 shows the S_{23} (I_{op}) and S_{21}, S_{31} (XPI) of the new finline OMT1, the former measured with a vector network analyzer (VNA). In the measurement, a circular horn antenna and square-waveguide to circular-waveguide transition were attached to the port 1, because wireless systems based on polarization multiplexing generally employ a circular horn

antenna that can transmit radio waves with any polarization.
The I_{op} is below 33 dB, and the XPI is below 23 dB in the operation band of the 120-GHz-band wireless link (116.5 ~ 133.5 GHz). Outside the operation band, there are sharp peaks at 115 and 137 GHz. These peaks come from resonance on the new finline. The achieved XPI meets our requirement (> 14 dB), but the achieved I_{op} missed the target by 17 dB. This indicated the need for further improvement to meet our goal of more than 50 dB.

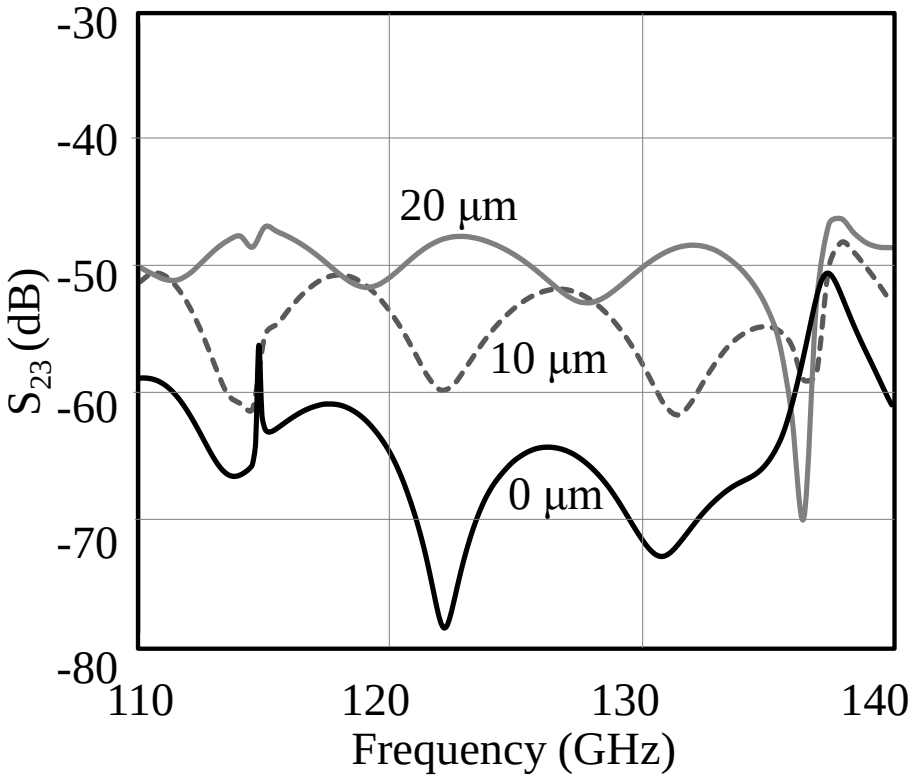

Figure. 5-8 Relationship between S_{23} (I_{op}) and waveguide fabrication precision.

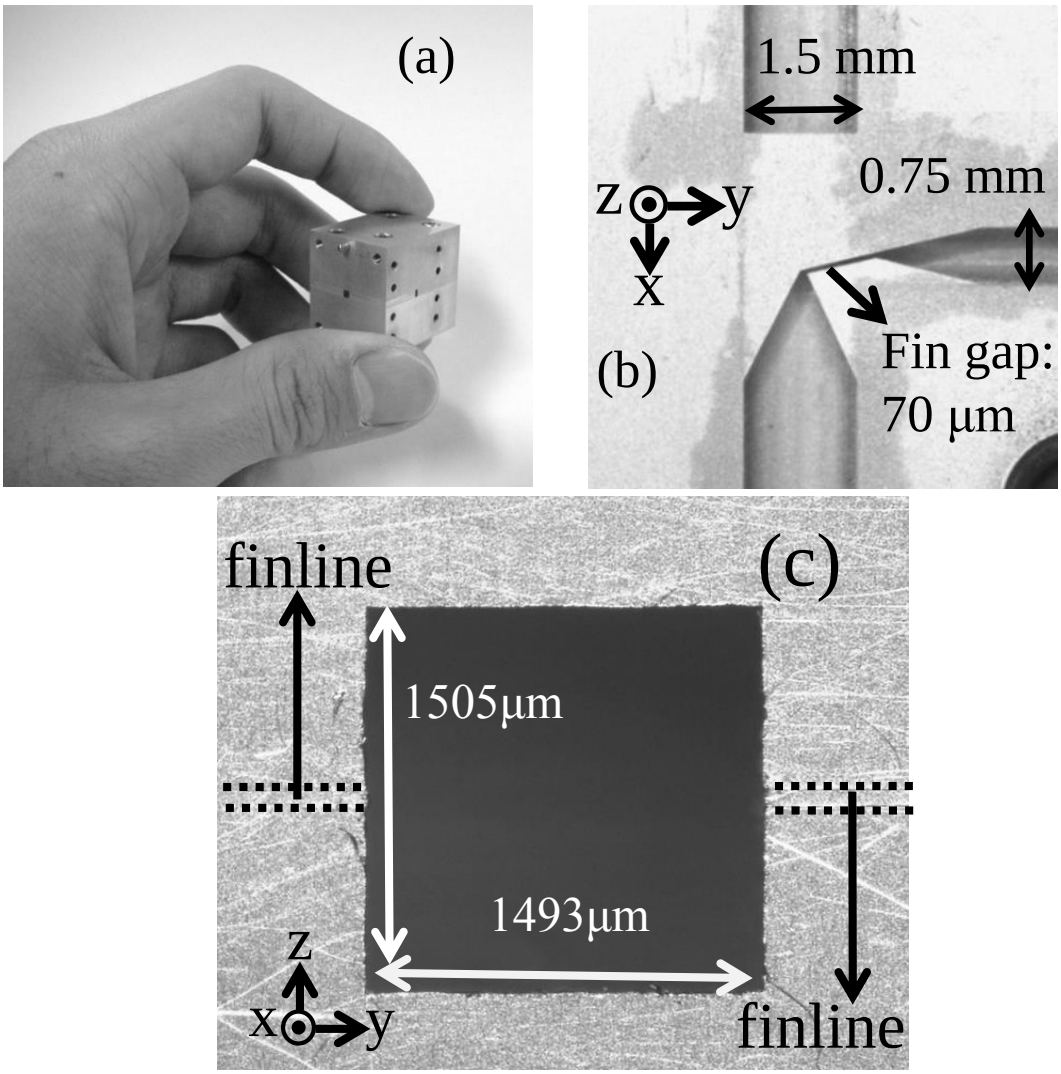

Figure. 5-9 (a) Outward appearance of the new finline OMT1. (b) Inside of the new finline OMT1. (c) Cross section of the new finline OMT1

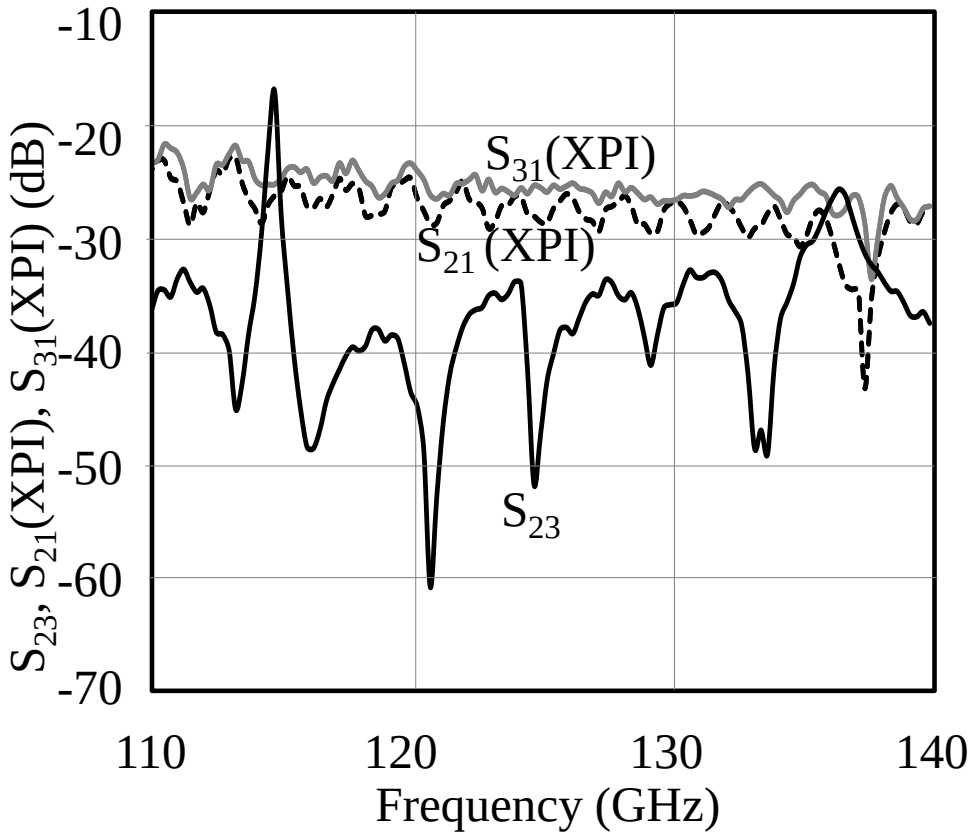

Figure. 5-10 First achieved S_{23} (I_{op}) and S_{21}, S_{31} (XPI) of the new finline OMT1.

5-2-3 Improvement of OMT isolation (Iop)

We evaluated the time-domain characteristics of I_{op}, and we found out that there were two points where polarization rotation happens. Fig. 5-11 shows propagation paths of radio waves inside the new finline OMT1-Basically, two kinds of waves determine I_{op}: a direct wave, for which we suppose that rotation of horizontal waves occurs due to the difference in the finline structure between the designed and fabricated finline; and reflected waves, which are once propagated to port 1, and reflected there, and then go back to port 2 with polarization rotation. The direct wave reaches port 2 earlier than the reflected one because its propagation distance

is shorter by 18 mm. Moreover, the direct wave is mainly affected by the difference in the finline structure between the design and the fabricated finline inside an OMT; it is not affected by the reflection characteristics at port 1.

To achieve high I_{op}, it is necessary to decrease the intensity of both the direct and reflected waves. One way to decrease the intensity of the reflected wave is to change the circular horn antenna attached at port 1 shown in Fig. 5-12 (a). The square-waveguide-to-circular-waveguide transition causes reflection at the joint plane. Moreover, radio wave signal can polarize at any direction on a circular horn antenna. As a result, millimeter-wave signal reflected at the circular horn antenna easily rotates into another polarization and these reflected waves degrade the I_{op}. In order to decrease the reflection and rotation of waves reflected at the antenna attached to port 1, we newly designed and fabricated the square horn antenna shown in Fig. 5-12 (b), which enables us to omit the square-waveguide-to-circular-waveguide transition that causes reflection at the interconnection plane. Moreover, the square horn antenna restricts the polarization to the vertical and horizontal directions, thereby preventing reflected waves from rotating polarizations. Fig. 5-13 shows the time-domain measurement results of S_{23} (I_{op}) with the circular horn antenna and square horn antenna. The first peak (dotted circle) is a direct wave. Some peaks after 1080 ps originate from the reflected wave from port 1 and the antenna attached at port 1. With a square horn antenna, the reflected wave is obviously smaller than that with the circular horn antenna. These results indicate that the use of the square horn antenna improves the I_{op} of the new finline OMT.

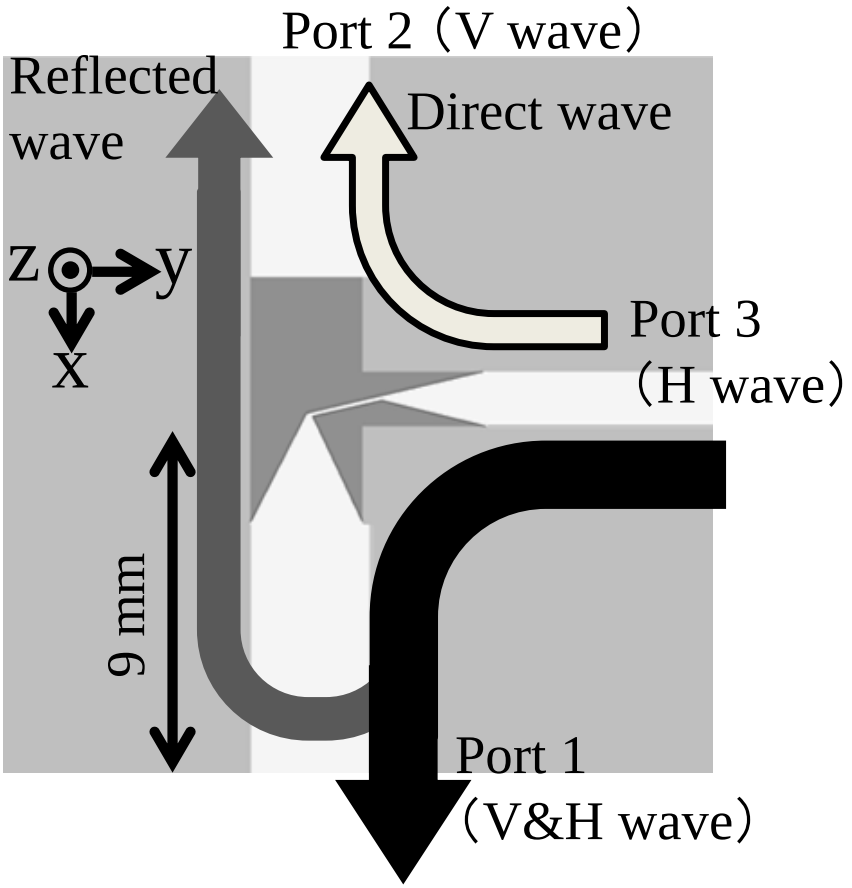

Fig. 5-11 Propagation of radio waves inside a finline OMT.

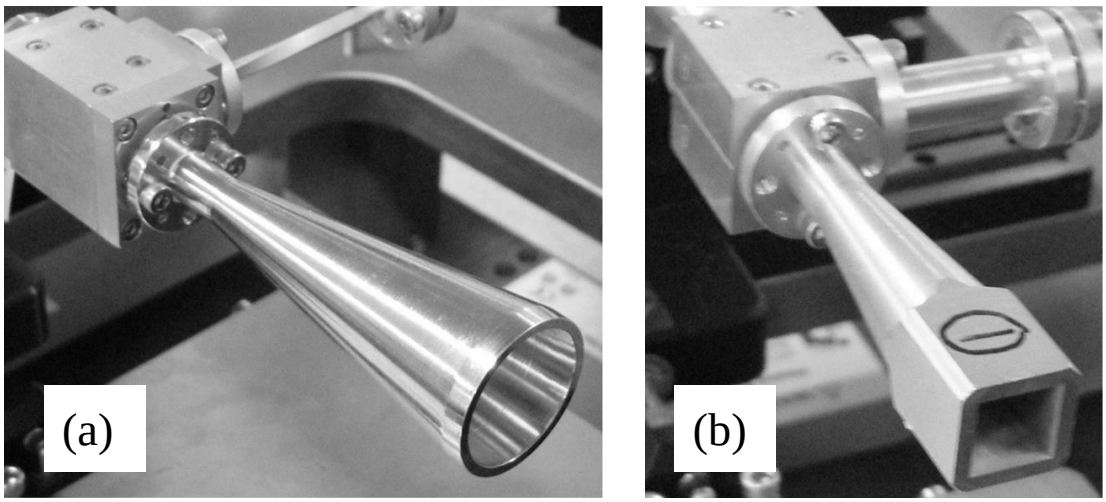

Fig. 5-12 (a) Conventional circular horn antenna. (b) New square horn antenna for preventing reflected waves from rotating polarizations.

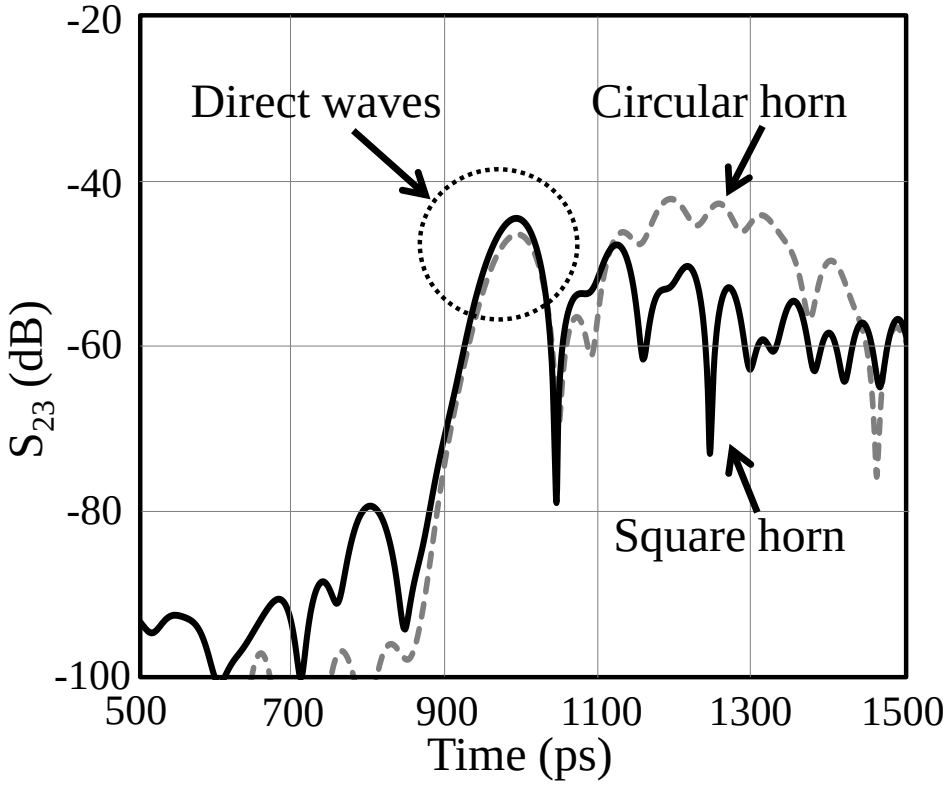

Fig. 5-13 Measured time-domain characteristics of S_{23} (I_{op}) with comparison of using circular horn antenna and square horn antenna.

Next, we investigated whether we could increase the I_{op} by changing the sandwiching structure of the finline plane. Fig. 5-14(a) shows a schematic of the cross section of the new finline OMT1-As shown in Fig. 11(c), the finline plane is sandwiched by two waveguide blocks. We suppose that the incomplete sandwich structure between waveguide blocks and finline causes a gap in the OMT, which deteriorates the I_{op}. As shown in Fig. 5-14(a)-1, in the new finline OMT described above (OMT1-a), the finline planes are sandwiched with flat planes with a wide area. Unevenness at the wide contact area, due to the limitations of the fabrication process, will cause a gap as shown Fig. 5-14(a)-2. At the gap, polarization rotation occurs and not only the intensity of the direct wave but also that of reflected ones increases. To reduce the contact area between waveguide block and finline OMT1-b, shown in Fig. 5-14(b), we therefore added a trench structure on the waveguide blocks as was done in a previously reported OMT [10]. This structure reduces the probability of gap formation. Fig. 5-15 shows the time-domain measurement results of S_{23} (I_{op}) for OMT1-a and OMT1-b with the square horn antenna. Finline OMT1-b successfully decreases the intensity of both direct and reflected waves.

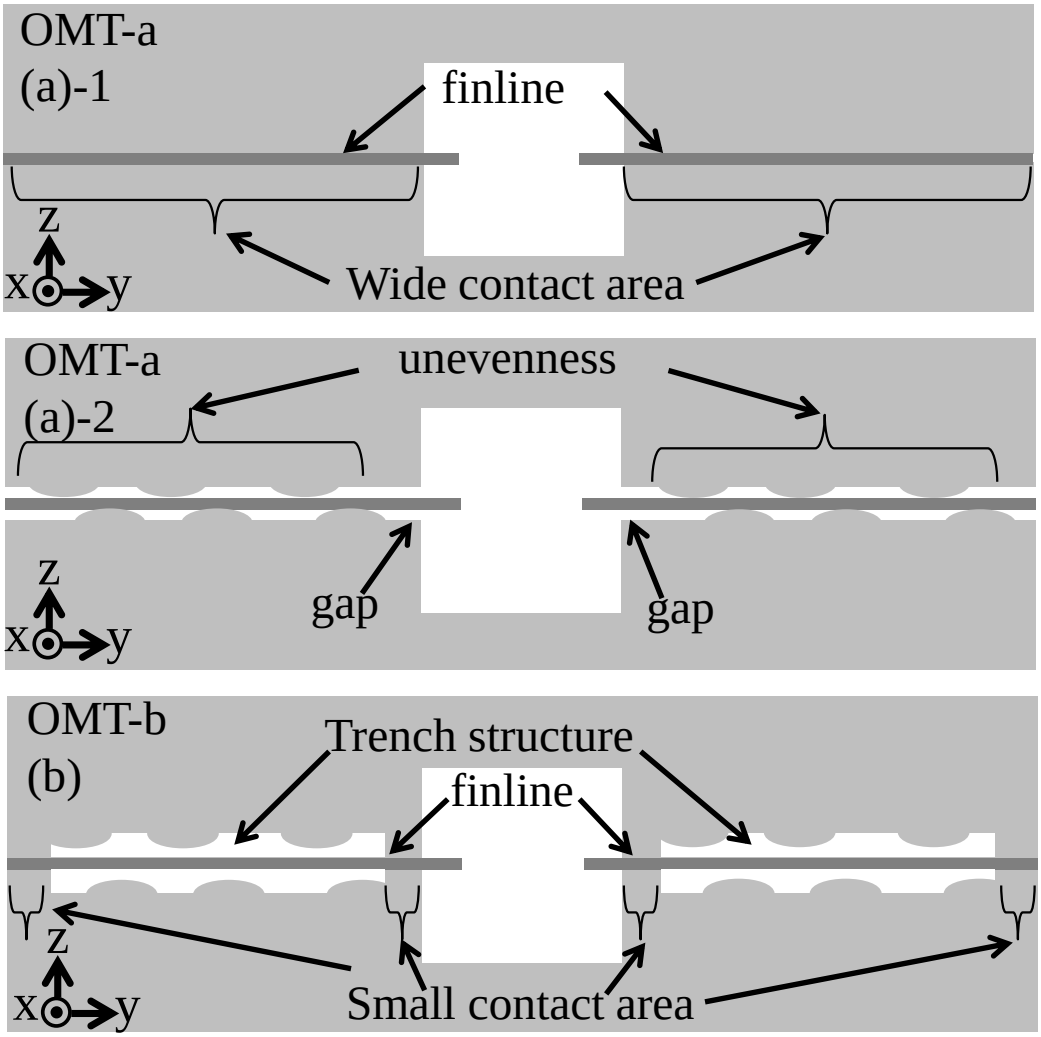

Fig. 5-14 Schematic of cross section of the new finline OMT: (a)-1 OMT1-a. (a)-2 Unevenness at the wide contact area of OMT1-a. (b) OMT1-b with trench structure for reducing the probability of a gap formation.

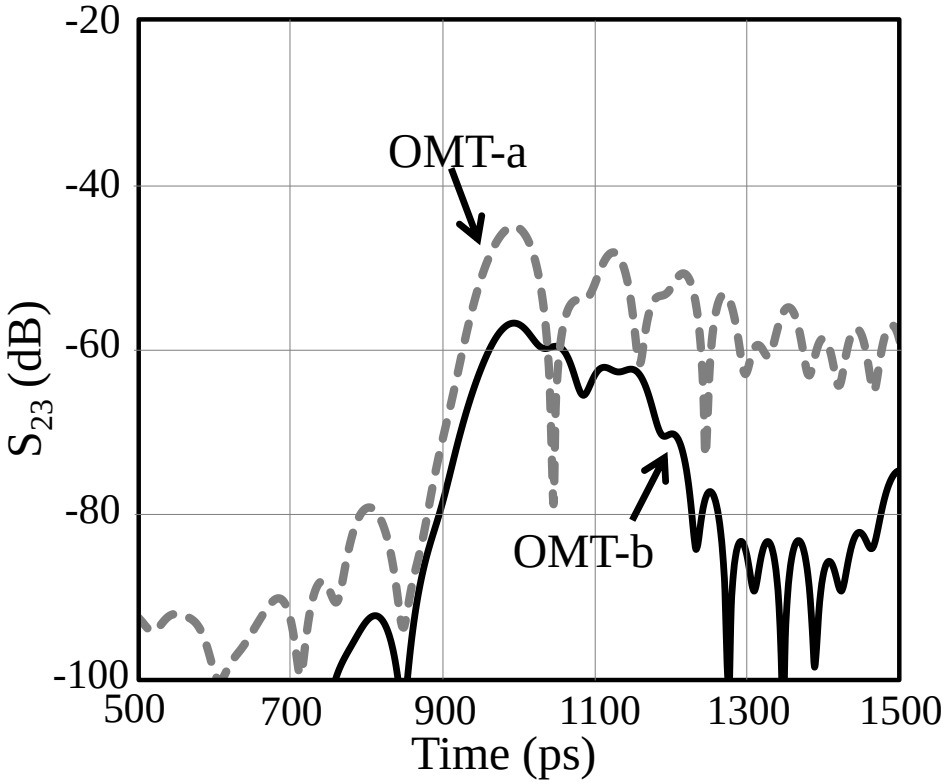

Fig. 5-15 Measured time-domain characteristics of S_{23} (I_{op}) for the new finline OMT1-a and OMT1-b with a square horn antenna.

5-2-4 Characteristics of the Improved finline OMT1

Next, we measured the frequency-domain characteristics of new finline OMT1-b. Fig. 5-16 shows the measured S_{23} (I_{op}) and S_{21}, S_{31} (XPI) of OMT1-b with the square horn antenna, measured with a VNA. The I_{op} is below 50 dB, and the XPI is below 31 dB in the operation band of the 120-GHz-band wireless link (116.5 ~ 133.5 GHz). Outside the operation band, there are sharp peaks at 115 and 137 GHz. These peaks come from resonance on the finline. The achieved I_{op} is insufficient for our requirement (> 60 dB). Thus, further improvement of finline OMT for higher I_{op} is necessary. The

achieved XPI is sufficient for the unidirectional 2-ch wireless link (> 23 dB). There is a difference between the simulated and measured I_{op}, which is probably due to the differences between the OMT structure used in the simulation and the actual structure of the fabricated OMT1-b. Fig. 5-17 shows the measured S_{21}, S_{31} (transmission loss) and S_{22}, S_{33} (return loss) of OMT1-b, measured with a VNA. The transmission loss is less than 1.2 dB, and the return loss is more than 12 dB for both polarization ports.

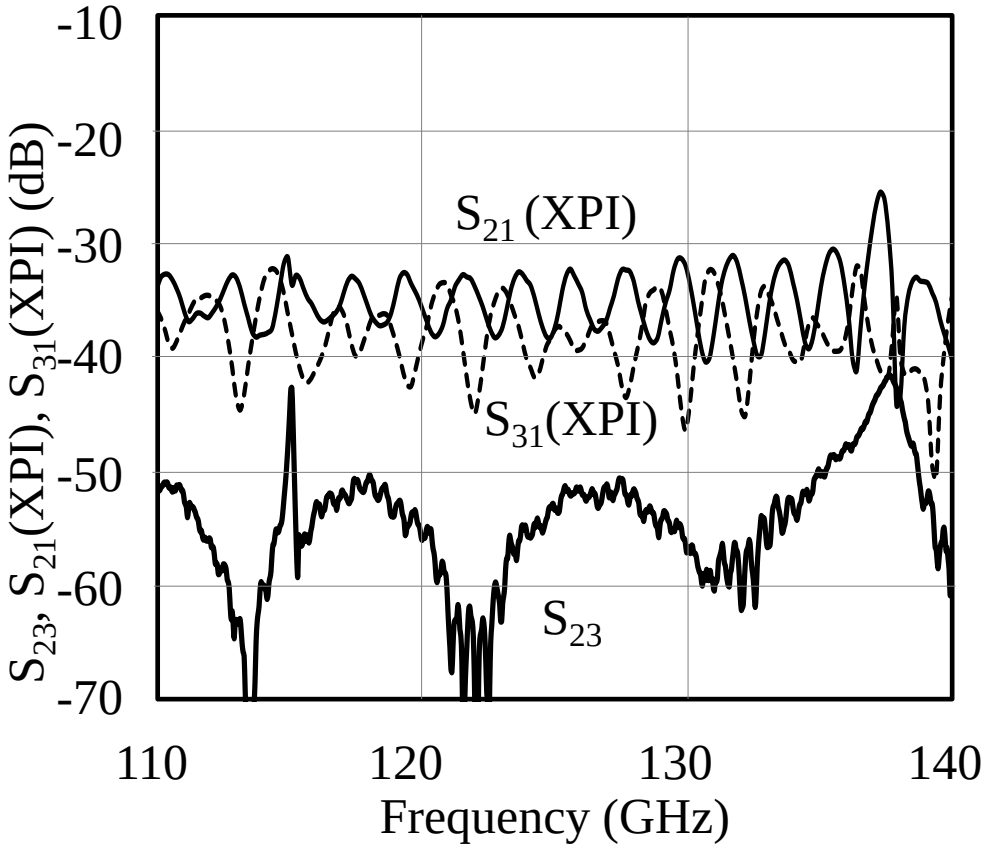

Fig. 5-16 Measured S_{23} (I_{op}) and S_{21}, S_{31} (XPI) of the new finline OMT1-b.

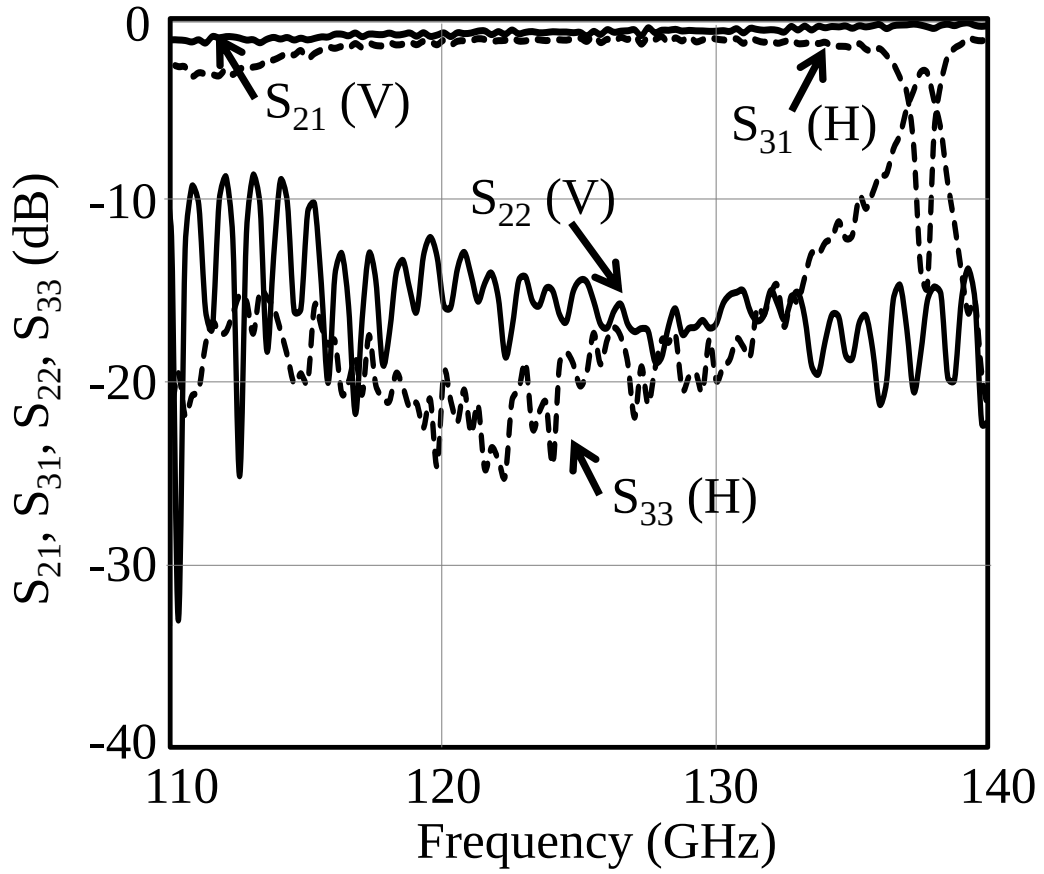

Fig. 5-17 Measured S_{21}, S_{31} (transmission loss) and S_{22}, S_{33} (return loss) of the new finline OMT1-b.

5-3 The Second Design and Fabrication of the New Finline OMT2

5-3-1 Improvement of OMT isolation (Iop)

As shown in Fig. 5-16, the measured I_{op} of OMT1 is more than 50 dB in the operation bandwidth of the 120-GHz-band wireless link (116.5~133.5 GHz). As explained above, I_{op} must be better than 60 dB for bidirectional wireless data transmission with an output power of 0 dBm. However, achieved I_{op} of 118 and 127 GHz is 50 dB, which misses our requirement by 10 dB. I_{op} of the OMT should be increased to improve the transmission

characteristics of the bidirectional 120-GHz-band wireless link.

The best way to increase the isolation is to fabricate the finline OMT much more precisely, because simulation results for an ideal finline OMT showed that the isolation would reach more than 60 dB in the operation bandwidth of the 120-GHz-band wireless link. However, the fabrication accuracy error of the current finline OMT1 is less than 10 μm, and it is quite difficult to further improve the fabrication accuracy.

To improve I_{op}, we chose to focus on the spectral characteristic of the 120-GHz-band wireless link. As explained in Chapter 2, 120-GHz-band wireless link uses ASK modulation. A theoretical calculation showed that a peak with a 50-% total power appears at the carrier frequency in the spectrum of ASK modulated wireless signal. This strong carrier component from the Tx module connected to the OMT causes frequency mixing with the data component of recived signals when the carrier component leaks into the other port, and it becomes a major source of noise at the receiver module. Therefore, I_{op} of more than 60 dB is necessary at the carrier frequency of 125 GHz to decrease the frequency mixing noise. As shown in Fig. 5-16, at 123 GHz, there is a point where I_{op} is over 60 dB. If the high I_{op} point can be set at 125 GHz, the frequency mixing noise caused by the leak carrier signal can be suppressed sufficiently.

We investigated the relationship between the high I_{op} point frequency and the structure of the finline OMT using an electromagnetic simulator with the finite element method. The simulation results indicate that the high I_{op} point mainly depends on the length of the rear part of the finline, L_c,shown in Fig. 5-2. And finline lengths L_a and L_b shown in Fig. 5-2 also affect the high I_{op} point. We optimized lengths L_a, L_b and L_c to 1.30, 2.20 and 1.30 mm, respectively, in order to shift the high I_{op} point to the carrier frequency of the 120-GHz-band wireless link. On the basis of the simulation results, we newly fabricated a finline OMT2. In that fabrication, we employed a new waveguide flange [14], which has fewer pins and holes for fine alignment of waveguide flange. Previous Finline OMT1 uses standard UG387/U-M flanges for waveguide interfaces, whose fabrication accuracy are within ± 30 μm. Fabrication accuracy error at waveguide interfaces causes polarization rotation, which deteriorates I_{op} and XPI. For finline OMT2, we therefore employed a new waveguide flange. The fabrication accuracy of waveguide flange design of finline OMT2 is within ± 15 μm.

Figure 5-18, 5-19, and 5-20 show the measurement results for OMT2. As shown in Fig. 5-18, the high I_{op} point is shifted from 123 to 125 GHz and the I_{op} at 125 GHz is 67 dB. The I_{op} of the previous OMT1 at 125 GHz was 53 dB, which means that we succeeded in improving I_{op} at 125 GHz by 14 dB. As shown in Fig. 5-19, the achieved XPI of OMT2 is more than 42 dB for the operation bandwidth of the 120-GHz-band wireless link, which is 12 dB better than that of finline OMT1. Figs.5-20 shows Measured S_{21}, and S_{31} (transmission loss) and S_{22}, S_{33} (return loss) of finline OMT2. Achieved transmission losses and return losses are sufficiently low for data transmission.

The I_{op} and XPI of finline OMT2 are sufficient for our requirement explained in Chapter 2, and the achieved I_{op} of OMT2 at 125 GHz is high enough to be used with an output power of 0 dBm.

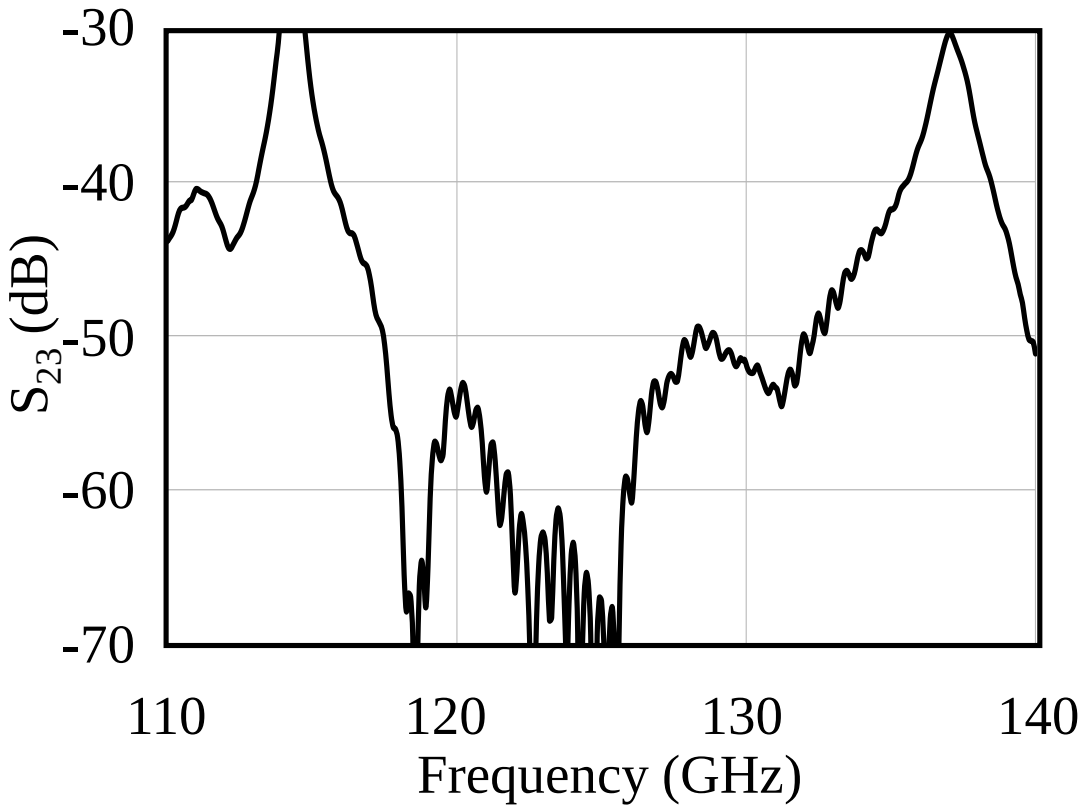

Fig. 5-18. Measured S_{23} (I_{op}) of finline OMT2.

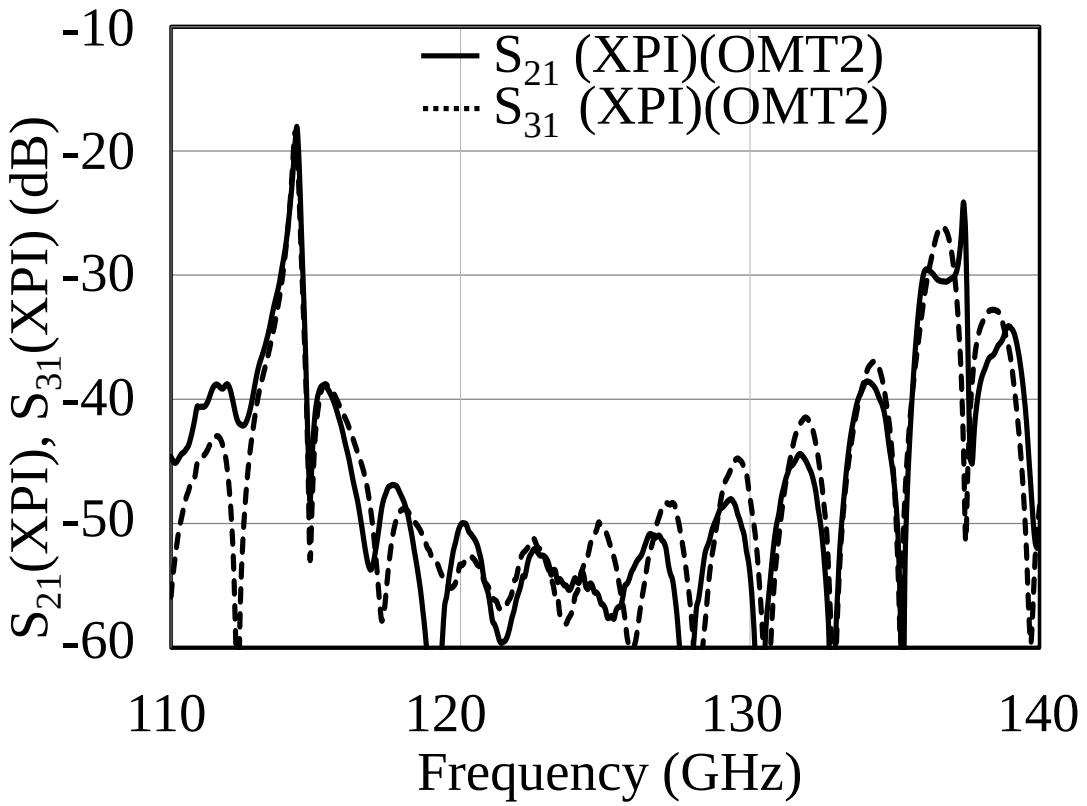

Fig. 5-19. Measured S_{21}, S_{31} (XPI) of finline OMT2.

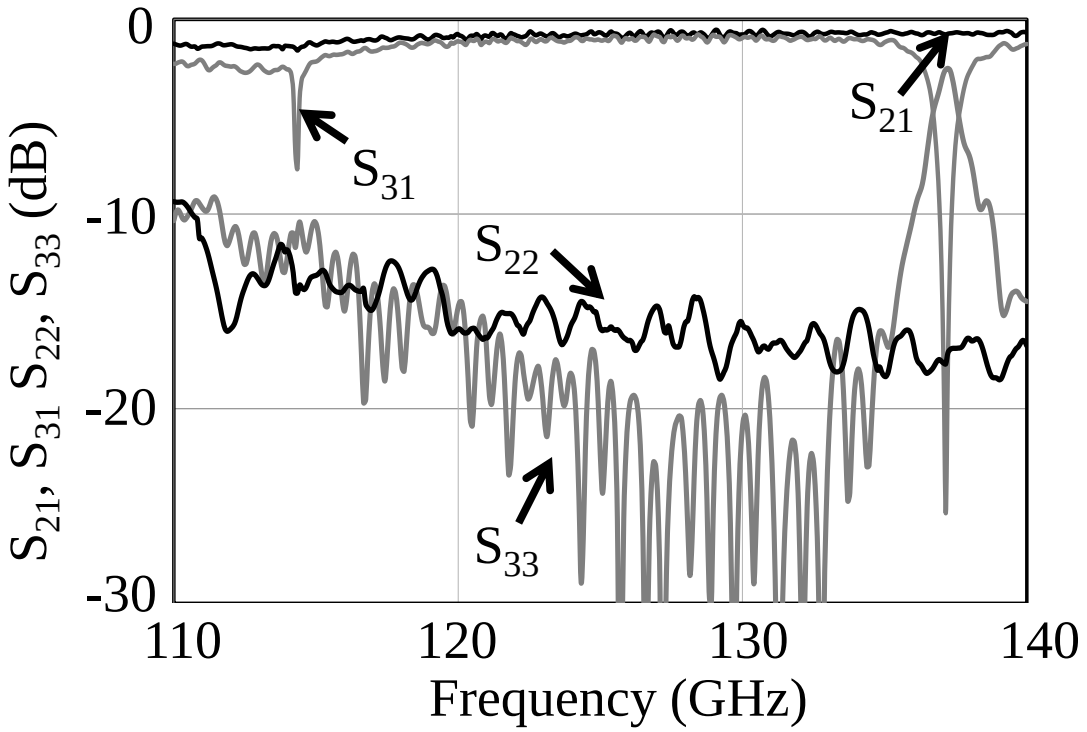

Fig. 5-20. Measured S_{21}, S_{31}, S_{22}, S_{33} of finline OMT2.

5-3-2 Improvement of group delay variation

Next, we improved the group delay variation of finline OMT2 for better data transmission characteristics. Figure 5-21 shows a schematic view of our finline OMT. As explained in Chapter 5-2-1, our finline OMT uses 1.5 mm × 1.5 mm square waveguide in order to use both polarizations and to allow only the basic modes. The cutoff frequency f_c of TE_{10} and TE_{01} basic modes in the 1.5 mm × 1.5 mm square waveguide is 100 GHz, which is higher than that of a standard F-band waveguide (1.016 mm × 2.032 mm) by 25 GHz. The operation bandwidth of the 120-GHz-band wireless link (116.5 ~ 133.5 GHz) is close to the f_c of the 1.5 mm × 1.5 mm square waveguide, so

that degradation of the group delay variation of 120-GHz-band signals occurs. The group delay variation of 120-GHz-band signals can be decreased by making waveguide length L_d small, which enables higher order modes to pass through the port. Thus, OMT waveguide length L_d should be designed to accommodate low group delay variation while preventing higher order modes from passing through. We simulated the relationship between waveguide length and the transmission characteristics of higher order modes. As shown in Fig. 5-22, simulation results showed that L_d can be reduced from 25 to 17 mm, which prevents transmission of higher order modes lower than -60 dB in the operation bandwidth of the 120-GHz-band wireless link (116.5~133.5 GHz). In the actual design, we employed L_d of 18 mm for a design margin. In addition, we reduced the length of the waveguide converters used for connecting the OMT waveguide and standard F-band waveguide. L_e and L_f were reduced from 30 to 25 mm. Fig. 5-23 shows the group delay variation of finline OMT1 (L_d= 25 mm, L_e and L_f = 30 mm) and the newly designed one (OMT2) (L_d = 18 mm, L_e and L_f = 25 mm). The simulation results (dotted circle) indicate that total simulated group delay variation of the OMT waveguide is reduced from 60 to 43 ps. Measured group delay variation of OMT2 is 43 ps, an improvement of 13 ps over that of OMT1 (56 ps). We use two OMTs for polarization multiplexing and demultiplexing so that the total group delay variation is reduced from 112 to 86 ps.

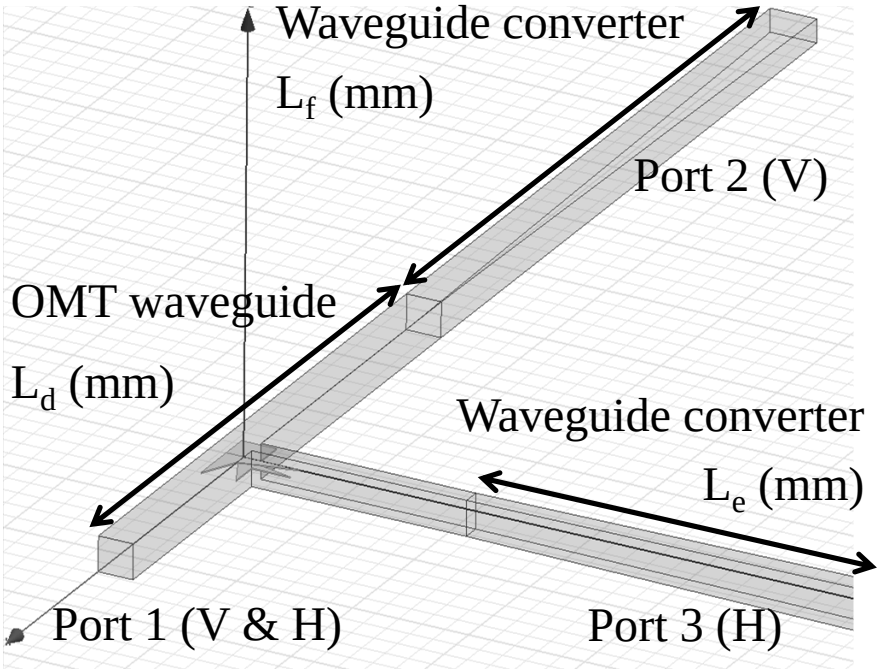

Fig. 5-21. Schematic view of the finline OMT.

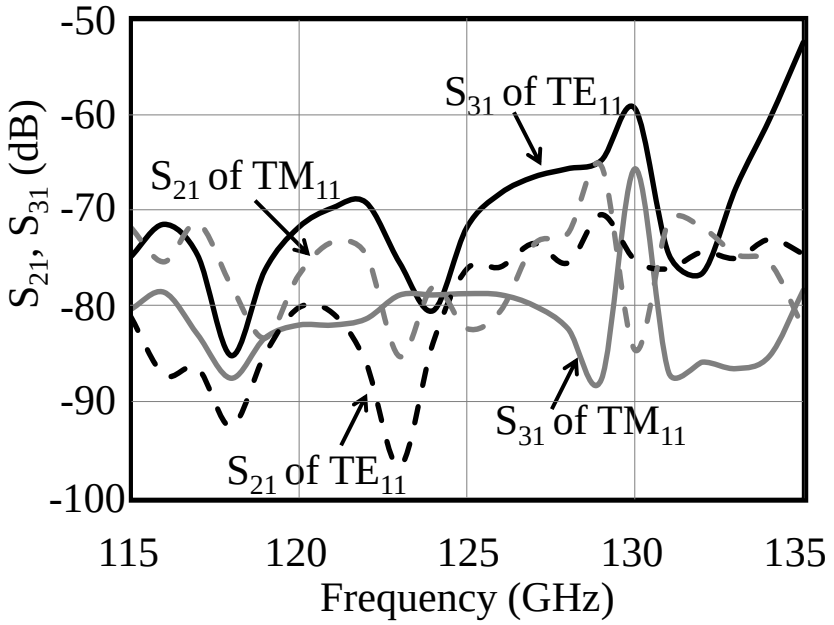

Fig. 5-22. Simulated transmission characteristics of higher order modes inside a 1.5 mm x 1.5 mm square waveguide (L_d = 17 mm).

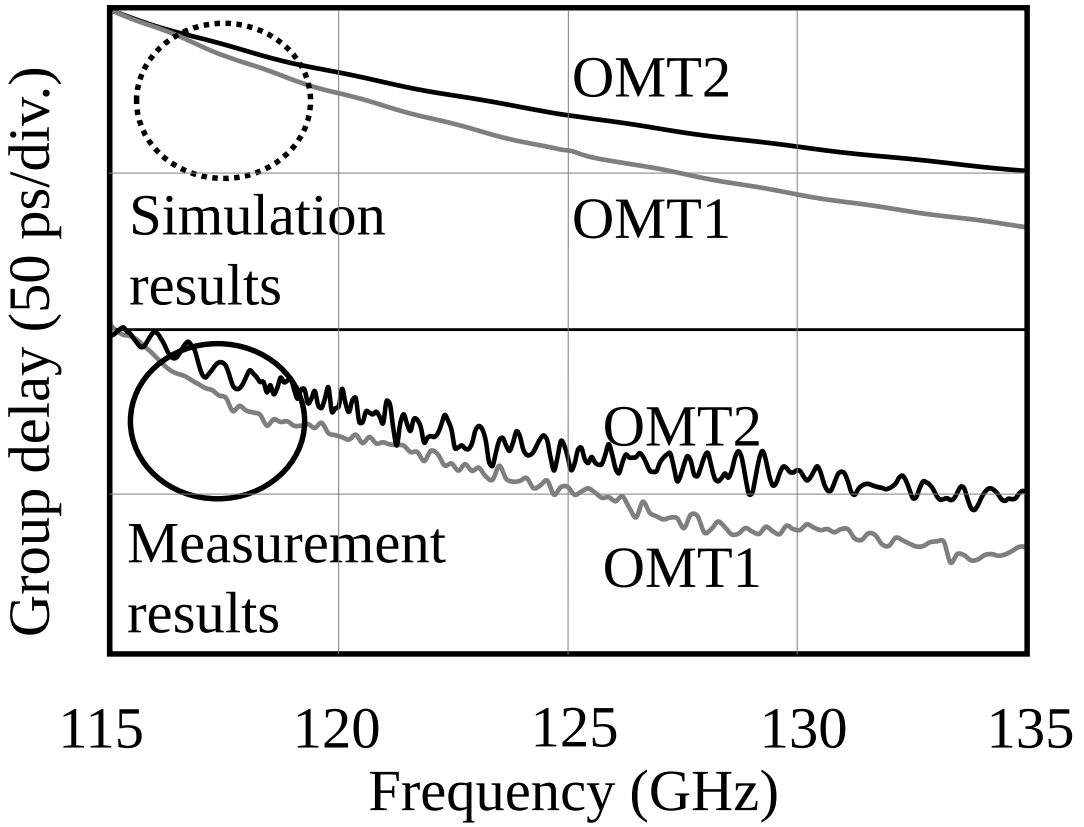

Fig. 5-23. Comparison of group delay variation of finline OMT1 and finline OMT2.

5-4 Wireless data Transmission Equipment using Polarization multiplexing with OMT

We made portable wireless equipment for polarization multiplexing data transmission experiments with OMT2.

Fig. 5-24 shows a photograph of the portable wireless equipment. A square horn antenna is used to transmit both V and H waves. Antenna gain of the square horn antenna is 22 dBi. The wireless equipment is 18 cm × 18 cm × 30 cm in size and almost the same as the former unidirectional equipment

which is referred in Chapter1 [22].

Fig. 5-25 shows a schematic of the portable wireless equipment assembled for 10-Gbps bidirectional data transmission. As shown in Fig. 5-25, the Tx and Rx modules and a square horn antenna are connected to the OMT. Fig. 5-26 shows a schematic of the portable wireless equipment assembled for 20-Gbps unidirectional data transmission. As shown in Fig. 5-26, two sets of Tx modules and a square horn antenna are connected to the OMT. The portable wireless equipment for the 20-Gbps unidirectional data receiver is assembled with two sets of Rx modules.

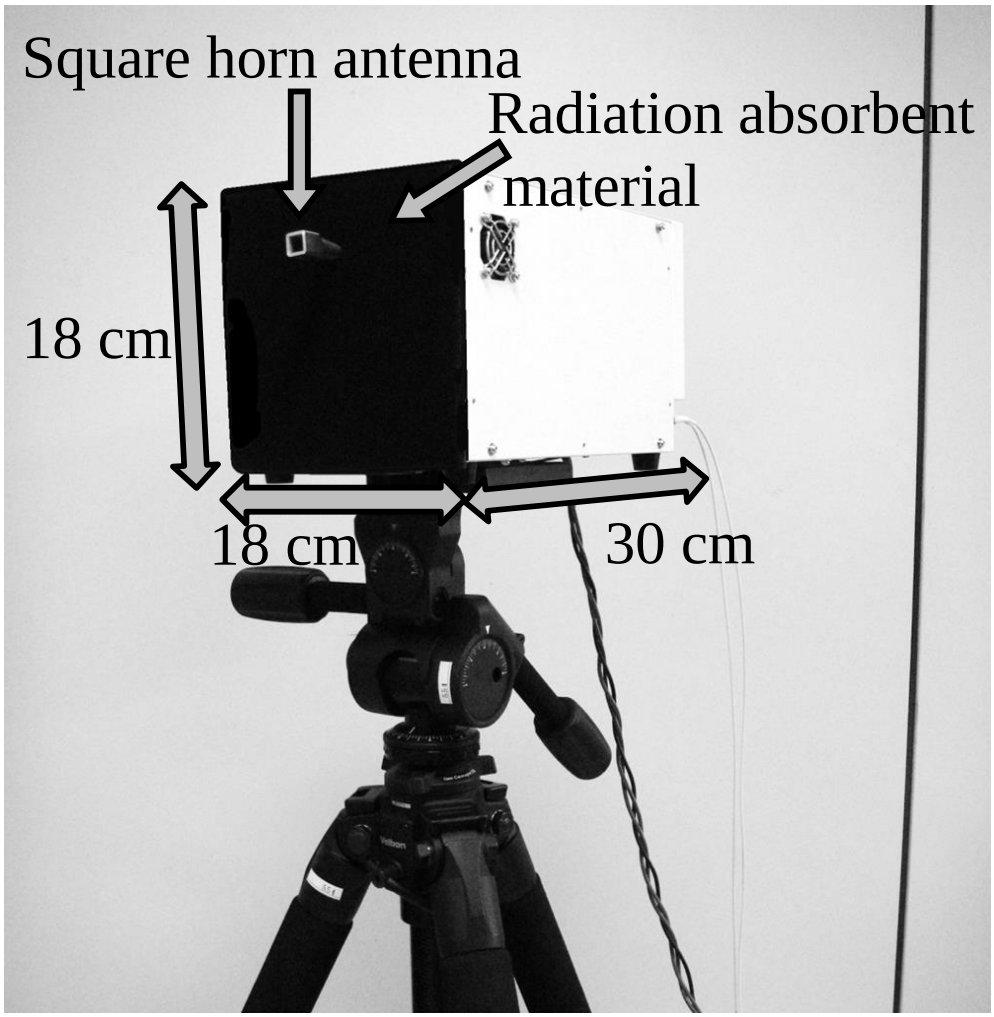

Fig. 5-24. Photograph of portable wireless equipment for polarization multiplexing.

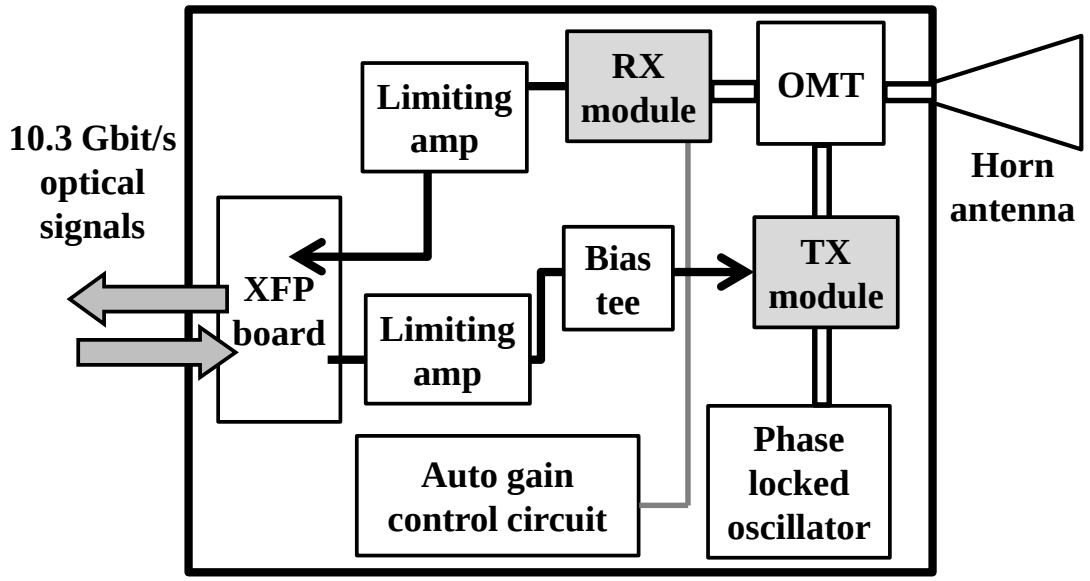

Fig. 5-25. Schematic view of portable wireless equipment assembled for 10-Gbps bidirectional data transmission.

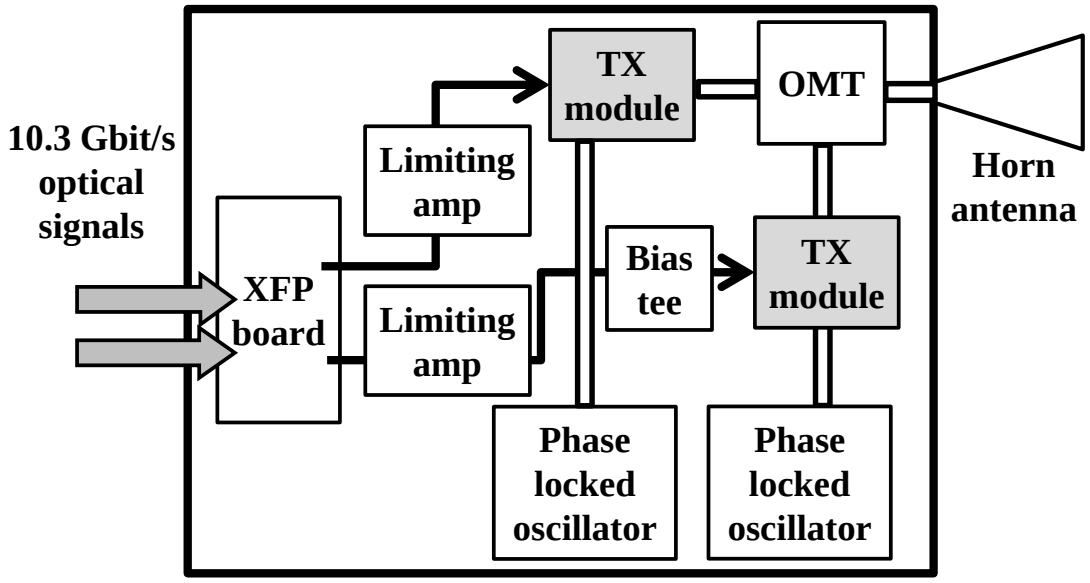

Fig. 5-26. Schematic view of portable wireless equipment assembled for 20-Gbps unidirectional data transmission.

5-5 Bidirectional data Transmission Experiment using Wireless Equipment

We carried out a bidirectional data transmission experiment using the equipment in an anechoic chamber. Fig. 5-27 is a schematic view of the setup, where dotted lines show the configuration for measuring data transmission characteristics, and solid lines show that for testing connectivity for 10-Gbit Ethernet (10GbE).

To measure the BER characteristics of the equipment, we used a pulse pattern generator (PPG) to generate 10.3-Gbps pseudorandom bit sequence (PRBS) data, an error detector (ED) to measure the BER, and FEC to control errors in data transmission. The FEC uses Reed-Solomon (RS) (255,239) coding with coding gain of 6 dB, and the output signal of FEC becomes 11.1 Gbps. V polarization waves generated by the equipment on the right are radiated from a 22-dBi horn antenna. They reach another 22-dBi horn antenna, and are input into the equipment on the left. At the same time, H polarization waves generated by the equipment on the left are transmitted to the equipment on the right. The output powers of both sets of equipment are basically 0 dBm and can reach 10 dBm by attaching an additional amplifier module in front of the Tx module. In this experiment, we varied the distance between the two antennas in order to change the received power and measure the BER characteristics. We also carried out the same experiment without FEC.

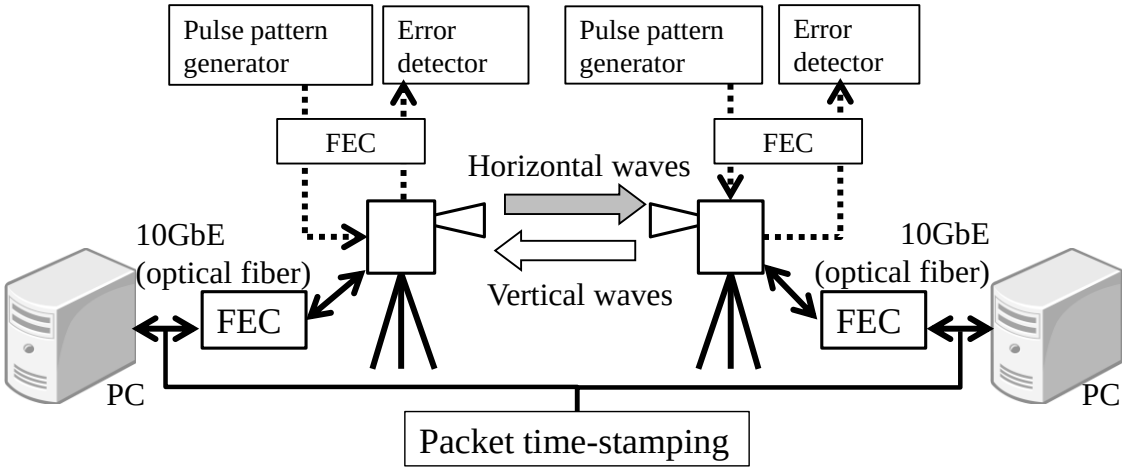

Fig. 5-27. Bidirectional wireless data transmission experiment: dotted line shows the configuration for measuring BER characteristics; and solid line shows the configuration for testing connectivity for 10GbE.

Fig. 5-28 shows the BER characteristics of the V and H channels. The BER of the wireless link was below 10^{-12} at both channels without FEC. With FEC, we succeeded in bidirectional transmission with a BER of below 10^{-12} over a distance of more than 1.8 m with an output power of 0 dBm and 2.8 m with 10 dBm. With a Cassegrain antenna with a 52-dBi gain and FEC, the maximum transmission distances calculated using the output power, antenna gain, received power necessary for BER of 10^{-12}, and absorption coefficient of air (about 1 dB/km), would be about 1.5 km with an output power of 0 dBm and 2.2 km with that of 10 dBm. As shown in Fig. 5-28, the BER characteristics of the H polarization channel of 10 dBm are worse than those of the V polarization channel. These characteristics appear when we change the polarity of the OMT, indicating that the deterioration of H polarization channel is due to the characteristics of the MMW amplifier attached to the Tx module for the H polarization channel.

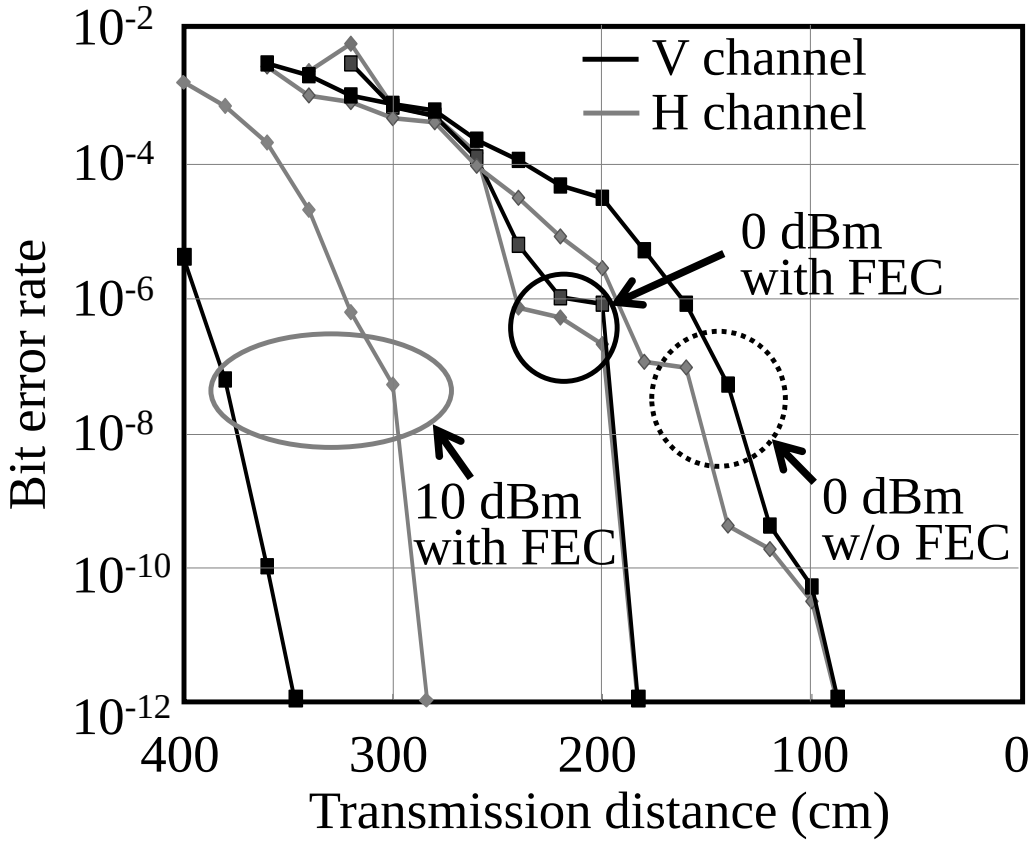

Fig. 5-28. BER characteristics of V and H polarization channel in the bidirectional data transmission system.

We carried out an experiment for connecting the bidirectional wireless data transmission equipment to 10GbE network. We connected the wireless equipment to two PCs that have a 10GbE interface, an application for controlling large numbers of data streams [15], large storage capacity for recording large data, and a packet time-stamping system. We evaluated the wireless data transmission characteristics by transmitting 11.2 GB of uncompressed picture data over the setup shown in Fig. 5-27 by solid lines. The 11.2 GB of data transmitted from one PC passes through the setup and is recorded by the other PC. Fig. 5-29 shows the relationship between the BER and average data transmission time of the 11.2-GB data. For a BER of below 10^{-12}, the transmission time was 9.1 seconds. The averaged bit rate of the PC is calculated as

$$11.2 \times 8 \div 9.1 = 9.85\ Gbit/s \quad (5\text{-}2)$$

The achieved bit rate of 9.85 Gbps is almost same as the theoretical maximum TCP throughput of 10GbE (9.92 Gbps). When the BER characteristics deteriorate above 10^{-8}, the data transmission time drastically increases. The BER of 10^{-8} significantly influences the TCP throughput because TCP considers every packet loss as an indicator of congestion and increases the data transmission time accordingly.

Fig. 5-30 shows average delay time versus connecting PCs without wireless system (only with optical fiber) and with wireless system. The average delay of using the wireless system was 9.6 μs. We suppose that the delay is mostly due to FEC because electro-optic conversion by the optical transceiver inside the wireless equipment takes less than 1μs.

These results indicate that the 120-GHz-band bidirectional wireless data transmission system using polarization multiplexing can be connected to a 10GbE network seamlessly.

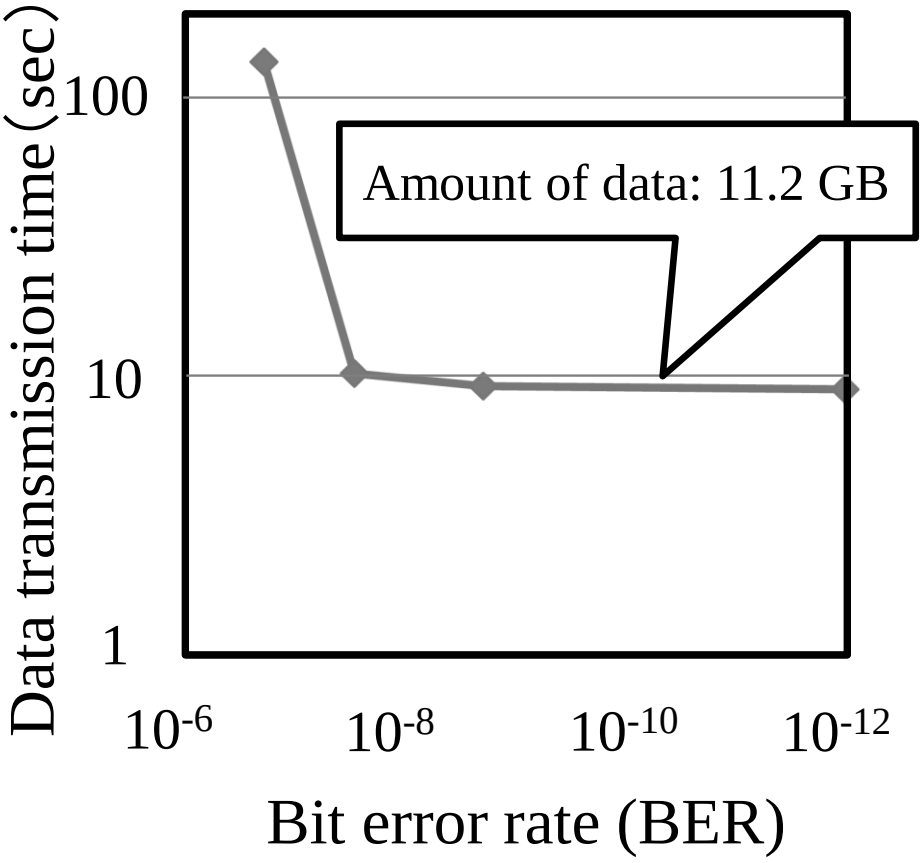

Fig. 5-29. Relationship between BER and average data transmission time of 11.2 GB data by wireless equipment.

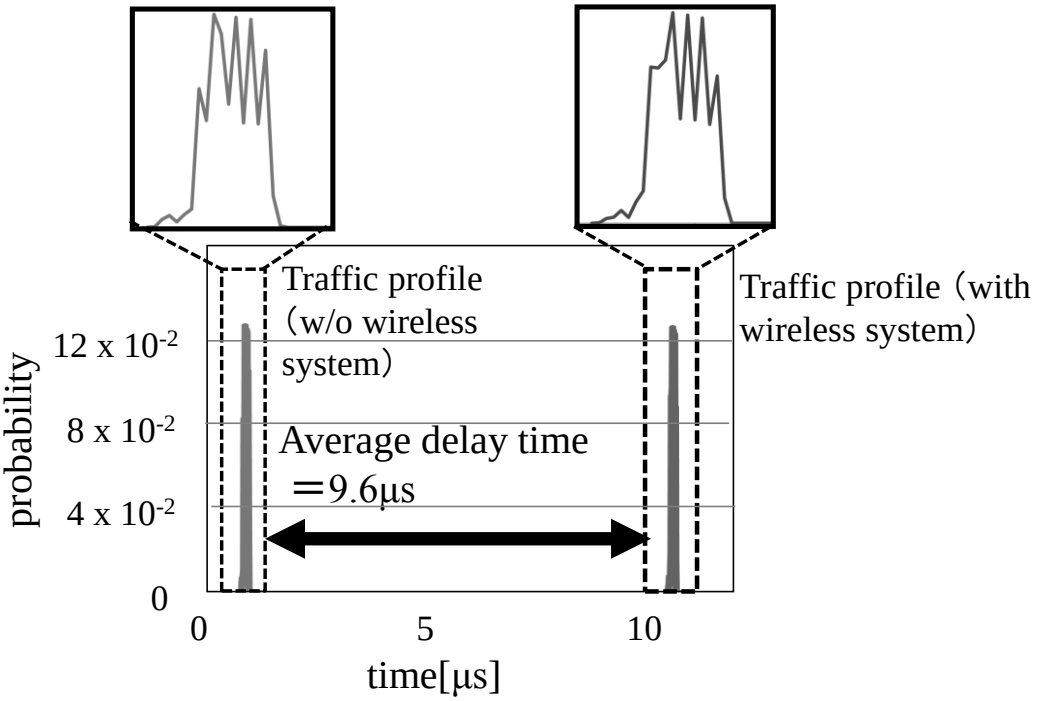

Fig. 5-30. Average delay time versus connecting PCs without wireless system and with wireless system.

5-6 Unidirectional data Transmission Experiment using Wireless Equipment

As explained in Chapter 5-4, we reassembled the wireless equipment to make unidirectional 20.6-Gbps (2 ch x 10.3 Gbps) wireless equipment with finline OMT2. We carried out a unidirectional 2-ch data transmission experiment using the equipment in an anechoic chamber. Fig. 5-31 shows a schematic view of the experimental setup, where the dotted lines show the configuration for measuring data transmission characteristics, and the solid lines show that for testing connectivity for multiplexed 12-ch of HD-SDI (uncompressed HDTV signal). To measure the BER characteristics of the equipment, we used a PPG to generate 10.3-Gbps PRBS data, FEC to control errors in data transmission, and an ED to measure the BER. The FEC uses RS (255,239) coding and the output signal of FEC becomes 11.1 Gbps. The

pieces of equipment used in this experiment were connected as shown by the dotted lines in Fig. 5-31. V and H polarization waves generated by the transmitter equipment on the left are radiated from a 22-dBi horn antenna. They reach another 22-dBi horn antenna and are input into the receiver equipment on the right. The output powers of both sets of equipment are basically 0 dBm and can reach 10 dBm by attaching an additional amplifier module in front of the Tx module. In this experiment, we varied the distance between the two antennas in order to change the received power and measure the BER characteristics. We also carried out the same experiment without FEC.

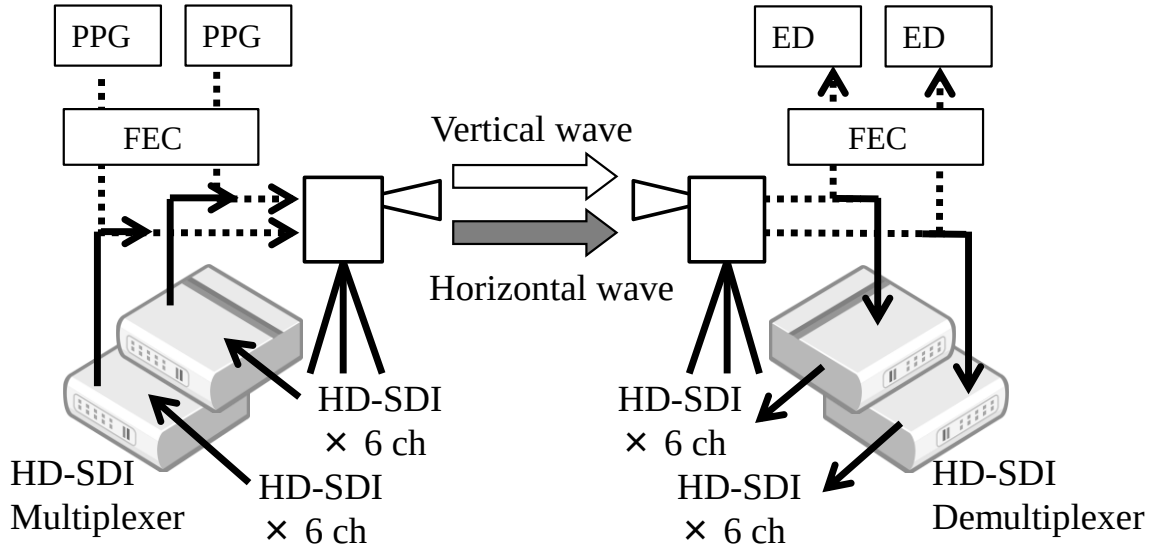

Fig. 5-31. Unidirectional 20.6-Gbps (2 ch x 10.3 Gbps) wireless data transmission experiment: dotted line means measuring BER characteristics, solid line means testing connectivity for multiplexed 12-ch of HD-SDI.

Fig. 5-32 shows the BER characteristics of the V and H channels. The BER of the wireless link was below 10^{-12} at both channels without FEC. Measurement results show that using a pair of OMTs increases the required C/N ratio by 2 dB, so the deterioration of data transmission characteristics caused by each OMT is 1 dB. With FEC, we succeeded in unidirectional transmission with a BER of below 10^{-12} over a distance of more than 4.2 m with an output power of 0 dBm. Because of the limited length of the anechoic chamber, we evaluated data transmission characteristics with an output

power of 10 dBm without FEC and achieved transmission with a BER of below 10^{-12} over a distance of more than 6.2 m. With a Cassegrain antenna with a 52-dBi gain and FEC, the maximum transmission distances, calculated using the output power, antenna gain, received power necessary for BER of 10^{-12} , and absorption coefficient of air (about 1 dB/km), would be about 3.0 km with an output power of 0 dBm with FEC and 3.9 km with 10 dBm without FEC. As shown in Fig. 5-32, the BER characteristics of the H polarization channel of 10 dBm are worse than those of the V polarization channel. These characteristics appear when we change the polarity of the OMT, indicating that the deterioration of H polarization channel is due to the characteristics of the amplifier attached to the Tx module for H polarization channel.

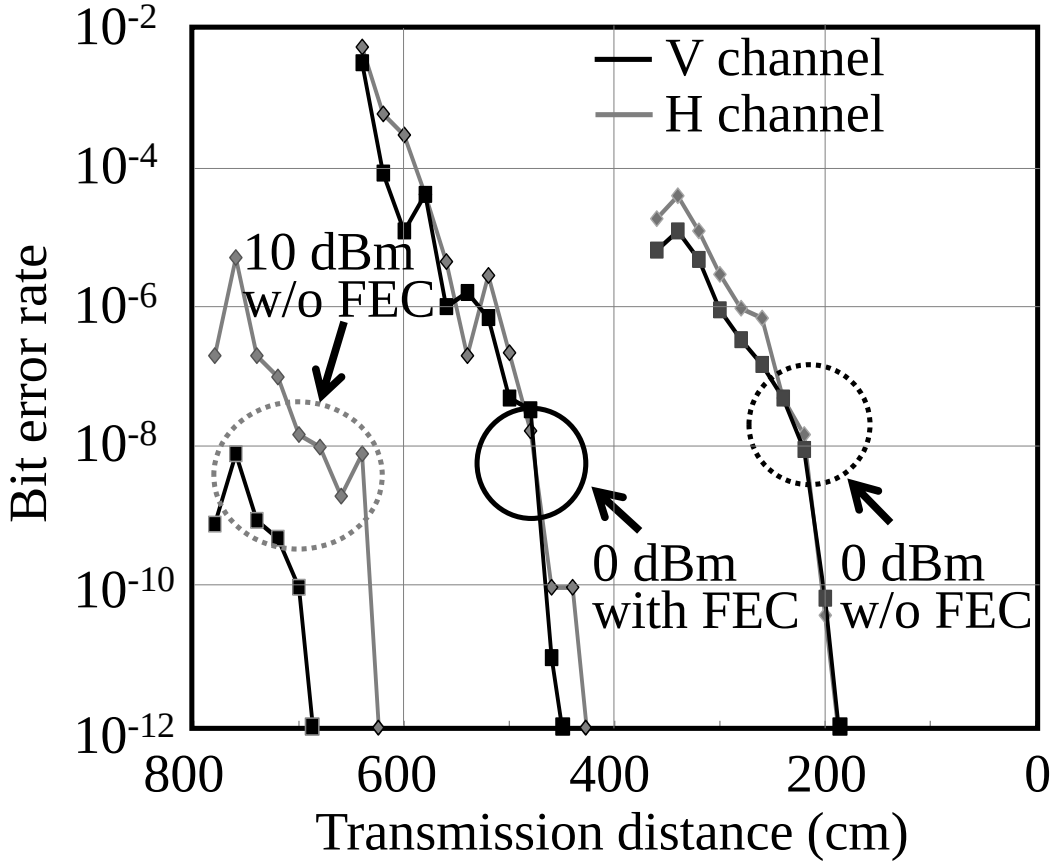

Fig. 5-32. BER characteristics of V and H polarization channel in the unidirectional data transmission system.

We carried out an experiment for unidirectional 12-ch wireless HD-SDI data transmission. The experimental setup is shown in Fig. 5-31 as indicated by the solid lines. The data transmission distance was 1 m. We used two pairs of the HD-SDI multiplexer and demultiplexer to multiplex and demultiplex six channels of HD-SDI signals. The HD-SDI multiplexer uses FEC of concatenating RS codes with different structures to achieve 6 dB of coding gain [16]. RS(986,966) code is used to encode each HDTV line format and then encoded HDTV signals are divided into the data packets by packet formation function inside the HD-SDI multiplexer. RS(252,236) is used to encode the data packets and then the sum of six channels of encoded data packets are multiplexed into one optical data stream. The data rate of the optical data stream rises from the sum of six channels of HD-SDI signals (approximately 9 Gbps) to 10.3 Gbps. We first evaluated the BER characteristics using PRBS data generated within the encoder of the HD-SDI multiplexer and error detector within the decoder of the HD-SDI demultiplexer. We succeeded in error-free transmission with a BER of below 10^{-12}. We next estimated the wireless data transmission characteristics of 12 channels of HD-SDI signals. Transmitted HD-SDI signals show no error, which was indicated on the HD-SDI monitors. Thus, we succeeded in transmitting 12-ch HD-SDI data by interconnecting our system.

5-7 Conclusion of Chapter 5

Chapter 5 describes polarization multiplexing by orthomode transducer. First, we designed and fabricated new OMT. Fabricated OMT shows high enough Iop and XPI for our requirement. Measured Iop was 67 dB at the carrier frequency of the 120-GHzband wireless link. Measured XPI was more than 42 dB for the operation bandwidth of the 120-GHz-band wireless link. Next, we made portable wireless equipment for polarization multiplexing data transmission experiments with OMT. The wireless equipment was successfully assembled 18 cm × 18 cm × 30 cm in size and almost the same as the former unidirectional equipment which is referred in Chapter1 [22]. Finally, we measured data transmission characteristics of polarization multiplexing by the portable wireless equipment with OMT. The bidirectional

equipment succeeded in the transmission of 10-Gbps bidirectional data and seamless connection to a 10GbE network. The unidirectional 2-ch equipment succeeded in the transmission of 20-Gbps data and 12 channels of uncompressed HDTV signals.

References in Chapter 5

[1] R. W. Kreutel Jr, D. F. Difonzo, W. J. English, R. W. Gruner, "Antenna technology for frequency reuse satellite communications," Proceeding of the IEEE, vol. 65, No.3, 1977.

[2] M. Kamikura, M. Naruse, S. Asayama, N. Satoru, W. Shan, Y.Sekimoto, "Development of a 385-500 GHz Orthomode Transducer (OMT)," 19th International Symposium on Space Terahertz Technology, PP. 557-562,April, 2008.

[3] http://www.antesky.com/

[4] G. Pisano, L. Pietranera, K. Isaak, L. Piccirillo, B. Johnson, B. Maffei, S. Melhuish, "A Broadband WR10 Turnstile Junction Orhomode Transducer," IEEE Microwave and Wireless Components Letters, vol. 17, No.4, 2007.

[5] E. J. Wollack, W. Grammer, and J. Kingsley, "The Boifot Orthomode Junction," ALMA Memo Series 425.

[6] G. Chattopadhyay, B. Philhour, J.E. Carlstrom, S. Church, A. Lange, J. Zmuidzinas, "A 96-GHz Ortho-Mode Transducer for the Polatron," IEEE Microwave and Guided wave Letters, vol. 8, No.12, pp. 421-423, 1998.

[7] S. D. Robertson, "Recent advances in finline circuits", IRE Transactions on Microwave Theory and Techniques, pp. 263-267, 1956.

[8] G. Chattopadhyay and J.E. Carlstrom, "Finline ortho-mode transducer for millimeter waves," IEEE Microwave Guided Wave Lett.,vol. 9, pp. 339–341, Sept. 1999.

[9] J.D. Pandian, L. Baker, G. Cortes, P.F. Goldsmith, A.A. Deshpande, R. Ganesan, J. Hagen, L. Locke, N. Wadefalk, S. Weinreb, "Low-noise 6-8 GHz receivver," IEEE Microwave Magagine.,vol. 7, issue: 6, pp. 74–84, Dec. 2006.

[10] S. J. Skinner and G. L. James, "Wide-band orthomode transducers," IEEE Trans. Microwave Theory Tech., vol. 39, pp. 294–300, Feb. 1991.

[11] J. Takecuhi, A. Hirata, H. Takahashi, N. Kukutsu, "10-Gbit/s Bidirectional and 20-Gbit/s Uni-directional Data Transmission over a 120-GHz-band Wireless Link using a Finline Ortho-mode Transducer", APMC 2010, pp.195-198, 2010.

[12] J. Takecuhi, A. Hirata, H. Takahashi, N. Kukutsu, "10-Gbit/s Bidirectional Wireless Data Transmission System using 120-GHz-band Ortho-mode Transducers.", RWS 2012, pp.63-66, 2012.

[13] J. Takecuhi, A. Hirata, H. Takahashi, N. Kukutsu, "20-Gbit/s Unidirectional Wireless System using Polarization Multiplexing for 12-ch HDTV Signal Transmission.", APMC 2012, pp.142-144 , 2012.

[14] M. Horibe, K. Noda, “Modification of Waveguide Flange Design for Millimeter and Submillimeter-wave measurements,” 77th ARFTG Conference, pp.1-7, 2011.

[15] S. Kobayashi, Y. Yamada, K. Hisadome, O. Kamatani, O. Ishida, "Scalable Parallel Interface for Terabit LAN," IEICE TRANS. COMMUN., VOL.E92–B, NO.10 OCTOBER, pp. 3015- 3021, 2009.

[16] S. Okabe, T. Ikeda, F. Suginoshita, K. Shogen, A. Hirata, M. Yaita, N. Kukutsu, Y. Kado, “10-Gbps forward error correction system for 120-GHz-band wireless transmission.”, RWS 2010, pp.472-475, 2010.

Chapter 6
Conclusion

6-1 Summary of Preceding Chapter

Chapter 1 presents the background of this research.

Chapter 2 presents theoretical calculation of required Iop and XPI for polarization multiplexing. From the theoretical calculation, required Iop for bidirectional transmission is more than 60 dB when the output power of Tx is 0 dBm, required XPI for unidirectional two channel data transmission is more than 23 dB.

Chapter 3 presents the polarization multiplexing using two Cassegrain antennas. Measured XPI was 29 dB at 125 GHz. Measured isolation between Tx and Rx for bidirectional data transmission was 80 dB at 125 GHz even when two pairs of wireless links use same polarization. We have succeeded in outdoor bidirectional 10 Gbps data transmission and unidirectional 20 Gbps data transmission. Moreover, we have experimentally shown that the rain attenuation of V- and H- polarization 120-GHz-band signal is almost the same.

Chapter 4 presents the polarization multiplexing using two planar slot array antennas. Measured XPI was 40 dB at 125 GHz. Measured Iop was 70 dB at 125 GHz. We have succeeded in bidirectional 10 Gbps data transmission and unidirectional 20 Gbps data transmission.

Chapter 5 presents the polarization multiplexing using OMT. We have designed and fabricated finline OMT for high Iop. Measured XPI was z50 dB at 125 GHz. Measured Iop was 67 dB at 125 GHz. We have fabricated wireless data transmission equipment using OMT. We have succeeded in bidirectional 10 Gbps data transmission and unidirectional 20 Gbps data transmission. Moreover we have succeeded in experiment for connecting the bidirectional wireless data transmission equipment to 10GbE network. We also have

succeeded in experiment for unidirectional 12-ch wireless HD-SDI data transmission.

Finally, Chapter 6 summarizes this study and discusses the future study.

6-2 Conclusions for the Future Research and development

Results of Chapter 3 indicate that the interference between 120-GHz-band wireless links with high-gain antennas is small even when they are arranged close to each other, and that space and polarization multiplexing is effective for frequency reuse in the 120-GHz-band wireless link system for both bidirectional data transmission and unidirectional 2ch data transmission. High gain Cassegrain antennas are already practically used for the millimeter wave wireless links and are suitable for space and polarization multiplexing. The disadvantage of using Cassegrain antennas is bulky size of them. Using Cassegrain antennas for space and polarization multiplexing needs wide area for installation. Thus they should be used at vast area like golf course or rooftop of big buildings.
Results of Chapter 4 indicate that using planar slot array antennas is also good candidate for space and polarization multiplexing because of its high Iop and XPI. Especially, its thin structure allows to be installed at narrow area where Cassegrain cannot be installed. The disadvantage of using planar slot array antennas is group delay variation of waveguide inside the antenna. Large antenna size for higher gain of planar slot array antenna needs long line of waveguide feeding inside the antenna, which deteriorates the group delay variation. Moreover, small diameter of the waveguide also deteriorates the group delay variation. The cutoff frequency of waveguides inside the antenna is designed close to the lower frequency band of wireless signal in order to make the diameter of waveguide small. Small diameter of the waveguides is required because waveguide feeding structure inside the antenna is crowded. Currently,

new planar slot array antennas which have coaxial cable structure are studied in Hirokawa Laboratories because coaxial cable structure never deteriorates group delay variation in principle.

Results of Chapter 5 indicate that using OMTs is also good candidate for polarization multiplexing because of its high Iop and XPI. An OMT multiplexes and de-multiplexes V and H wave with one antenna. Using OMT enables space-saving assembly of wireless equipment which is much smaller than using two pairs of antennas system and is suitable for portable wireless system. The disadvantage of using OMT is limitation of Iop. In the OMT, V and H wave are physically connected and space multiplexing cannot be applied, that situation increases difficulty of achieving high Iop. The other way of achieving high Iop is decreasing fabrication accuracy error and is fitting the Iop spectrum to wireless data spectrum. As explained in Chapter 5, decreasing fabrication accuracy error is at the limit. As shown in Chapter 5, fitting the Iop spectrum to wireless data spectrum which uses ASK modulation has succeeded, but this method cannot be applied to wireless data spectrum which uses OFDM modulation because it requires high Iop at the entire operation band. Therefore using OMT for bidirectional data transmission is suitable for short distance usage model like a data transmission in stadium because current Iop is high enough for that usage. As the future work, high-gain Cassegrain antenna that uses the OMT is required for data transmission over a distance of a few kilometers. The Cassegrain antenna will require new reflector design and new feed antenna design which are suitable for high Iop and XPI of the OMT.

Figure 6-1 shows relationship between this work and future work. As explained above, 2 channels multiplexing of 120-GHz-band wireless link system has succeeded. One of the methods of 2 channels multiplexing is using two pairs of antennas. Using two pairs of antennas can be categorized as a kind of space division multiplexing because it uses only one polarization at each antenna. The other method of 2 channels multiplexing is using OMT. OMT enables using two polarizations at each antenna. These results indicate that using both two pairs of antennas and OMT enables 4 channels multiplexing of 120-GHz-band wireless link system. 4 channels multiplexing will enable 20 Gbps bidirectional and 40 Gbps unidirectional 4 ch data transmission.

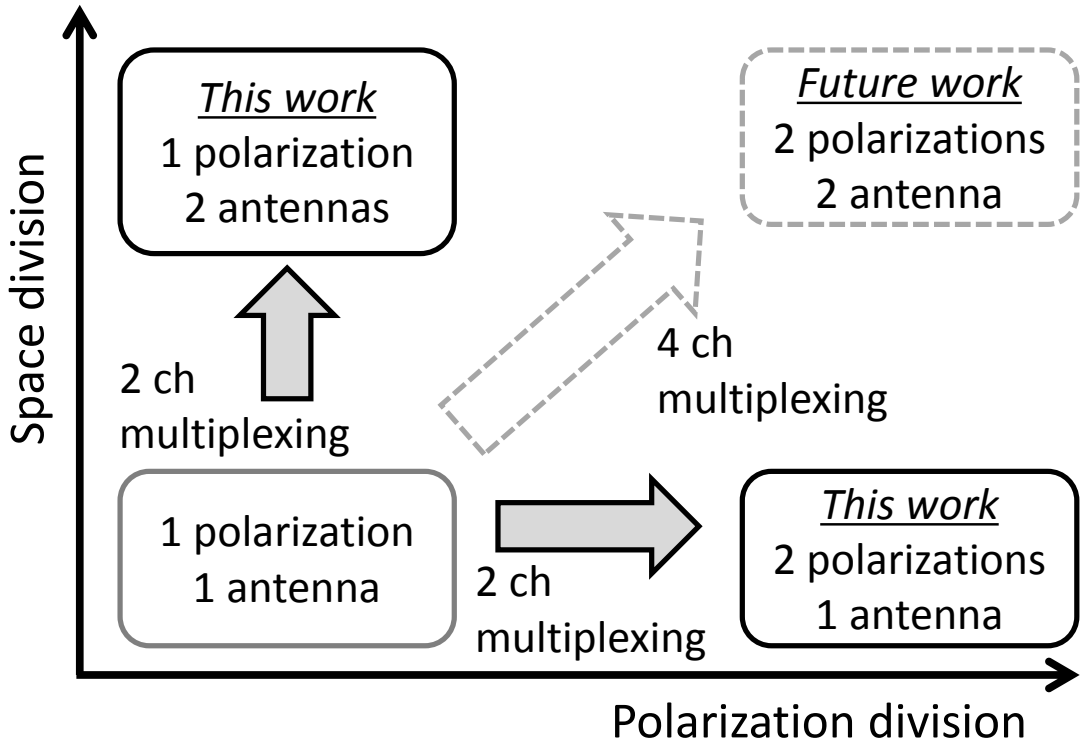

Fig. 6-1. Relationship between this work and future work.

List of Publications
(Related to this paper)

1-1. Journal Paper (Lead author)

1) **Jun Takeuchi,** Akihiko Hirata, Hiroyuki Takahashi, Naoya Kukutsu, "A Finline Orthomode Transducer for 120-GHz-band Wireless Links," IEICE Transactions on Electronics, Vol.E97-C, No.2, pp.111-119, 2014.

2) **Jun Takeuchi,** Akihiko Hirata, Hiroyuki Takahashi, Naoya Kukutsu, Yoshiaki Yamada, Kei Kitamura, Mitsuhiro Teshima, "10-Gbit/s Bidirectional and 20-Gbit/s Unidirectional 2-ch Wireless Data Transmission System using 120-GHz-band Finline Orthomode Transducers," IEICE Transactions on Electronics, Vol.E97-C, No.2, pp.101-110, 2014.

3) **Jun Takeuchi,** Akihiko Hirata, Hiroyuki Takahashi, Naoya Kukutsu, "Evaluation of Interference between Parallel 120-GHz-Band Wireless Link Systems with High-Gain Cassegrain Antenna," IEICE Transactions on Electronics, Vol.E96-C, NO.10, pp. 1294-1300, 2013.

1-2. Journal Paper (Co-author)

1) A. Hirata, T. Kosugi, H. Takahashi, **J. Takeuchi**, H. Togo, M. Yaita, N. Kukutsu, K. Aihara, K. Murata, Y. Sato, T. Nagatsuma, Y. Kado, "120-GHz-Band Wireless Link Technologies for Outdoor 10-Gbit/s Data Transmission," IEEE Transactions on Microwave Theory and Techniques, pp. 881-895, 2012.

2) Dongjin Kim, J. Hirokawa, K. Sakurai, M. Ando, T. Takada, T. Nagatsuma, **J. Takeuchi**, A. Hirata, “Design and measurement of the plate laminated waveguide slot array antenna and its feasibility for wireless link system in the 120 GHz band,” IEICE Transactions on Communications, Vol.E96-B, No.8, pp.2102-2111, 2013.

3) Dongjin Kim, J. Hirokawa, M. Ando, **J. Takeuchi**, A. Hirata, “64 x 64-Element and 32 x 32-Element Slot Array Antennas Using Double-Layer Hollow-Waveguide Corporate-Feed in the 120 GHz Band,” IEEE Transactions on Antennas and Propagation, Vol.62, No.3, pp.1507 – 1512, 2014.

2-1. International Conference (Lead author)

1) **Jun Takeuchi,** Akihiko Hirata, Hiroyuki Takahashi, Naoya Kukutsu, "10-Gbit/s Bi-directional and 20-Gbit/s Uni-directional Data Transmission over a 120-GHz-band Wireless Link using a Finline Ortho-mode Transducer," Asia-Pacific Microwave Conference 2010 (APMC 2010), pp.195-198, 2010.

2) **Jun Takeuchi,** Akihiko Hirata, Hiroyuki Takahashi, Naoya Kukutsu, "10-Gbit/s Bidirectional Wireless Data Transmission System using 120-GHz-band Ortho-mode Transducers," IEEE Radio and Wireless Symposium 2012 (RWS 2012), pp.63-66, 2012.

3) **Jun Takeuchi,** Akihiko Hirata, Hiroyuki Takahashi, Naoya Kukutsu, "20-Gbit/s Unidirectional Wireless System using Polarization Multiplexing for 12-ch HDTV Signal Transmission," Asia-Pacific Microwave Conference 2012 (APMC 2012), pp.142-144 , 2012.

2-2. International Conference (Co-author)

1) A. Hirata, T. Kosugi, H. Takahashi, **J. Takeuchi**, K. Murata, N. Kukutsu, Y. Kado, S. Okabe, T. Ikeda, F. Suginosita, K. Shogen, H. Nishikawa, A. Irino, T. Nakayama, and N. Sudo,
"5.8-km 10-Gbps data transmission over a 120-GHz-band wireless link," 2010 IEEE International Conference on Wireless Information Technology and Systems (ICWITS), pp.1-4 , 2010.

2) A. Hirata, **J. Takeuchi**, H. Takahashi, N. Kukutsu, H. Nishikawa, A. Irino, T. Nakayama, and N. Sudo,
"Space division multiplexing of 120-GHz-band wireless links using high-gain antennas," 2011 41st European Microwave Conference (EuMC), pp.25-28, 2011.

3) A. Hirata, H. Takahashi, **J. Takeuchi**, N. Kukutsu, Dongjin Kim, J. Hirokawa,
"120-GHz-band antenna technologies for over-10-Gbps wireless data transmission," 2012 6th European Conference on Antennas and Propagation (EUCAP), pp. 2564-2568, 2012.

4) A. Hirata, **J. Takeuchi**, H. Takahashi, N. Kukutsu,
"Rain attenuation fade-slope characteristics of 120-GHz-band wireless links," 2012 IEEE Antennas and Propagation Society International Symposium (APSURSI), pp. 1-2, 2012.

5) A. Hirata, **J. Takeuchi**, Dongjin Kim, J. Hirokawa,
"10-Gbit/s dual channel transmission of 120-GHz-band wireless link using planar slot array antennas," 2013 European Microwave Conference (EuMC), pp.744-747, 2013.

6) J. Hirokawa, Dongjin Kim, M. Ando, **J. Takeuchi**, A. Hirata,
"43dBi gain, 60% efficiency and 10% bandwidth hollow-waveguide slot array antenna in the 120GHz band," 2013 Asia-Pacific Microwave Conference Proceedings (APMC), pp.307-309, 2013.

3-1. Domestic Conference (Lead author)

1) **竹内淳**, 枚田明彦, 高橋宏行, 矢板信, 久々津直哉, 門勇一, 小杉敏彦, 村田浩一
「120GHz 帯無線の偏波多重通信に向けた基礎検討」, 電子情報通信学会 2009 ソサイエティ大会, C-2-85, 2009 年 9 月

2) **竹内淳**, 枚田明彦, 高橋宏行, 久々津直哉, 門勇一
「120GHz 帯無線通信用フィンライン型偏波分離器の特性評価」, 電子情報通信学会 2010 ソサイエティ大会, C-2-31, 2010 年 8 月

3) **竹内淳**, 枚田明彦, 高橋宏行, 久々津直哉
「偏波多重による 120GHz 帯無線の双方向 10Gbit/s,単方向 20Gbit/s 伝送」, 電子情報通信学会 2011 総合大会, C-2-127, 2011 年 3 月

4) **竹内淳**, 枚田明彦, 高橋宏行, 久々津直哉
「120GHz 帯無線リンクの双方向 10Gbit/s、単方向 20Gbit/s データ伝送実現に向けた偏波分離器の研究」, 電子情報通信学会 マイクロ波研究会, 電子情報通信学会技術研究報告. OPE, 光エレクトロニクス 111(148), pp.1-6, 2011 年 7 月

5) **竹内淳**, 枚田明彦, 高橋宏行, 久々津直哉
「フィンライン型偏波分離器を使用した 120GHz 帯偏波多重無線システムの交差偏波識別度評価」, 電子情報通信学会 2011 ソサイエティ大会, C-2-56, 2011 年 8 月

6) **竹内淳**，枚田明彦，高橋宏行，久々津直哉
「偏波分離器を搭載した 120GHz 帯無線機による双方向 10 Gbit/s 伝送」，電子情報通信学会 2012 総合大会, C-2-90, 2012 年 3 月

7) **竹内淳**，枚田明彦，高橋宏行，久々津直哉
「偏波分離器を用いた 120 GHz 帯無線機による単方向 20 Gbit/s 伝送」，電子情報通信学会 2013 総合大会, C-2-118, 2013 年 3 月

8) **竹内淳**，高橋宏行，枚田明彦，矢板信
「ミリ波偏波分離器の偏波間アイソレーション特性の一改善法」，電子情報通信学会 2013 ソサイエティ大会, C-2-77, 2013 年 9 月

9) **竹内淳**，枚田明彦，広川二郎
「平面スロットアレーアンテナを使用した 120 GHz 帯 2 チャンネル伝送システムの検討」，電子情報通信学会 マイクロ波研究会，電子情報通信学会技術研究報告, Vol. 113, No.378, pp.103-108, 2014 年 1 月

3-2. Domestic Conference (Co-author)

1) 枚田明彦，**竹内淳**，高橋宏行，久々津直哉，門勇一，西川寛，入野晃彦，中山稔啓，須藤直宏
「偏波分離を用いた 120GHz 帯ミリ波無線の干渉電力評価」，電子情報通信学会 2010 総合大会, B-5-172, 2010 年 3 月

2) 枚田明彦，小杉敏彦，高橋宏行，**竹内淳**，村田浩一，久々津直哉，門勇一，岡部聡，池田哲臣，杉之下文康，正源和義，西川寛，入野晃彦，中山稔啓，須藤直宏
「120GHz 帯無線による 10Gbit/s データの 5km 伝送」，電子情報通信学会 2010 ソサイエティ大会, B-5-124, 2010 年 8 月

3)　枚田明彦，高橋宏行，**竹内淳**，久々津直哉
「120GHz 帯ミリ波無線信号のガラス吸収特性」，電子情報通信学会 2011 総合大会，B-5-183, 2011 年 3 月

4)　岡部 聡，杉之下文康，**竹内淳**，　枚田明彦
「120GHz 帯無線を用いた偏波多重伝送実験」，電子情報通信学会 2012 総合大会，B-5-127, 2012 年 3 月

5)　津持純，岡部聡，杉之下文康，**竹内淳**，高橋宏行，枚田明彦
「降雨時における 120GHz 帯無線伝送装置の伝送特性」,映像情報メディア学会 2012 冬季大会, 5-10, 2012 年 12 月

6)　枚田明彦，**竹内淳**，高橋宏行，久々津直哉
「120GHz 帯無線の気象条件に起因する減衰変化速度の評価」，電子情報通信学会技術研究報告. ED，電子デバイス 112(380), 29-33, 2013 年 1 月

7)　枚田明彦，**竹内淳**, Dongjin Kim，広川二郎
「平面スロットアレーアンテナを使用した 10Gbit/s データ伝送実験」，電子情報通信学会 2013 総合大会, C-2-117, 2013 年 3 月

4-1. Award (Lead author)

1)　**Jun Takeuchi,** Akihiko Hirata, Hiroyuki Takahashi, Naoya Kukutsu
APMC Prize at the 2010 Asia-Pacific Microwave Conference, " 10-Gbit/s Bi-directional and 20-Gbit/s Uni-directional Data Transmission over a 120-GHz-band Wireless Link using a Finline Ortho-mode Transducer" December 2010.

2) **Jun Takeuchi,** Akihiko Hirata, Hiroyuki Takahashi, Naoya Kukutsu
APMC Prize at the 2012 Asia-Pacific Microwave Conference, "20-Gbit/s Unidirectional Wireless System using Polarization Multiplexing for 12-ch HDTV Signal Transmission." December 2012.

3) **竹内淳** 枚田明彦 高橋宏行 久々津直哉
一般社団法人 電子情報通信学会, 学術奨励賞(平成 24 年度(第 75 回)),「偏波分離器を搭載した 120 GHz 帯無線機による双方向 10 Gbit/s 伝送」, 2013 年 3 月

4) **竹内淳**
マイクロシステムインテグレーション研究所 所長表彰 若手奨励賞(平成 23 年度),「120GHz 帯無線の周波数利用効率向上に向けた偏波多重伝送システムの研究開発」, 2012 年 3 月

4-2. Award (Co-author)

1) J. Hirokawa, Dongjin Kim, M. Ando, **J. Takeuchi**, A. Hirata,
APMC Prize at the 2013 Asia-Pacific Microwave Conference, "43dBi gain, 60% efficiency and 10% bandwidth hollow-waveguide slot array antenna in the 120GHz band," 2013 Asia-Pacific Microwave Conference Proceedings (APMC), pp.307-309, 2013.

5. Patent (Lead author)

1) **竹内淳**, 枚田明彦, 久々津直哉
「偏波分離器および偏波分離器の製造方法」, 日本特許, 特願 2010–021505, 2010 年 2 月

2) **竹内淳**, 枚田明彦, 久々津直哉
「フィンライン型導波管構造、偏波分離器およびフィンライン型導波管構造の製造方法」, 日本特許, 特願 2010–021507, 2010 年 2 月

3) **竹内淳**, 枚田明彦, 久々津直哉
「フィンライン型導波管構造、偏波分離器およびフィンライン型導波管構造の製造方法」, 日本特許, 特願 2010–021511, 2010 年 2 月

4) **竹内淳**, 枚田明彦, 高橋宏行, 久々津直哉
「フィンライン型偏波分離器」, 日本特許, 特願 2010–283081, 2010 年 12 月

5) **竹内淳**, 枚田明彦, 高橋宏行, 久々津直哉
「フィンライン型偏波分離器」, 日本特許, 特願 2011–263604, 2011 年 12 月

6) **竹内淳**, 枚田明彦, 高橋宏行, 久々津直哉
「偏波分離器」, 日本特許, 特願 2012-031673, 2012 年 2 月

List of Publications
(Unrelated to this paper)

1. Journal Paper (Co-author)

1) H. Takahashi, T. Kosugi, A. Hirata, **J. Takeuchi**, K. Murata, N. Kukutsu, "120-GHz-Band Fully Integrated Wireless Link Using QSPK for Realtime 10-Gbit/s Transmission," IEEE Transactions on Microwave Theory and Techniques, Vol.61, No. 12, pp.4745 – 4753, 2013.

2) Dongjin Kim, J. Hirokawa, M. Ando, **J. Takeuchi**, A. Hirata, "4x4-element Corporate-feed Waveguide Slot Array Antenna with Cavities for the 120 GHz-band," IEEE Transactions on Antennas and Propagation, Vol.61, No.12, pp.5968 – 5975, 2013.

3) H. Takahashi, T. Kosugi, A. Hirata, **J. Takeuchi**, K. Murata, N. Kukutsu, "120-GHz-Band Amplifier Module with Hermetic Sealing Structure for 10-Gbit/s Wireless System," IEICE Transactions on Electronics, Vol.E97-C, No.6, pp.583-591, 2014.

2. International Conference (Co-author)

1) H. Takahashi, T. Kosugi, A. Hirata, **J. Takeuchi**, K. Murata, N. Kukutsu, "Hermetic sealing technique for F-band waveguides and packages," 2011 41st European Microwave Conference (EuMC), pp. 269-272, 2011.

2) H. Takahashi, A. Hirata, **J. Takeuchi**, N. Kukutsu, T. Kosugi, K. Murata, "120-GHz-band 20-Gbit/s transmitter and receiver MMICs using quadrature phase shift keying," 2012 7th European Microwave Integrated Circuits Conference (EuMIC), pp. 313-316, 2012.

3) Dongjin Kim, J. Hirokawa, M. Ando, **J. Takeuchi**, A. Hirata, "4×4-element corporate-feed waveguide slot array antenna with cavities for the 120 GHz-band," 2013 IEEE Antennas and Propagation Society International Symposium (APSURSI), pp. 230-231, 2013.

4) Duong Nhu Quyen, M. Sano, J. Hirokawa, M. Ando, **J. Takeuchi**, A. Hirata, "Design of a linear array of transverse slots without cross-polarization to any directions on a hollow rectangular waveguide," 2013 Proceedings of the International Symposium on Antennas & Propagation (ISAP), pp.918-920, 2013.

3-1. Domestic Conference (Lead author)

1) **竹内淳**, 高橋宏行, 枚田明彦, 矢板信
「120GHz 帯無線モジュールにおける温度特性安定化の検討」, 電子情報通信学会 2014 総合大会, C-2-110, 2014 年 3 月

3-2. Domestic Conference (Co-author)

1) 高橋宏行, 枚田明彦, **竹内淳**, 久々津直哉
「120GHz 帯可変位相 MMIC の基礎検討」, 電子情報通信学会 2011 ソサイエティ大会, C-2-13, 2011 年 8 月

2) 枚田明彦, 高橋宏行, **竹内淳**, 矢板信, 久々津直哉
「120GHz 帯ミリ波無線におけるアンテナ方位自動調整機構の検討」, 電子情報通信学会 2011 ソサイエティ大会, C-2-92, 2011 年 8 月

3) 高橋宏行, 小杉敏彦, 枚田明彦, **竹内淳**, 村田浩一, 久々津直哉
「F 帯方形導波管の気密封止構造」, 電子情報通信学会 マイクロ波研究会, 電子情報通信学会技術研究報告. MW, マイクロ波 111(313), pp.59-64, 2011 年 11 月

4) ユンニーウィン，佐野誠，広川二郎，安藤真，**竹内淳**，枚田明彦
「交さ偏波を放射しない中空導波管横方向スロット 1 次元アレーの設計」，電子情報通信学会 2013 総合大会, B-1-61, 2013 年 3 月

5) 高橋宏行，小杉敏彦，枚田明彦，**竹内淳**，村田浩一，久々津直哉
「120 GHz 帯無線リンク用 10 Gbit/s QPSK 受信 MMIC に対する高感度化の検討」，電子情報通信学会 2013 総合大会, C-2-25, 2013 年 3 月

6) ユンニーウィン，佐野誠，広川二郎，安藤真，**竹内淳**，枚田明彦
「交さ偏波を放射しない横方向スロット 1 次元アレーの広帯域設計」，電子情報通信学会 2013 ソサイエティ大会, B-1-138, 2013 年 9 月

7) 高橋宏行，**竹内淳**， 枚田明彦
「10Gbit/s QPSK 変調 120GHz 帯無線リンク」，電子情報通信学会 2013 ソサイエティ大会, C-2-91, 2013 年 9 月

8) ユンニーウィン，佐野誠，広川二郎，安藤真，**竹内淳**，枚田明彦
「交さ偏波を放射しない 120GHz 帯中空導波管横方向スロット 1 次元アレーアンテナ」，電子情報通信学会 マイクロ波研究会，電子情報通信学会技術研究報告, Vol. 113, No.378, pp.91-96， 2014 年 1 月

9) 高橋宏行，**竹内淳**， 枚田明彦
「InP HEMT による QPSK 送信、受信 MMIC を用いた 120GHz 帯 10 Gbit/s 無線装置」，電子情報通信学会 マイクロ波研究会，電子情報通信学会技術研究報告, Vol. 113, No.378, pp.97-102， 2014 年 1 月

10) 橋本敬裕，広川二郎，安藤真，**竹内淳**，枚田明彦
「120 GHz 帯偏波共用並列給電 32×32 素子導波管スロットアレーアンテナの設計」，電子情報通信学会 2014 総合大会, B-1-95, 2014 年 3 月

11)　ユンニーウィン，佐野誠，広川二郎，安藤真，**竹内淳**，枚田明彦
「交さ偏波を放射しない中空導波管横方向スロット 1 次元アレーアンテナのビームチルト設計」，電子情報通信学会 2014 総合大会, B-1-98, 2014 年 3 月

12)　津持純，岡部聡，杉之下文康，**竹内淳**，高橋宏行，枚田明彦
「SHV 信号伝送用 120GHz 帯 FPU の 1.25km 伝送実験」，電子情報通信学会 2014 総合大会, C-2-111, 2014 年 3 月

4. Award (Co-author)

1)　高橋宏行，**竹内淳**，小杉敏彦，枚田明彦，
マイクロシステムインテグレーション研究所 所長表彰 研究開発賞 革新研究部門（平成 24 年度），「ミリ波 QPSK 無線回路による 22Gbps 非圧縮伝送技術の実現」, 2013 年 2 月

5-1. Patent (Lead author)

1)　**竹内淳**，枚田明彦，高橋宏行，久々津直哉
「ミリ波無線装置」，日本特許，特願 2013-003421, 2013 年 1 月

2)　**竹内淳**，枚田明彦，広川二郎
「積層型二次元スロットアレイアンテナ」，日本特許，特願 2013-071144, 2013 年 3 月

3)　**竹内淳**，枚田明彦，高橋宏行，久々津直哉，広川二郎
「導波管スロットアレーアンテナの配置およびビームの向きの設定方法」，日本特許，特願 2013-152417, 2013 年 7 月

4)　**竹内淳**，枚田明彦
「導波管接続機構」，日本特許，特願 2014-067886, 2014 年 3 月

5) **竹内淳**, 枚田明彦
「アンテナ装置と電波到来方向推定方法」, 日本特許, 特願 2014-065536, 2014 年 3 月

5-2. Patent (Co-author)

1) 枚田明彦, **竹内淳**, 久々津直哉
「無線装置」, 日本特許, 特願 2008-212980, 2008 年 8 月

2) 枚田明彦, **竹内淳**, 久々津直哉
「無線装置」, 日本特許, 特願 2008-212982, 2008 年 8 月

3) 枚田明彦, **竹内淳**, 久々津直哉
「無線装置」, 日本特許, 特願 2010-008866, 2010 年 1 月

4) 緒方祐介, 玉木秀和, 柏木啓一郎, **竹内淳**, 福富隆明
「健康維持増進システム及び健康維持増進方法」, 日本特許, 特願 2011-004909, 2011 年 1 月

5) 枚田明彦, 久々津直哉, 高橋宏行, **竹内淳**,
「スペクトル測定システム」, 日本特許, 特願 2011-066227, 2011 年 3 月

6) 枚田明彦, 久々津直哉, 高橋宏行, **竹内淳**,
「複合ねじ、および導波管接続方法」, 日本特許, 特願 2011-070567, 2011 年 3 月

7) 高橋宏行, 枚田明彦, **竹内淳**, 久々津直哉,
「安定化フィルタ」, 日本特許, 特願 2011-085383, 2011 年 4 月

8)　高橋宏行，枚田明彦，**竹内淳**，久々津直哉
「電力検出器付導波管」，日本特許，特願 2012-032379, 2012 年 2 月

9)　高橋宏行，枚田明彦，**竹内淳**，久々津直哉
「導波管接続構造」，日本特許，特願特願 2012-031481, 2012 年 2 月

10)　枚田明彦，高橋宏行，**竹内淳**，久々津直哉
「ミリ波イメージング装置」，日本特許，特願 2012-047705, 2012 年 3 月

11)　枚田明彦，**竹内淳**，高橋宏行，久々津直哉，広川二郎
「アンテナ装置、および電波到来方向推定方法」，日本特許，特願 2012-093007, 2012 年 4 月

12)　枚田明彦，**竹内淳**，高橋宏行，久々津直哉
「アンテナ装置」，日本特許，特願 2013-059597, 2013 年 3 月

13)　高橋宏行，**竹内淳**，枚田明彦，久々津直哉
「差動増幅器」，日本特許，特願 2013-149427, 2013 年 7 月

14)　枚田明彦，**竹内淳**，高橋宏行，久々津直哉，広川二郎
「一次元スロットアレーアンテナ」，日本特許，特願 2013-158781, 2013 年 7 月

Acknowledgement

I would like to express my gratitude to Associate Professor Jiro Hirokawa for his continuous guidance and encouragement. I also wish to express my gratitude to Professor Makoto Ando for his fruitful advice.
I am very grateful to Dr. Akihiko Hirata in NTT Device Technology Laboratories and Dr. Hiroyuki Takahashi in NTT Access Network Service Systems Laboratories for their helpful advices during my doctor degree course.
I would like to thank Mr. Kimio Sakurai, Dr. Takuichi Hirano for their technical assistance. I wish to thank Ms. Keiko Nagao for her helps in my daily life. Many thanks are due to Dr. Miao Zhang, Mr. Keisuke Hashimoto and the other members of Ando and Hirokawa Laboratories for their fruitful helps.
I deeply appreciate for my wife Takayo's devoted support for every moment in my life. She is my good partner, best friend and a great adviser in my life.
Finally, I express my respects to my parents and my brother for their support.